comptes rendus
palevol
2021 • 20 • 23

The anatomy, phylogenetic relationships, and autecology of the carnivorous lizard *"Saniwa" feisti* Stritzke, 1983 from the Eocene of Messel, Germany

Krister T. SMITH & Jörg HABERSETZER

art. 20 (23) — Published on 9 June 2021
www.cr-palevol.fr

PUBLICATIONS SCIENTIFIQUES
MUSÉUM NAT. HIST. NATURELLE

Comptes Rendus Palevol est indexé dans / Comptes Rendus Palevol *is indexed by:*
– Cambridge Scientific Abstracts
– Current Contents® Physical
– Chemical, and Earth Sciences®
– ISI Alerting Services®
– Geoabstracts, Geobase, Georef, Inspec, Pascal
– Science Citation Index®, Science Citation Index Expanded®
– Scopus®.

Les articles ainsi que les nouveautés nomenclaturales publiés dans *Comptes Rendus Palevol* sont référencés par / *Articles and nomenclatural novelties published in* Comptes Rendus Palevol *are registered on:*
– ZooBank® (http://zoobank.org)

Comptes Rendus Palevol est une revue en flux continu publiée par les Publications scientifiques du Muséum, Paris et l'Académie des sciences, Paris
Comptes Rendus Palevol *is a fast track journal published by the Museum Science Press, Paris and the Académie des sciences, Paris*

Les Publications scientifiques du Muséum publient aussi / *The Museum Science Press also publish:*
Adansonia, ***Geodiversitas***, ***Zoosystema***, ***Anthropozoologica***, ***European Journal of Taxonomy***, ***Naturae***, ***Cryptogamie*** **sous-sections** ***Algologie***, ***Bryologie***, ***Mycologie.***

L'Académie des sciences publie aussi / *The Académie des sciences also publishes:*
Comptes Rendus Mathématique, Comptes Rendus Physique, Comptes Rendus Mécanique, Comptes Rendus Chimie, Comptes Rendus Géoscience, Comptes Rendus Biologies.

Diffusion – Publications scientifiques Muséum national d'Histoire naturelle
CP 41 – 57 rue Cuvier F-75231 Paris cedex 05 (France)
Tél. : 33 (0)1 40 79 48 05 / Fax : 33 (0)1 40 79 38 40
diff.pub@mnhn.fr / https://sciencepress.mnhn.fr

Académie des sciences, Institut de France, 23 quai de Conti, 75006 Paris.

ISSN (imprimé / *print*) : 1631-0683/ ISSN (électronique / *electronic*) : 1777-571X

The anatomy, phylogenetic relationships, and autecology of the carnivorous lizard "*Saniwa*" *feisti* Stritzke, 1983 from the Eocene of Messel, Germany

Krister T. SMITH
Department of Messel Research and Mammalogy, Senckenberg Museum,
Senckenberganlage 25, 60325 Frankfurt am Main (Germany)
and Faculty of Biological Sciences, Institute for Ecology, Diversity and Evolution,
Max-von-Laue-Strasse 13, University of Frankfurt, 60438 Frankfurt am Main (Germany)
krister.smith@senckenberg.de (corresponding author)

Jörg HABERSETZER
Department of Messel Research and Mammalogy, Senckenberg Museum,
Senckenberganlage 25, 60325 Frankfurt am Main (Germany)

Submitted on 16 March 2020 | Accepted on 28 April 2020 | Published on 9 June 2021

urn:lsid:zoobank.org:pub:60DC0CFE-1FC8-4A79-B19C-25B70FC4EFB0

Smith K. T. & Habersetzer J. 2021. — The anatomy, phylogenetic relationships, and autecology of the carnivorous lizard "*Saniwa*" *feisti* Stritzke, 1983 from the Eocene of Messel, Germany, *in* Folie A., Buffetaut E., Bardet N., Houssaye A., Gheerbrant E. & Laurin M. (eds), Palaeobiology and palaeobiogeography of amphibians and reptiles: An homage to Jean-Claude Rage. *Comptes Rendus Palevol* 20 (23): 441-506. https://doi.org/10.5852/cr-palevol2021v20a23

ABSTRACT
The evolution and interrelationships of carnivorous squamates (mosasaurs, snakes, monitor lizards, Gila Monsters) are a contentious part of reptile systematics and go to the heart of conflict between morphological and molecular data in inferring evolutionary history. One of the best-preserved fossils in this motley grouping is "*Saniwa*" *feisti* Stritzke, 1983, represented by complete skeletons from the early-middle Eocene of Messel, Germany. We re-describe it on the basis of superficial examination, stereoradiography, and high-resolution X-ray computed tomography of new and published specimens. The scalation of the lizard is unique, consisting of small, keeled scales on the head (including a row of enlarged medial supraorbitals) and large, rhomboidal, keeled scales (invested by osteoderms) that covered the rest of the body. Two paired longitudinal rows of enlarged scales ran down the neck. The head was laterally compressed and box-shaped due to the presence of a strong canthal-temporal ridge; the limbs and tail were very long. Notable osteological features include: a toothed, strap-like vomer; septomaxilla with a long posterior process; palpebral with a long posterolateral process; a lacrimal boss and a single lacrimal foramen; a well-developed cultriform process of the parabasisphenoid; two hypoglossal (XII) foramina in addition to the vagus; a lack of resorption pits for replacement teeth; and possibly the presence of more than one wave of developing replacement teeth per locus. There are no osteological modifications suggestive of an intramandibular hinge, but *postmortem* displacement of the angular-prearticular-surangular complex in multiple specimens suggests that there might have been some degree of mobility in the lower jaw based on soft-tissue modifications. Using phylogenetic analyses on a data-set comprising 473 morphological characters and 46 DNA loci, we infer that

a monophyletic Palaeovaranidae Georgalis, 2017, including *Eosaniwa* Haubold, 1977, lies on the stem of Varanidae Merrem, 1820, basal to various Cretaceous Mongolian taxa. We transfer *feisti* to the new genus *Paranecrosaurus* n. gen. Analysis of gut contents reveals only the second known specimen of the cryptozoic lizard *Cryptolacerta hassiaca* Müller, Hipsley, Head, Kardjilov, Hilger, Wuttke & Reisz, 2011, confirming a diet that was at least partly carnivorous; the preservation of the teeth of *C. hassiaca* suggests that the gastric physiology of *Paranecrosaurus feisti* (Stritzke, 1983) n. comb. had high acidity but low enzyme activity. Based on the foregoing and linear discriminant function analysis, we reconstruct *P. feisti* n. comb., as a powerful, widely roaming, faunivorous-carnivorous stem monitor lizard with a sensitive snout. If the molecular phylogeny of anguimorphs is correct, then many of the features shared by Helodermatidae Gray, 1837 and Varanidae must have arisen convergently, partly associated with diet. In that case, a reconciliation of morphological and molecular data would require the discovery of equally primitive fossils on the helodermatid stem.

KEY WORDS
Palaeovaranids,
Eocene,
Messel,
Germany,
carnivorous squamates,
phylogenetic
relationships,
new genus,
new combination.

RÉSUMÉ
*Anatomie, interrelations phylogénétiques et autécologie du lézard carnivore "*Saniwa*"* feisti *Stritzke, 1983 de l'Eocène de Messel, Allemagne.*
L'évolution et la phylogénie des squamates carnivores (mosasauriens, serpents, lézards monitor, monstres de Gila) font partie du contentieux qui règne dans la systématique des reptiles et sont au cœur du conflit entre données morphologiques et moléculaires, en éclairant l'histoire évolutive de ce groupe. L'un des fossiles les mieux conservés de ce groupement composite est "*Sawina*" *feisti* Stritzke, 1983, représenté par des squelettes complets dans l'Eocène inférieur et moyen de Messel, en Allemagne. Nous le redécrivons sur la base d'un examen superficiel, de la stéréoradiographie et de la tomodensitométrie X haute résolution. Son type d'écailles est unique, consistant en de petites écailles carénées sur la tête (incluant une rangée de supraorbitales médianes élargies) et en de larges écailles carénées rhomboïdales (investies par des ostéodermes) qui recouvrent le reste du corps. Deux paires de rangées longitudinales d'écailles élargies descendent le long du cou. La tête est compressée latéralement et en forme de boîte, en raison de la présence d'une crête canthale-temporale ; les membres et la queue sont très longs. Des traits ostéologiques notables consistent en un vomer denté en forme de sangle ; un manchon lacrimal et un foramen lacrimal unique ; un processus cultriforme bien développé du parabasisphénoïde ; deux foramens hypoglossaux (XII) en plus du vagus ; une absence de trous de résorption pour les dents de remplacement ; et la présence possible de plus d'une vague de développement de dents de remplacement per locus. Il n'y a pas de modifications ostéologiques suggérant une charnière intra-mandibulaire, mais un déplacement *post mortem* du complexe angulaire-préarticulaire-surangulaire chez de nombreux specimens suggère qu'il pourrait y avoir eu un certain degré de mobilité de la mâchoire inférieure, sur la base de modifications du tissu mou. En utilisant des analyses phylogénétiques sur une base de données comportant 473 caractères morphologiques et 46 locus DNA, nous déduisons qu'un Palaeovaranidae Georgalis, 2017 monophylétique, incluant *Eosawina* Haubold, 1977, existe sur la tige des Varanidae Merrem, 1820 à la base de nombreux taxons crétacés mongoliens. Nous transférons *feisti* dans le nouveau genre *Paranecrosaurus* n. gen. L'analyse de contenus de l'intestin révèle seulement le second spécimen connu du lézard cryptozoïque, *Cryptolaceria hassiaca* Müller, Hipsley, Head, Kardjilov, Hilger, Wuttke & Reisz, 2011, confirmant une alimentation au moins partiellement carnivore ; la préservation des dents de *C. hassiaca* suggère que la physiologie gastrique de *Paranecrosaurus feisti* (Stritzke, 1983) n. comb. ait eu une forte acidité, mais une faible activité enzymatique. En nous fondant sur la forme des dents et sur une analyse discriminante linéaire, nous reconstituons *P. feisti* n. comb. comme étant un lézard monitor puissant, largment errant, de souche faunivore-carnivore et à museau sensible. Si la phylogénie moléculaire des angimorphes est correcte, de nombreux caractères partagés par les Helodermatidae Gray, 1837 et les Varanidae doivent être apparus de manière convergente, en partie associés à l'alimentation. Dans ce cas, une réconciliation entre données morphologiques et données moléculaires devrait requérir la découverte de fossiles également primitifs sur la tige des Helmodermatidae.

MOTS CLÉS
Paléovaranidés,
Eocène,
Messel,
Allemagne,
squamates carnivores,
interrelations
phylogénétiques,
genre nouveau,
combinaison nouvelle.

INTRODUCTION

The clade of squamate reptiles known as Anguimorpha has attracted the attention of professionals and hobbyists alike (Pianka *et al.* 2004). Many of its members are carnivorous, seeking out and taking in part vertebrate prey. Some of the rarest (*Shinisaurus* Ahl, 1930, *Lanthanotus* Steindachner, 1878) and most charismatic (*Varanus* Merrem, 1820) lizards are contained in it, together with the venomous Gila Monster and Beaded Lizard (*Heloderma* spp.). Furthermore, it has been suspected that the dramatically transformed snakes and the extinct mosasaurs may belong, or be closely related, to it.

Snakes are noteworthy for their high present species diversity, most of which arose during the Cenozoic (Hsiang *et al.* 2015), and mosasaurs dominated megapredator niches in Late Cretaceous oceans (Everhart 2005). Yet, morphological and molecular evidence on the relationships of anguimorph lizards to each other (Rieppel 1980b; Borsuk-Białynicka 1984; Pregill *et al.* 1986; Norell & Gao 1997; Conrad 2006a; Vidal *et al.* 2012), and to other squamates clades (Lee 1997; Vidal & Hedges 2005; Gauthier *et al.* 2012; Reeder *et al.* 2015), remains strongly at odds. In particular, if the relationships supported by molecular data are correct, then the carnivorous adaptations seem in Helodermatidae Gray, 1837 and Varanidae Merrem, 1820 must have risen independently on different continents.

The fossil record is a unique archive of extinct terminal or ancestral lineages: the only direct evidence of past evolutionary history. Well-preserved fossils offer a means to test hypotheses of relationship founded on molecular or morphological data from extant taxa. One understudied extinct taxon relevant to anguimorph phylogeny is the genus now known as *Palaeovaranus* Zittel, 1887-1890, formerly known as "*Necrosaurus*" (Georgalis 2017). It was first reported from the Paleogene phosphorites of Quercy, France, by Filhol (1873a: 89; 1873b), who noted its large size, "égalant l'Iguane", and its similarity to "l'ancien genre Monitor de Cuvier." Although the type specimen was only a dentary (Augé 2005), large portions of the skeleton of the type species, *Palaeovaranus cayluxi* Zittel, 1887-1890, are now known (de Stefano 1903; de Fejérváry 1935; Hoffstetter & Gasc 1968; Rage 1978; Augé 2005). Furthermore, specimens of closely related species have been reported from Eocene localities in Germany, specifically *Palaeovaranus giganteus* (Kuhn, 1940) (on taxonomy, see Georgalis 2017) from Geiseltal (Kuhn 1940; Haubold 1977) and "*Saniwa*" *feisti* Stritzke, 1983 from Messel (Stritzke 1983; Smith *et al.* 2018a).

Leaving aside the transient associations of *Palaeovaranus* material with glyptosaurine anguids (Filhol 1877: 488; Lydekker 1888a: 279) and with shinisaurs (Hoffstetter 1954; McDowell & Bogert 1954; Hoffstetter 1955; Haubold 1977), there have historically been two main views on the relationships of *Palaeovaranus* (for a detailed review, see Georgalis 2017). According to the one view *Palaeovaranus* is in fact closely related to its namesake, *Varanus* (Zittel 1887-1890; Lydekker 1888b: 111; de Stefano 1903; de Fejérváry 1918, 1935). The other view, first promulgated by Hoffstetter (Hoffstetter 1943), draws attention to a number of primitive features of *Palaeovaranus* and places it on the stem of the putative clade Varanoidea (Hoffstetter 1962; Kuhn 1966; Hoffstetter & Gasc 1968; Estes 1983; Borsuk-Białynicka 1984; Pregill *et al.* 1986; Gao & Norell 1998; Conrad 2008). This latter view had been dominant until the widespread use of molecular techniques disrupted Anguimorpha (see above). If the molecular hypothesis of Paleoanguimorpha (*Shinisaurus* + Varanidae) (Vidal *et al.* 2012) is correct, with extinct taxa from the Cretaceous of Mongolia on the stem of Varanidae (Reeder *et al.* 2015), there might be a kind of ironic validity to several of these views, insofar as *Palaeovaranus* could be related to *Shinisaurus* and/or Varanidae but not Helodermatidae.

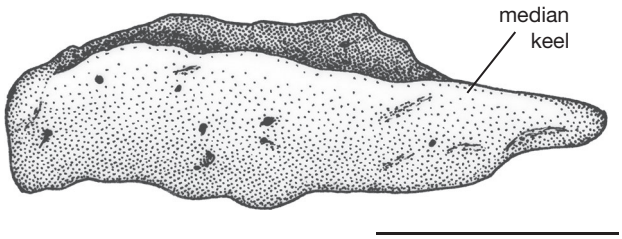

FIG. 1. — Body osteoderm of *Paranecrosaurus feisti* (Stritzke, 1983) n. comb. SMF-ME 10954 (juvenile) from posterior dorsum. Scale bar: 1 mm.

The palaeovaranid from Messel, named *Saniwa feisti* by Stritzke (1983), is represented by several well-preserved skeletons (Smith *et al.* 2018c). It is among the most complete fossil carnivorous squamates ever discovered and potentially a key taxon for reconciling molecular and morphological evidence. It has long been recognized that the initial assignment of this species to *Saniwa* was in error (e.g. Augé 2005; Georgalis 2017). This paper has three purposes. First, we re-describe the morphology of the species, including ontogenetic variation, using modern radiographic techniques based on the holotype, the paratype, and previously unpublished specimens. Second, we assess its phylogenetic relationships based on these new data. Third, we use multivariate statistical techniques and gut contents to analyze its ecological role in the Messel community and its significance for understanding anguimorph evolution.

INSTITUTIONAL ABBREVIATIONS

ANSP	Academy of Natural Sciences, Drexel University, Philadelphia;
BSP	Bayerische Staatssammlung für Geologie und Paläontologie, Munich;
GMH	Geiseltalmuseum, Martin-Luther-Universität, Halle an der Saale;
HLMD-Me	Messel Collection, Hessisches Landesmuseum, Darmstadt;
SMF-ME	Messel Collection, Naturmuseum und Forschungsinstitut Senckenberg, Frankfurt am Main;
SMF-PH	Paleoherpetology Collection, Naturmuseum und Forschungsinstitut Senckenberg, Frankfurt am Main;
SMNK-PAL	Paleontology Collection, Staatliches Museum für Naturkunde, Karlsruhe;
UCMP	University of California, Museum of Paleontology, Berkeley;
UF	University of Florida, Museum of Natural History, Gainesville;
USNM	National Museum of Natural History, Smithsonian Institution, Washington;
YPM	Yale Peabody Museum of Natural History, New Haven.

MATERIAL AND METHODS

MATERIAL

All specimens derive from the Middle Messel Formation of the Messel Pit, Germany (Smith *et al.* 2018a). Messel fossils are generally discovered by splitting laminated mudstone, or "oil-shale" (see Goth 1990), slabs, which frequently results in a division of the skeleton between part and counterpart. The first-exposed surface of a specimen is therefore commonly

TABLE 1. — Metadata for computed tomography scans of specimens of "*Saniwa*" *feisti* Stritzke, 1983. Sequence follows (estimated) snout-vent length (see Table 2).

Specimen	Focus	Institution	Device	No. steps	µA	kV	Mode	Voxel Resolution (µm)
SMF-ME 10954	Skull	AUDI CT-Lab Neckarsulm & Senckenberg Research Institute	Rayscan 200	*c*. 1200	65	160	HQ	18.5
Pohl-Perner	Belly	Technische Hochschule Deggendorf	TomoScope HV 500	1600	150	200	2	25.2
	Skull	Technische Hochschule Deggendorf	TomoScope HV 500	1600	150	200	2	34.7
HLMD-Me 13709 (holotype)	Skull	Technische Hochschule Deggendorf	TomoScope HV 500	1600	150	185	2	34.6
SMNK-Me 1124 (paratype)	Skull	University of Frankfurt	GE-Phoenix nanotom	800	45	150	2	30.0
	Skull	University of Tübingen	Phoenix	2700	200	190	2	38.4

broken. Because the oil-shale contains upward of 40% water (Harms *et al.* 1999) and desiccates and crumbles rapidly when exposed to air, it must be removed. The first-exposed surface is cleaned and embedded in a stable substance (polyester reinforced with glass fibers or, nowadays, epoxy). The oil-shale is then prepared away from the other side, nearly completely freeing the fossil from the matrix (Wedmann *et al.* 2018).

At least five specimens are now known from the Middle Messel Formation. Two of these specimens, a nearly complete skeleton and a partial one, formed the briefly described hypodigm of the new species that Stritzke (1983) named *Saniwa feisti*.

1. The holotype, specimen A in Stritzke (1983), is a nearly complete skeleton missing only the distal part of the tail. It was first illustrated in Hillmer *et al.* (1980: fig. 13). Previously in the private Feist collection, it was subsequently acquired by the Hessisches Landesmuseum in Darmstadt, Germany, and catalogued as HLMD-Me 13709. Pregill *et al.* (1986), though they were apparently unaware of Stritzke's (1983) paper, used a cast of a skeleton from Messel to score "*Necrosaurus*" in their study of varanoid phylogeny (J. A. Gauthier, pers. comm., 2007). That cast (UCMP 123607) is of the holotype.

2. The paratype comprises a disarticulated skull, partial dorsal vertebral column, and forelimbs. The part is specimen B in Stritzke (1983); it was previously in the private Tandler collection and was subsequently acquired by the Staatliches Museum für Naturkunde in Karlsruhe, Germany (catalogued as SMNK-Me 1124). The counterpart of the paratype was apparently not available to Stritzke (1983); it is or was in the private Eisvogel collection, according to the label on the HLMD cast. Casts of the counterpart are available in public collections (SMF-ME A258, HLMD-Me 14259). The specimen, unlike the others, is partly disarticulated, with the skull bones lying in a pile but some of the dorsal vertebrae and ribs and parts of the left forearm in articulation. A small crocodylian tooth lies atop the dorsal vertebral series in SMNK-Me 1124, suggesting the possibility that this was a decomposing carcass test-bitten as it floated at the surface (for a similar case, see Franzen & Frey 1993).

3. SMF-ME 10954 is a complete skeleton. It is the only specimen to preserve the tail completely. The part (SMF-ME 10954a) contains most of the specimen, the counterpart (SMF-ME 10954b) a section of 5½ caudal vertebrae missing from the part. The specimen was first reported by Harms (2000) and figured by Smith *et al.* (2018c).

4. Another specimen is a very well-preserved skeleton, missing the distal part of the tail (as in the holotype). The part, illustrated in Behnke *et al.* (1986: 77, 101), passed through the private Burkhardt collection into the private Pohl collection. The counterpart was until recently in the private Perner collection. This specimen is here referred to as the Pohl-Perner specimen.

5. We also examined a poorly preserved skeleton. Though referable to "*Saniwa*" *feisti* on the basis of co-occurrence, general body form, and osteoderm shape and coverage, little more can be said about the specimen. It passed through the private M. Keller collection into the private Pohl collection.

6. SMNK, specimen NAOM 115o118/88, is a poorly preserved skeleton. The specimen appears to have been regurgitated by a predator; osteoderms are not clearly visible, the bones are poorly exposed in the skull, and the bone surfaces are corroded. A definitive referral is not possible at present, although CT scans could probably provide some additional data.

METHODS

Radiography and CT scanning

High-resolution radiography and stereoradiography (Appendices 6-11) were performed on SMF-ME 10954 at the Senckenberg Research Institute. Additionally, six µCT scans were conducted on four specimens, focusing on the skull but also (in the Pohl-Perner specimen) the belly. Table 1 presents metadata for the CT scans. The Tübingen scan of SMNK-Me 1124 was additionally conducted in multiscan mode (4 individual scans) with detector shift activated to improve resolution. Analysis and segmentation of these scans was performed using VGStudioMAX v3.2 on a high-end workstation at the Senckenberg Research Institute.

Phylogenetic analysis

The phylogenetic relations of "*Saniwa*" *feisti* were assessed using the combined morphological data matrices of Gauthier *et al.* (2012) and Reeder *et al.* (2015), which were focused on osteology and scalation, respectively. Ingroup taxa include all of their sampled Anguimorpha and Mosasauria, and outgroups were taken to be Rhynchocephalia and the pleurodont iguanian

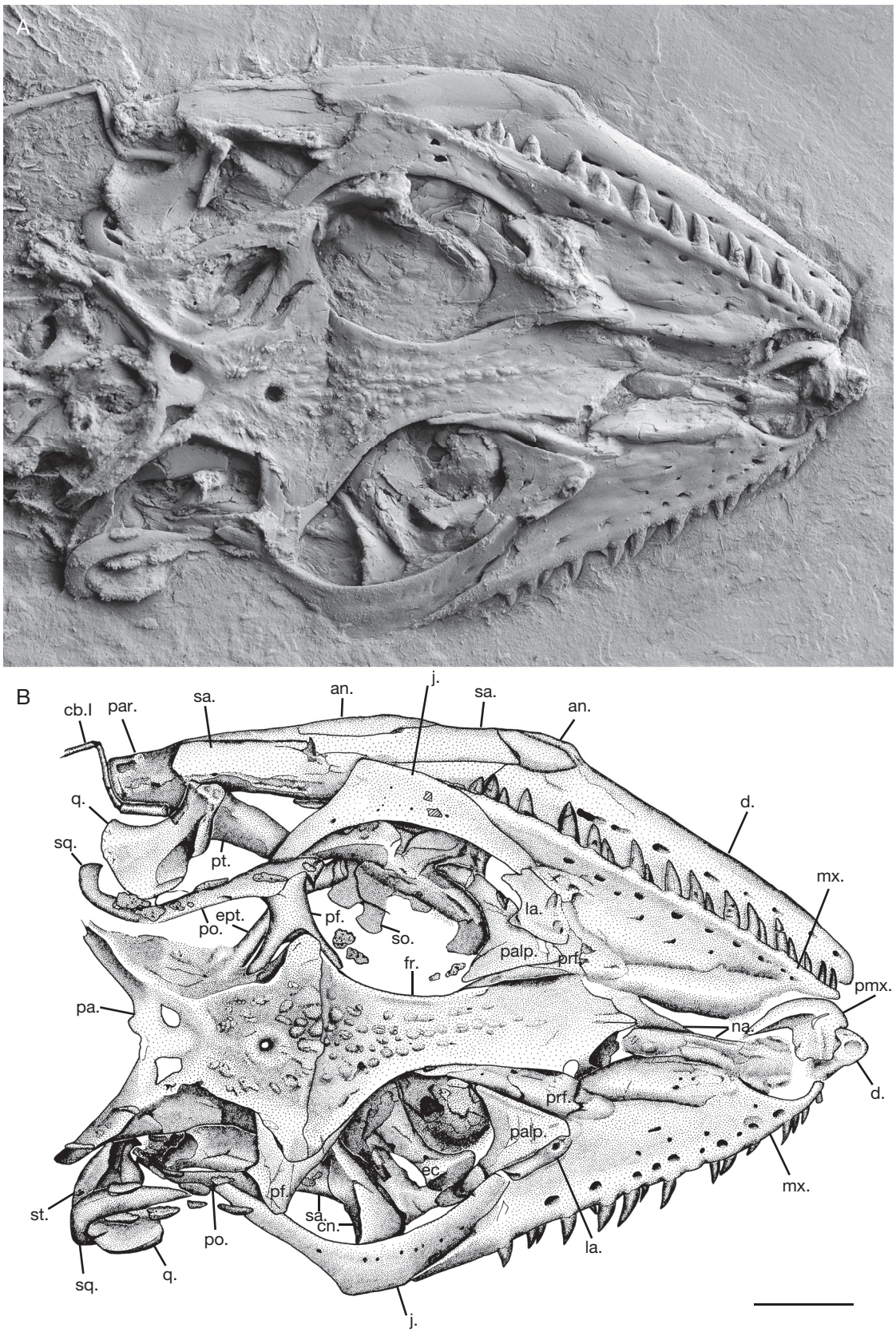

FIG. 2. — **A**, **B**, Photograph and interpretive drawing, respectively, of the skull of *Paranecrosaurus feisti* (Stritzke, 1983) n. comb. SMF-ME 10954 in dorsal view. Specimen coated with ammonium chloride in photograph. Abbreviations: **an.**, angular; **cb.I**, ceratobranchial I; **cn.**, coronoid; **d.**, dentary; **ec.**, ectopterygoid; **ept.**, epipterygoid; **fr.**, frontal; **j.**, jugal; **la.**, lacrimal; **mx.**, maxilla; **na.**, nasal; **pa.**, parietal; **palp.**, palpebral; **par.**, prearticular; **pmx.**, premaxilla; **pf.**, postfrontal; **po.**, postorbital; **prf.**, prefrontal; **pt.**, pterygoid; **q.**, quadrate; **sa.**, surangular; **so.**, scleral ossicle; **sq.**, squamosal; **st.**, supratemporal. Scale bar: 5 mm.

TABLE 2. — Body size of the four well-preserved specimens of "*Saniwa*" *feisti* Stritzke, 1983. Frontal length for the holotype is somewhat greater than given by Stritzke (1983), and for the paratype somewhat less. SVL for SMNK-Me 1124 estimated by regression equation log10(SVL) = 1.175 × log10(frontal length) + 0.7800. Mass estimated by regression equation for Varanidae, log10(mass) = 3.235 × log10(SVL) – 5.301, from Meiri (2010).

Specimen	Appendix no.	Frontal length (mm)	SVL (mm)	Mass (g)
SMF-ME 10954	1-2	15.7	148.8	54
Pohl-Perner specimen	3	19.6	187.6	113
HLMD-Me 13709 (holotype)	4	18.2	198.9	136
SMNK-Me 1124 (paratype)	5	30.8	338 (est.)	759

Pristidactylus torquatus. Characters that were invariant for the chosen taxa were eliminated. Thirty new characters of special relevance for fossil anguimorphs were added. Simões *et al.* (2017) levelled certain criticisms at the osteological portion of this matrix. Rather than deleting characters with injudicious formulations, we rewrote them wherever they could be interpreted in a more satisfactory manner (the "John Roberts approach"). The resulting matrix has 473 morphological characters (Appendix 12). Ordering of additive multistate characters follows the original authors.

Taxa potentially closely related to "*Saniwa*" *feisti* were also added, specifically *Eosaniwa koehni* Haubold, 1977 and *Palaeovaranus* spp. The recognition of a second species of *Palaeovaranus* in Quercy (Georgalis *et al.* 2021) makes the attribution of isolated elements more complicated. However, since only one species has been found in previously published collections, we tentatively accept the prior attribution of these elements. In particular, the locality at Sainte-Neboule has yielded numerous specimens corresponding to a single species, *P. cayluxi* (Rage 1978). However, we have excluded *Palaeovaranus giganteus* from this analysis, as the taxon is currently under study.

Some characters were rewritten and states renumbered to reflect the decreased variation observed among included taxa. A few corrections (cells coloured in light blue) were also made. In some cases it might appear that characters of osteology (osteoderms) and scalation (the scales overlying them) are non-independent. For instance, the keeling of dorsal body osteoderms and of dorsal body scales seem linked. However, these can develop and evolve independently, because osteoderms need not fill the entire scale. Examples of this are the ventral body osteoderms in *Heloderma horridum* (Wiegmann, 1829) (KTS, pers. obs.), which do not completely fill the scales anteriorly, and the osteoderms underlying the crested caudal scales of *Lanthanotus borneensis* Steindachner, 1877, in which dissection revealed that the keels are supported by thick wedges of connective tissue overlying the irregular osteoderms (Smith 2017a).

Our molecular data partition is taken from Reeder *et al.* (2015), which included data for both extant outgroup and 14 ingroup species. The data are up to 35 673 base pairs representing 46 loci (Appendix 13). Sequence alignment, models of molecular evolution, and priors were also taken from (Reeder *et al.* 2015).

The matrix was analysed using two methods: maximum parsimony (MP) in PAUP* (Swofford 2003) and standard Bayesian inference (BI) in MrBayes (Ronquist *et al.* 2012). In each case analyses with and without the molecular partition were conducted. For BI we used *Sphenodon* Gray, 1831 as an outgroup and enforced a monophyletic Squamata.

Paleoecology

In addition to drawing on generalizations from the literature, we used two specimen-based methods to assess the autecology of "*Saniwa*" *feisti*. First, we checked known specimens for gut contents, which would provide direct data on diet.

Second, we conducted multivariate statistical analyses of body proportions (Appendix 14). Except for the neck, "*Saniwa*" *feisti* has general body proportions similar to those of *Varanus* and in our combined analyses is more closely related to Varanidae than to any other anguimorph group (see results below); furthermore, *Varanus* displays a diversity of ecomorphs. Therefore, after checking the data in Mertens (1942c) (Appendix 15), we took the dataset of Thompson & Withers (1997) (Appendix 16) on body proportions (9 independent variables) and autecology (1 response variable with 4 levels) for 18 species of Australian *Varanus* (goannas); those authors classified the species into 8 climbing species (arboreal or saxicolous), 3 sedentary species, 6 widely foraging species, and 1 semiaquatic species. We measured the Pohl-Perner specimen of "*S.*" *feisti*, whose body is so clearly outlined by the scales that the same measurements can be conducted, except for tail length, which we scaled based on SMF-ME 10954. Limb measurements were conducted along the middle of the extremity in question. Due to flattening of all specimens, head width is the least well constrained of the variables. Following Thompson & Withers (1997), we divided all linear measurements by thorax length, which they determined to be the best measure of overall body size, to normalize size.

We then conducted principle components (PCA) and linear discriminant (LDA) analyses of the data using R v3.5.0 (R Core Team 2016). While both techniques use dimensionality reduction, LDA seeks to maximise the separation of classes. It is applied to a training dataset and then used to classify new observations (in this case, of "*Saniwa*" *feisti*). For PCA, we scaled variables to unit variance and ran analyses with and without "*S.*" *feisti*; we also explored different plausible values for head width. For LDA, we used the data on modern *Varanus* as a training dataset and then predicted the ecological class of "*S.*" *feisti*, using default prior probabilities (the proportions of classes in the training dataset). Because "*S.*" *feisti* is not in the varanid crown, we judged it unhelpful to conduct analyses based on phylogenetically independent contrasts, nor (given the unambiguousness of the LDA results) did we seek to apply LDA to the PCA results (rather than just untransformed data).

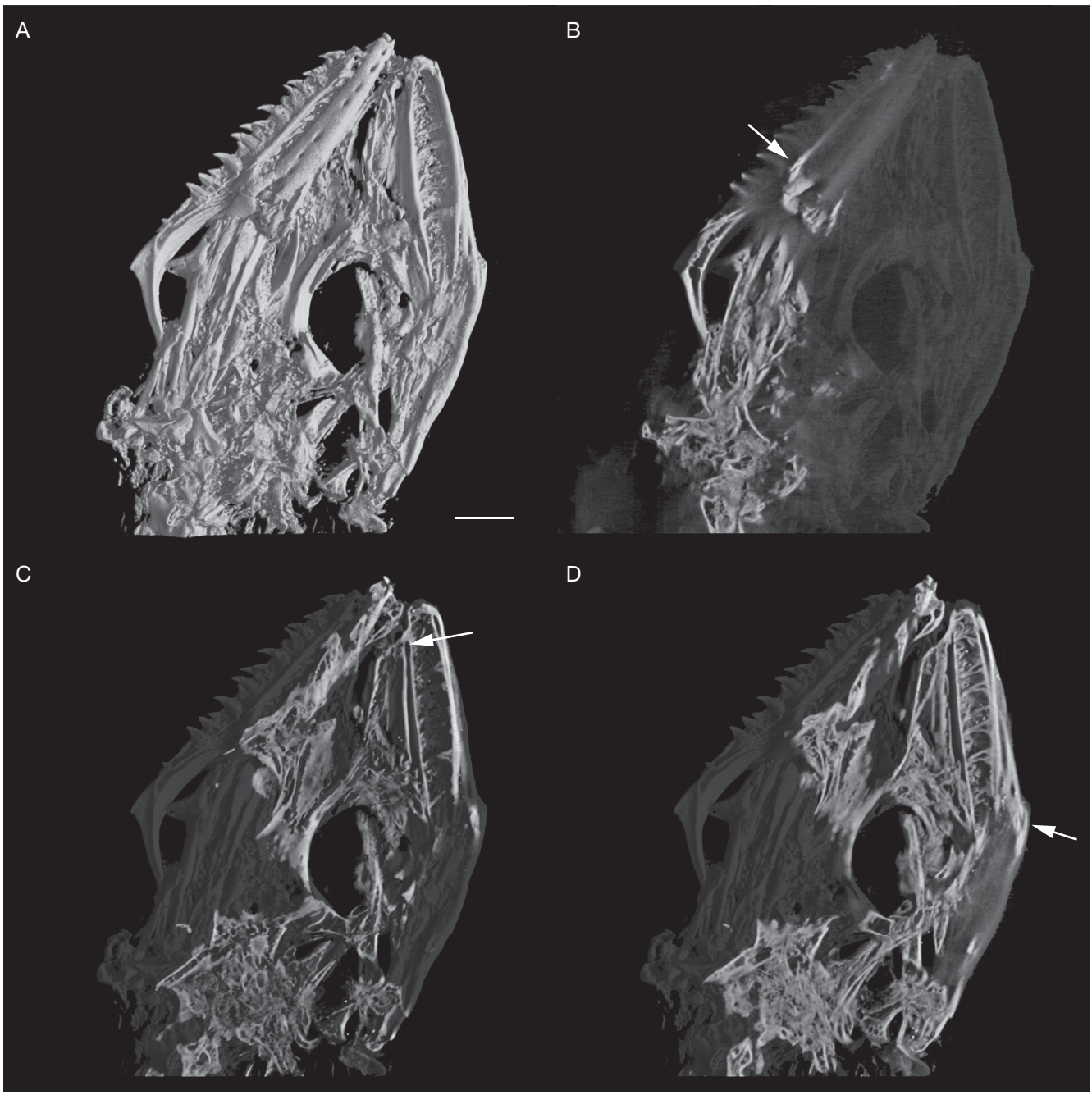

FIG. 3. — **A**, CT reconstruction of ventral surface of skull of *Paranecrosaurus feisti* (Stritzke, 1983) n. comb. SMF-ME 10954; **B**, cutaway showing slice xz505 from CT scan, **arrow** points to right palatine-maxilla articulation; **C**, cutaway showing slice xz546 from CT scan, **arrow** points to anterior superior alveolar foramen piercing left maxilla medial to crista transversalis; **D**, cutaway showing slice xz551 from CT scan, **arrow** points to the nexus of the left prearticular, splenial, angular, and dentary. Scale bar: 5 mm.

RE-DESCRIPTION

SMF-ME 10954, with a frontal length of *c*. 15.7 mm, is the smallest specimen and clearly represents a skeletally immature individual (Appendices 1; 2). The Pohl-Perner specimen (Appendix 3), with a frontal length of 19.6 mm, and the holotype, HLMD-Me 13709 (Appendix 4), with a frontal length of *c*. 18.2 mm, are somewhat larger in linear dimensions. The animal represented by SMNK-Me 1124 (Appendix 5) is the largest known individual. The length of the frontal is 30.8 mm, making it larger even than GMH Ce-III-4139-1933, the holotype of *Palaeovaranus giganteus* (Kuhn 1940) and the largest specimen attributed to the species by Estes (1983). Still, on the left humerus of SMNK-Me 1124 (Appendix 5A) the distal epiphysis appears to have been unfused, indicating that even this large individual was not yet fully skeletally mature. Table 2 gives an estimate of size (snout-vent length, or SVL, and mass in life) for each specimen. We draw on the conclusions of Blob (1998) that the vent is normally located at the middle of the second caudal vertebra. SVL for SMNK-

Me 1124 was estimated by regressing the logarithm of frontal length on the logarithm of SVL for the three specimens in which both parameters can be determined; as an extrapolation based on few data-points, this estimate is particularly uncertain. Mass in life was estimated based on parameters of the linear regression equations in Meiri (2010) for Varanidae. The mass of the largest specimen is estimated to be 759 g.

The head is large, and the body robust. The neck is short by comparison with Varanidae. The body may have been slightly compressed, to judge by the shape of the ribs. Unlike in Varanidae, and especially *Varanus*, the external nares are small and anteriorly located. The snout is not elongated.

The detailed description begins with the integument. Here we closely follow the terminology of Savage *et al.* (2008). The description of the skull is organized according to the functional units of Frazzetta (1962), who recognized more divisions than did Versluys (1912). The description then proceeds to the remainder of the axial skeleton (the vertebral column and ribs) and finally the extremities, including girdles.

Free osteoderms and scalation

Scales

Description. Osteoderms invest virtually every scale in larger individuals. In the smallest individual (SMF-ME 10954), osteodermal tissue is principally confined to the keel of larger scales (Fig. 1), consistent with the observations on osteoderm development in *Shinisaurus* (Bhullar & Smith 2008). Thus, it is the larger individuals that provide the best picture of scalation. The largest individual is disarticulated (Appendix 5). Furthermore, the holotype shows few indications of osteoderms outside of the skull and tail. The reasons for this are unknown; individual variation in the ontogenetic timing of osteoderm ossification could be a factor, but it cannot be discounted that some free osteoderms were lost during preparation. Thus, it is the Pohl-Perner specimen in which the scalation and external appearance of the living animal are most clear. We use the term "scale" to refer to the epidermal structure only, where its morphology can reasonably be inferred on the basis of the osteoderm. Only over the frontal and parietal bones do the osteoderms appear to be co-ossified with the underlying bone; the remaining osteoderms are free.

The scales of the head are generally much smaller than those of the body (Fig. 5; Appendix 3), and large, discrete shields are not to be found. Even the interparietal scale, one of the largest on the head and which covered the parietal foramen, is smaller than the body scales. The scales of the loreal region, on the lateral part of the snout between the nasal opening and orbit, were apparently flat, as indicated by the lack of keeling on the small plates of osteoderm on the maxilla (Fig. 5); as noted above, however, absence of keeling of osteoderms is not dispositive with respect to the presence of keeling on scales. Here, the osteoderm probably did not fully invest each scale. There is no indication of osteoderms in the supralabial scales that must have been located below the labial foramina.

Virtually all the scales over the dorsal roofing bones are keeled (Figs 5; 7). On the dorsal part of the snout around the canthal ridges the scales have the form of elongate hexagons and appear to have been flat (Fig. 5). More medially, between the canthal ridges in the internasal region, the scales had keels that are oriented slightly obliquely, converging anteriorly on the midline. A row of scales appears to have run along the orbital margin of the frontal, but the appertaining osteoderms have largely slid off the side and are seen only edge-on. In the anterior half of the frontal in the Pohl-Perner specimen there are (including the scales along the orbital margin) five longitudinal rows of scales that diverge and grow larger anteriorly (Fig. 5). Based on rugosities, SMF-ME 10954 appears also to have had five longitudinal rows of scales in this position. The number is reduced to four anteriorly in HLMD-Me 13709 (Fig. 7). More posteriorly on the frontal discrete rows are difficult to make out in the Pohl-Perner specimen, but in HLMD-Me 13709 they are clearer. At the frontoparietal suture there may have been 10-11 scales in a transverse row (Figs 5; 7).

A row of five shields, the medial supraocular scales, is present on each side just lateral to the interorbital constriction of the frontal, which largely fill the space posteromedial to the palpebral (Fig. 5). The medial supraoculars overlap each other from front to back. The most anterior and most posterior medial supraoculars are shorter than the three in the middle. The most anterior is nearly oval, whereas the succeeding three are narrow rectangles. The most posterior again shows more rounded anterior and posterior margins. The first four medial supraoculars are distinctly transversely keeled, whereas the fifth is less distinctly keeled. In the osteoderms of all five, numerous tiny ridges extend anteriorly and posteriorly from the transverse keel. The lateral supraocular scales were also invested with bone. They extend from the medial supraoculars as far as the lateral edge of the palpebral. Their osteoderms lie atop the palpebral and appear to have been flat, except the anteromedial-most ones. They are generally longer than wide (Figs 5; 7).

Over the parietal the scales are slightly larger than those of the posterior part of the frontal. Their keels are oriented obliquely, converging slightly posteriorly toward the interparietal scale. The interparietal scale was presumably devoid of pigmentation immediately over the parietal foramen to allow light to pass to the parietal (or parapineal) organ lying immediately beneath (see Smith *et al.* 2018b). Posteriorly on the parietal osteoderms are absent in both HLMD-Me 13709 and the Pohl-Perner specimen. There are no clear rugosities over the parietal in this region of SMF-ME 10954 either. Given the consistency among specimens, it is likely that osteoderms were lacking in this region, although it is unknown why that should be the case.

The temporal scales over the supratemporal fenestra are keeled (Fig. 5). They grow in size from medial to lateral, at least as far as the presumed ridge marked by the supratemporal bar. Here the scales first begin to achieve the nearly oval shape common to the scales of the rest of the body.

In the lower jaw, scales over the dentary were apparently largely devoid of osteoderms (Fig. 6), so that little can be said about them. The small patches of osteoderm over the left dentary of the Pohl-Perner specimen (Fig. 6B), if these pertain to scales in this region, suggest that the scales were flat rather than keeled. Some of the scales over the posterior

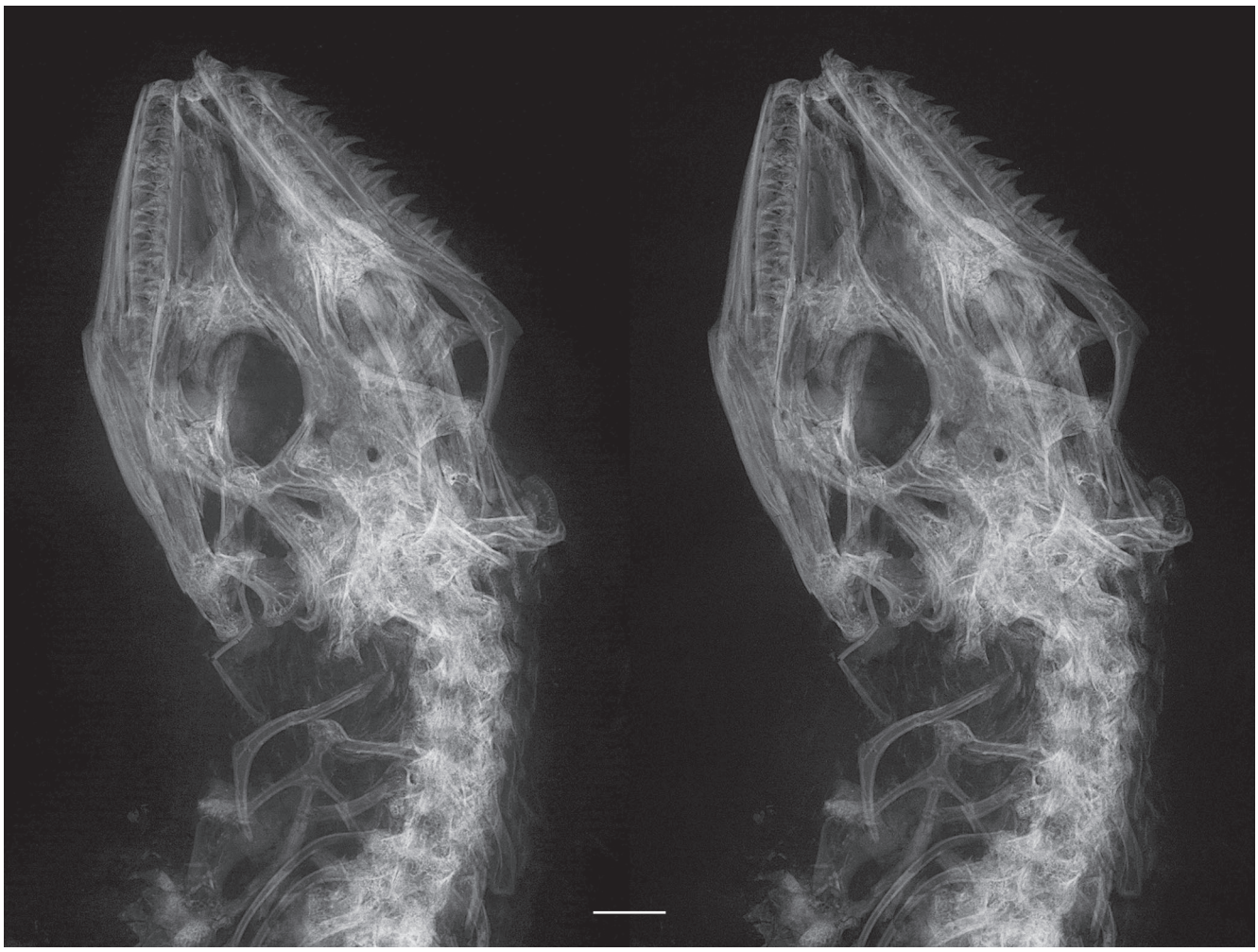

Fig. 4. — Stereo X-radiograph of skull and torso of *Paranecrosaurus feisti* (Stritzke, 1983) n. comb. SMF-ME 10954. A stereo JPEG (.jps) is found in Appendix 7. Scale bar: 5 mm.

half of the mandible were invested with osteoderms, especially dorsolaterally near the angle of the mouth. Ventrolateral scales over the posterior mandible appear to have been weakly keeled, whereas dorsolateral scales were more strongly keeled. These scales were long and narrow, probably rectangular.

The scales of the neck were not homogeneous (Appendix 3A). Dorsally they consist of two longitudinal rows of large, strongly keeled scales of oval to rhomboidal shape separated by at least three rows of much smaller scales on the midline. This pattern is established immediately behind the parietal (even between the supratemporal processes of that bone) and continues as far posteriorly as the shoulders. The scales on the lateral aspect of the neck are considerably smaller than the enlarged rows of the dorsal aspect but otherwise similar in shape. Those on the ventral aspect are again similar in shape and larger than the lateral ones but do not approach the enlarged dorsal scales in size (Appendix 3B). A gular fold in iguanian lizards is frequently, but not always, accompanied by a marked change in scalation (Frost & Etheridge 1989), with especially small scales in the fold. There is no change in the size or morphology of the osteoderms on the ventral surface of the neck that would indicate the presence of a gular fold.

The scales on the remainder of the dorsum are oval to rhomboidal, with a strong median keel that may grow more prominent distally and with the distal end sometimes drawn out into a point (Appendix 3A). Beginning at the shoulder there is no longer any heterogeneity of scale morphology. There are approximately 18-19 longitudinal rows of scales at mid-body on the dorsum. The number of transverse rows of scales per vertebra is about 1.6. Except on the posterior-most part of the torso, the keels of the scales appear to be slightly offset, so that extensive, longitudinal ridges are not formed. The osteoderms of some scales close to the boundary between dorsum and venter are distinctly narrower and shorter than the adjacent scales, similar to the body osteoderms of immature individuals (see above), suggesting the possibility of some kind of a lateral fold, as seen in the heavily armored clades Cordyliformes (Lang 1991) and Anguidae (Keller 2009).

There are approximately 21 longitudinal rows of scales on the venter (Appendix 3B). The number of transverse rows of scales per vertebra is approximately 1.4. The osteoderms differ in shape from those of the dorsum in several ways. They are narrower and tend to be rectangular. They are less strongly keeled than those of the dorsum.

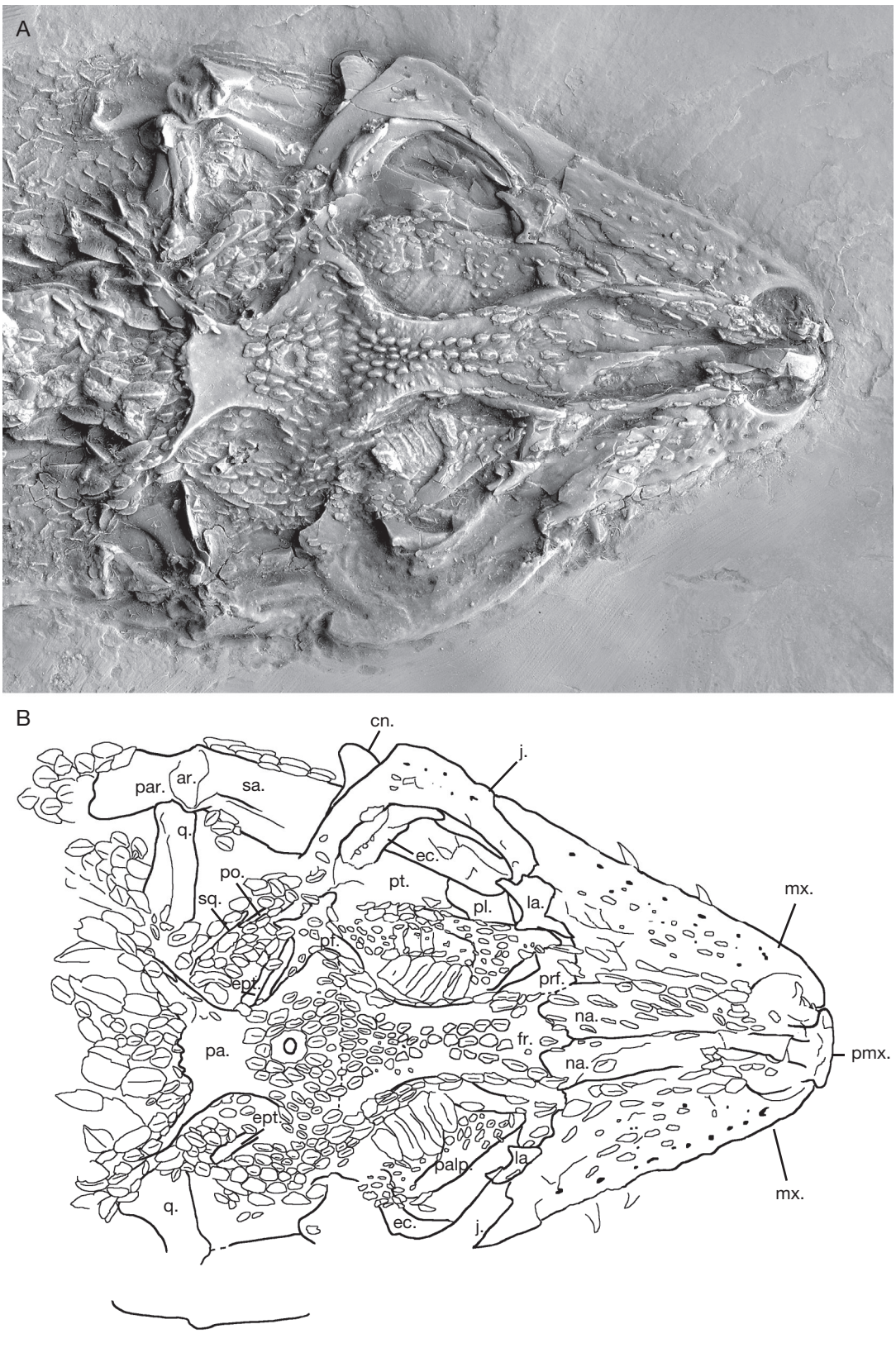

FIG. 5. — **A**, **B**, Photograph and interpretive drawing, respectively, of the skull of *Paranecrosaurus feisti* (Stritzke, 1983) n. comb. (Pohl specimen) in dorsal view. Abbreviations: **ar.**, articular; **cn.**, coronoid; **d.**, dentary; **ec.**, ectopterygoid; **ept.**, epipterygoid; **fr.**, frontal; **j.**, jugal; **la.**, lacrimal; **mx.**, maxilla; **na.**, nasal; **pa.**, parietal; **palp.**, palpebral; **par.**, prearticular; **pf.**, postfrontal; **pl.**, palatine; **pmx.**, premaxilla; **po.**, postorbital; **prf.**, prefrontal; **pt.**, pterygoid; **q.**, quadrate; **sq.**, squamosal; **sa.**, surangular. Scale bar: 5 mm.

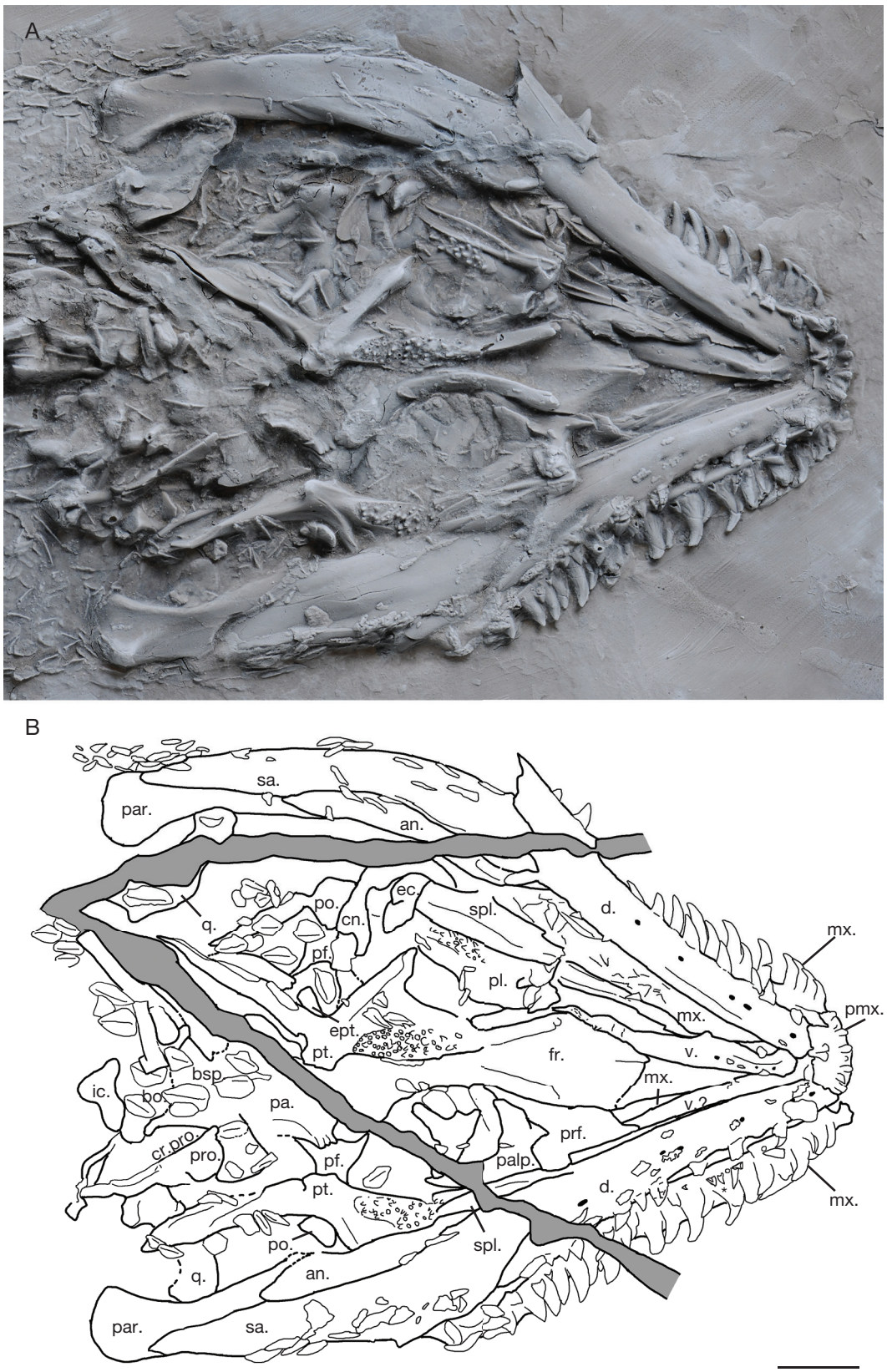

FIG. 6. — **A**, **B**, Photograph and interpretive drawing, respectively, of the skull of *Paranecrosaurus feisti* (Stritzke, 1983) n. comb. (Perner specimen) in ventral view. Abbreviations: **an.**, angular; **bo.**, basioccipital; **bsp.**, basisphenoid; **cn.**, coronoid; **cr.pro.**, crista prootica; **d.**, dentary; **ec.**, ectopterygoid; **ept.**, epipterygoid; **fr.**, frontal; **ic.**, atlantal intercentrum; **mx.**, maxilla; **palp.**, palpebral; **pa.**, parietal; **par.**, prearticular; **pf.**, postfrontal; **pl.**, palatine; **pmx.**, premaxilla; **po.**, postorbital; **prf.**, prefrontal; **pro.**, prootic; **pt.**, pterygoid; **q.**, quadrate; **sa.**, surangular; **spl.**, splenial; **v.**, vomer. Scale bar: 5 mm.

Moreover, the keel is not symmetrical, running down the midline, but rather it tends to extend from the anteromedial to the posterolateral corner.

Because osteoderms are lacking ventrally around the second caudal vertebra, there is no evidence of distinctive scalation around the vent (Appendix 3). The scales of the tail are long and narrow. They tend to be more lenticular dorsally and rectangular ventrally. Some of the lateral scales have slightly asymmetrical keels; dorsally these extend somewhat laterally, and ventrally somewhat medially. In SMF-ME 10954, where osteoderms have formed only in the keels of the scales, these scales are seen to cross one another in a regular fashion (Appendices 1; 2; see also Fig. 18). The number of longitudinal scale rows decreases in the proximal part of the tail, from about 14 below the 3rd caudal vertebra to about 12 below the 7th caudal vertebra (Appendix 3B). There are two transverse rows of scales per caudal vertebra (Appendix 3).

In contrast to the scales of the torso, the scales of the limbs have keels that are typically aligned proximally to distally, forming strong longitudinal ridges (Appendix 3). Curiously, this alignment is not present on the posteroventral surface of the thigh. Here, the scales, while they have the same form as those on the rest of the limbs, are arranged such that the keels run anteroposteriorly, like those on the torso and tail. The keels on the ventral scales are less prominent than those of the dorsal ones, as on the torso, and in one place on the undersurface of the thigh keels appear to be absent entirely (Appendix 3B, right side). The scales around moveable joints tend to be smaller than adjacent scales. This is true of the shoulder and elbow (Appendix 3A, right side) and most especially the hip (Appendix 3A, left side) and knee (Appendix 3B, right side). Rows of keeled scales are present on the dorsal surface of the metacarpus (Appendix 3B, left side) and metatarsus (Appendix 3A, right and left sides). Small bits of osteodermal tissue are present even on in the digits (especially clear in Appendix 3B, left manus), although there is no indication here of keeling.

Comparisons. The head scales of "*Saniwa*" *feisti*, particularly those over the skull roofing bones, are small and keeled and are much smaller than the scales of the body. The torso is covered with fairly homogeneous, oval to rhomboidal scales (with relatively small differences between dorsum and venter), except for the nape, where there is a paired longitudinal row of enlarged scales. The scales of the limbs are similar to those of the body in form, but the keels of proximodistally adjacent scales are aligned, forming longitudinal ridges. Overall, this scalation is unique with respect to extant anguimorphs. Only *Varanus dumerilii* Schlegel, 1839 (e.g. USNM 24022, 26205) – with its small head scales, enlarged keeled neck scales, and keeled scales elsewhere on the body (KTS, pers. obs.) – and *V. rudicollis* Gray, 1845 come close. These and other aspects of scalation are treated in more detail below.

Keeled scales on the frontal and parietal are described for *Palaeovaranus* sp. (Georgalis *et al.* 2021), like "*Saniwa*" *feisti*. However, most anguimorphs, including the palaeovaranid *P. giganteus* (KTS, pers. obs.), do not have distinctly keeled scales on the top of the head (Reeder *et al.* 2015). The epidermal shields are basically flat-topped in Anguidae (Meszoely 1970), the proposed stem varanids (cf. Gauthier *et al.* 2012; Reeder *et al.* 2015) *Gobiderma pulchrum* Borsuk-Białynicka, 1984 and *Carusia intermedia* (Borsuk-Białynicka, 1985) (Borsuk-Białynicka 1984; Conrad *et al.* 2011a), *Varanus*, the proposed stem xenosaur *Entomophontes incrustatus* Smith & Gauthier, 2013, and stem shinisaurs (Conrad 2006a; Klembara 2008; Smith & Gauthier 2013), and they are flat-topped or rounded in proposed stem (Nydam 2000; Longrich *et al.* 2012) and extant Helodermatidae. Extant *Shinisaurus* (Zollweg & Kühne 2013) does tend to develop keeled scales in the temporal region on either sides of the dorsolateral crest, but only *Lanthanotus* is similar to "*S.*" *feisti* in having keeled scales over much of the head (Reeder *et al.* 2015).

Fragmentation of the epidermal shields on the dorsal skull is recognized as a derived character in Anguimorpha (Gauthier 1982; Estes *et al.* 1988) found in *Xenosaurus* Peter, 1861, *Shinisaurus*, *Heloderma* Wiegmann, 1829 and Varanidae. Indeed, only Anguidae are thought to preserve them among extant anguimorphs. Smith and Gauthier (Smith & Gauthier 2013), however, suggested that early Eocene *Entomophontes incrustatus* from Wyoming, United States, which has large shields on the frontal bone, may represent a transitional morphology on the line leading to *Xenosaurus*, which would be consistent with the independent fragmentation in this lineage. Large shields do not occur in any known member of Palaeovaranidae Georgalis, 2017 (although it should be noted that the cephalic scalation is essentially unknown in *Palaeovaranus cayluxi*), but there is variation in the degree of fragmentation. In *P. giganteus* the scales over the frontal and parietal are relatively broader than in "*Saniwa*" *feisti*, so that there are only 2-3 scales between the orbital margins at mid-length on the frontal (KTS, pers. obs.); there appear to be 3 in *Palaeovaranus* sp. (Augé 2005: fig. 189a; Georgalis *et al.* 2021: fig. 40C).

Enlarged, medial supraoculars are found in numerous squamates, but these scales in "*Saniwa*" *feisti* are distinct from those in most Anguimorpha. In *Lanthanotus*, *Heloderma* and *Xenosaurus* the medial supraoculars tend not to be distinct from lateral supraoculars and other head scales (Bhullar 2011; Schwandt 2019). In Anguidae, the medial supraoculars tend to be large, blocky and irregular. In *Shinisaurus* there are three enlarged medial supraoculars of similar shape (Bever *et al.* 2005), although they are not as narrow as those of "*Saniwa*" *feisti*. Amongst anguimorphs, the medial supraocular scales of "*Saniwa*" *feisti* are most similar to those of some *Varanus* like *V. salvator* Laurenti, 1768 (Koch *et al.* 2013). Similar scales also occur in some Iguania, particularly among phrynosomatines (e.g. Cope 1898) and tropidurines (e.g. de Avila Pires 1995).

The lack of (fusion of) osteoderms to the posterior part of the parietal is widely seen in anguimorphs with otherwise fused osteoderms, including *Shinisaurus* (Conrad 2006a; Smith & Gauthier 2013), *Heloderma*, various Anguidae (Meszoely 1970; Smith & Gauthier 2013), and, to a lesser extent, *Xenosaurus* (Bhullar 2011).

Paired longitudinal rows of enlarged, keeled scales on the nape, like those in "*Saniwa*" *feisti*, are otherwise only seen in *Lanthanotus*, among extant anguimorphs, and the species of

Varanus noted above. Notably, however, a similar morphology is seen in *Shinisaurus*, although the rows are multiple (McDowell & Bogert 1954), and occasionally more posteriorly in *Xenosaurus* (Lemos-Espinal *et al.* 2012).

Near-complete dorsal body armor, with adjacent scales in close contact, is seen in Anguidae and *Heloderma*, amongst extant anguimorphs (Gauthier 1982). The type material of "*Necrosaurus eucarinatus*" (see Georgalis 2017) from Geiseltal and "*Saniwa*" *feisti* are presumably primitive with respect to Anguidae in lacking well-developed overlap structures. With the caveat that articulated osteoderms are yet unknown in *Palaeovaranus cayluxi*, the squamation of Palaeovaranidae appears to separate it from all other anguimorphs where the body scalation and osteoderms are known. The scales are homogeneous, unlike in *Xenosaurus*, *Shinisaurus* and *Lanthanotus* (Steindachner 1878: pl. 2; Barrows & Smith 1947: pl. 11; McDowell & Bogert 1954: pls. 5-1, 6-1). Their relatively large size differentiates the taxon from *Varanus* (Mertens 1942c). Their shape, (degree of) keeling, and minor imbrication differentiate it from Anguidae and Helodermatidae.

Smith (2017a) noted that at least one member of the total clade of *Shinisaurus* was present in the Paleogene of Europe, more specifically at Messel, and that the isolated crestal osteoderms of the dorsum of extant *Shinisaurus* are similar in outward shape and cross-section to isolated osteoderms of *Palaeovaranus*. The Pohl-Perner specimen shows that many of the body osteoderms of these two species are rhomboidal, forming a nearly unbroken cuirass. Rhomboidal scales of this form are unknown in described extant or fossil pan-shinisaurs (on this term, see Smith & Gauthier 2013). Thus, rhomboidal scales might confidently be attributed to Palaeovaranidae. However, in the disarticulated holotype of *P. giganteus* (GMH 4139), numerous osteoderms with an apparently oval to lenticular outline are present in the region of the head and neck (KTS, pers. obs.); a detailed study of that species will be necessary to determine its similarities to *Palaeovaranus*.

McDowell and Bogert (McDowell & Bogert 1954) observed that the osteoderms in the type specimen of "*Necrosaurus eucarinatus*" Kuhn, 1940 are also non-imbricate. In fact, some osteoderms do very slightly overlap (although not nearly to the extent seen in Anguidae). Narrow and elongate facets appear to be developed on the apical side of the proximal edges of the osteoderms for the insertion of the distal edges of more proximal ones (e.g. GMH 4021); these facets are roughly equal in length and, unsurprisingly, are especially obvious where the scales are more rhomboidal than oval.

Unlike in some Anguidae (e.g. *Gerrhonotus* Wiegmann, 1828), there is no clear alignment of keels of dorsal scales in "*Saniwa*" *feisti*. The aligned scale keels of the limbs in "*Saniwa*" *feisti*, in contrast, are not found in Anguidae. They could have been similar to those of *Smaug* Stanley, Bauer, Jackman, Branch, Le Fras & Mouton, 2011 and, to a lesser extent, *Shinisaurus*. In *Smaug*, the distal margins of the scales project and so are free of the surrounding tissue, so that well-defined longitudinal ridges do not form.

The ratio of the number of transverse rows of scales to vertebral count in the trunk was examined by Camp (1923) and more quantitatively by Kerfoot (1970). Among Anguimorpha, Camp (1923) found that the ratio was about 2 in examined members of Anguidae, *Xenosaurus*, and *Heloderma* but greater in *Varanus*. More generally, he considered that a reduced ratio, characteristic of his taxon Autarchoglossa, is related, by m. rectus lateralis, to a propensity to evolve serpentiform locomotion. Kerfoot (1970) summarized more recent studies implicating instead the costocutaneous muscles. The number of ventral transverse scale rows per vertebra has not been studied, to our knowledge, in *Shinisaurus* or *Lanthanotus*. Presumably because of the large size of the trunk scales of "*Saniwa*" *feisti*, the ratio is lower (1.6 and 1.4 for the dorsum and venter, respectively) than in the anguimorphs studied by Camp.

The autotomy septum imposes additional constraints on the arrangement of caudal scales in those species showing autotomy. Smith (2017b) showed how in *Anolis cuvieri* Merrem, 1820, the otherwise hexagonal scales are transformed in such a way to form a transverse suture that corresponds to the autotomy plane through the vertebrae, and that the scales of the regrown tail do not show this segmental arrangement but instead are homogeneous and hexagonal (but now highly elongate). It seems evident that the creation of transverse boundaries at the autotomy planes is beneficial in contributing to a clean break, and this is especially true in taxa in which osteoderms invest the scales. It is therefore not surprising that in the tail of *Shinisaurus* and its extinct relative from Messel, there are precisely two transverse rows of scales per caudal vertebra, with one of the two whorl boundaries corresponding to the autotomy plane (Smith 2017a). It is less obvious that this should be the case in "*Saniwa*" *feisti*, where autotomy planes are absent (see Vertebrae). Particularly given the lower ratio on the trunk (see above), this possibly indicates that the lineage leading to "*Saniwa*" *feisti* was primitively autotomic and that it shows phylogenetic inertia.

The muzzle unit

Premaxilla

Description. The premaxilla has a maximal median length of approximately 8.0 mm in SMF-ME 10954 and 9.8 mm in HLMD-Me 13709. The bone bears a long nasal process (Figs 2-5; 7), which first rises dorsally then arches sharply posterodorsally. The degree of curvature is best preserved in SMF-ME 10954 (Fig. 2), whereas in other specimens it is exaggerated by breakage. The process is triangular in transverse section, with a flat, smooth, external surface. Anterior premaxillary foramina are absent. At the base of the process is a small posterior premaxillary foramen. The distal end of the nasal process, which can be followed in CT scans, is separated from the anterior tip of the frontal in SMF-ME 10954 (Fig. 3A) and HLMD-Me 13709. In HLMD-Me 11307 the posterior-most end it has a T-shaped cross-section. Ventrolaterally on the nasal process are longitudinal impressions that extend at least half the length of the process and into which the nasal bones would have inserted. The lateral process of the premaxilla shows weak irregularities for the maxillary overlap and is weakly bifurcate (Figs 2; 6). Its dorsal surface is bounded by small ridges labially and lingually (Fig. 2).

The ventral aspect of the bone is only clearly seen in the counterpart of the Pohl-Perner specimen (Fig. 6). Nine tooth spaces are present, with every second space (starting with the midline tooth) as well as the third space on the left side retaining an ankylosed tooth. A palatal flange is present lingual to the teeth, but distinct vomerine processes are absent. A bifurcated incisive process projects ventrally from the palatal flange. Its anterior margin is rounded, and posteriorly it is bounded on either side by a deep notch of unknown significance.

Comparisons. In lacking anterior premaxillary foramina, "*Saniwa*" *feisti* is similar to the referred premaxilla of *Palaeovaranus cayluxi* (Augé 2005). Smith (2009a: 343-344) noted that these foramina are absent in most Anguidae, and probably in the most recent common ancestor of that clade, as well as *Heloderma*, but are present in *Xenosaurus*, *Shinisaurus* and some *Varanus*. They are present in *Lanthanotus* (Gauthier *et al.* 2012) and *Estesia* Norell, McKenna & Novacek, 1992 (Yi & Norell 2013) but absent in *Ovoo* Norell, Gao & Conrad, 2007 (Norell *et al.* 2007) and *Saniwa ensidens* Leidy, 1870 (Rieppel & Grande 2007).

Georgalis (2017) included the long nasal process in his diagnosis of Palaeovaranidae, following Augé (2005), whereas Hoffstetter (1943: 135) curiously described it as short ("court"). In "*Saniwa*" *feisti*, the nasal process is long, well exceeding the interpreted vomeronasal cupola (see Septomaxilla) but is separated from the anterior end of the frontal in the two specimens in which this can be ascertained. *Varanus* is also characterized by a long nasal process that greatly surpasses the vomeronasal cupola and frequently reaches the frontal (Mertens 1942a), as it does in mosasaurs (Russell 1967) and, it seems, *Proplatynotia* Borsuk-Białynicka, 1984. In other anguimorphs the process is generally much shorter. The nasal process ("internarial bar") has been described as T-shaped in some mosasaurs (Williston 1898; Russell 1967).

A premaxillary tooth count of 9, as in "*Saniwa*" *feisti*, is common in many Anguimorpha (observations summarized in Smith 2009a: 346). Augé (2005) gives a tooth count of 10 for the referred premaxilla of *Palaeovaranus cayluxi*.

Elongate vomerine processes are absent in "*Saniwa*" *feisti*. In contrast, they are present and highly elongate in *Varanus*, greatly exceeding in length the distance between from the anterior tip of the premaxilla to the incisive process, although they articulate along their entire length with the maxilla. They are similarly long in many snakes. They are present also in at least some mosasaurs (e.g. *Clidastes propython* Cope, 1869 ANSP 10193; KTS, pers. obs.), and in *Lanthanotus*, although in the latter taxon they are not as long.

Nasal

Description. The paired nasals are long, narrow rectangular elements (Figs 2; 5). The articulation on the facial process of the maxilla and on the nasal process of the premaxilla is extensive. Posteriorly, where the premaxilla and anteromedian spine of the frontal were not interposed, they contacted each other on the midline. Thus, retracted nares can be ruled out completely. The posterior-most end of the nasal tapers, forming a triangular tab that overlies the subnasal lamina of the frontal between the latter bone's median and anterolateral spines. The medial border of the bone is straight posteriorly, but anteriorly it verges slightly away from the midline where it underlapped the nasal spine of the premaxilla. In the Pohl-Perner specimen it appears that the right nasal possesses a short, anteromedial process that continued along the premaxilla (Fig. 5), which would give the anterior end of the nasal a slightly concave anterior margin. The bone as a whole tapers slightly anteriorly.

Comparisons. The long, rectangular nasals are a distinctive feature of "*Saniwa*" *feisti*, and we can assume they were similarly built in *Palaeovaranus cayluxi*, based on the proportions of surrounding elements (maxilla, frontal, premaxilla). Such nasal bones have otherwise been described in *Eosaniwa* Haubold, 1977 from Geiseltal (Rieppel *et al.* 2007) and *Proplatynotia* from the Cretaceous of Mongolia (Borsuk-Białynicka 1984). In *Eosaniwa* also the bone tapers slightly anteriorly.

The long, tight junction between the nasal and maxillae suggest that the external nares were not retracted, as previously determined for "*Saniwa*" *feisti* (Pregill *et al.* 1986) and, based on isolated bones, for *Palaeovaranus cayluxi* (Hoffstetter 1943).

Septomaxilla

Description. An element preserved to the right of the nasal process of the premaxilla in HLMD-Me 13709 (Fig. 7) is identified as the right septomaxilla. The morphology of the dorsal surface, though unusual for an anguimorph septomaxilla, does not correspond to that of the vomer (see Vomer). Along the medial edge there is a strong, arching, dorsally projecting flange. From the posterior end of the arch the medial edge extends straight backwards. At mid-length on the lateral side is a dorsal bulge, convex in both transverse and sagittal section, which we interpret as covering Jacobson's organ. Between the bulge and the medial ridge runs a longitudinal groove. The anterior process of the bone, as far as it is preserved, appears shorter than the posterior process.

Comparisons. Attempts to digitally segment the bone were unsuccessful. A higher resolution CT scan might make this important endeavor possible.

Assuming the element in question really is the septomaxilla, it is unusual for an anguimorph in possessing a long, posterior extension of the medial flange. In most anguimorphs the bone terminates shortly behind Jacobson's organ (Yi & Norell 2013). Mosasaurs, however, are an exception. A long posterior extension of the septomaxilla has been described in *Plotosaurus bennisoni* (Camp, 1942) and a number of other mosasaurs (Konishi & Caldwell 2007). It may be present as well in *Clidastes propython* ANSP 10193 (KTS, pers. obs.), although because the snout is so long it does not extend as far posteriorly as the prefrontal.

Vomer

Description. The description of the vomer is based principally on the right element in the Pohl-Perner specimen, which is well preserved and exposed (Fig. 6). It is an elongate, strap-like, dentigerous element (Figs 6; 8; see also Fig. 3A).

Fig. 7. — Photograph of skull of *Paranecrosaurus feisti* (Stritzke, 1983) n. comb. HLMD-Me 13709 (holotype) in dorsolateral view. Scale bar: 5 mm.

Just behind the anterior terminus is an embayment of the lateral wall that marks the fenestra vomeronasalis (Rieppel *et al.* 2008). Just behind the fenestra is a rough, slightly projecting, apparently broken region that probably represents the maxillary process (Fig. 8A-C). However, it is unknown whether this process actually articulated with the maxilla or merely extended toward it (as in *Lanthanotus*); there is no clear articulation facet on the maxilla. The lacrimal groove, a marked crescentic depression normally present in squamates along the medial margin of the fenestra vomeronasalis, is poorly developed.

The medial ramus of the palatine branch of cranial nerve VII (palatine nerve) passes along a weak groove on the dorsal surface of the bone anteriorly (Fig. 8A). From that groove, several foramina pass ventrally through the bone, suggesting that the medial ramus gave off several branches onto the ventral surface; from the largest, anteriormost foramen of this series, a groove runs a short distance anteriorly before entering a horizontally trending canal. This series of foramina is broadly set in an elongate longitudinal depression demarcated by a strong ridge medially and a weak one laterally. The ultimate egress of the medial ramus of the palatine nerve is the vomerine foramen near the anterior end of the bone.

The medial margin of the bone is reflected dorsally to form a ridge that supported the nasal septum and paraseptal cartilages (Fig. 8B). The dorsal surface of this ridge appears to be broken, giving the impression of a canal for some neurovascular structure. The posterior end of the vomer appears to veer away from the midline, probably indicating a posteromedial articulation on the palatine, and in the Pohl-Perner specimen two tiny, conical teeth are present on the ventral surface near the tip (Figs 6; 8A).

Comparisons. In its overall strap-like construction, the vomer of "*Saniwa*" *feisti* is similar to that of Varanidae, including extinct *Saniwa ensidens* (see Gilmore 1928), *Heloderma* (Pregill *et al.* 1986) and various taxa from the Cretaceous of Mongolia (Borsuk-Białynicka 1984; Gao & Norell 2000; Norell *et al.* 2007; Yi & Norell 2013). The anterior tip of the vomer of "*Saniwa*" *feisti* is more similar to *Heloderma* in lacking the elongate anterior processes found in Varanidae and *Proplatynotia*.

The vomer of *Varanus* is characterized by a longitudinal, parasagittal channel (Gauthier *et al.* 2012, char. 222/3) formed by a ventrally reflected medial margin and a robust lateral ridge (the medial margin of the fenestra vomeronasalis). A similar channel is found on the ventral surface of the vomer of *Saniwa ensidens* USNM 2185, although it is not as prominent because the medial margin is only weakly reflected (KTS, pers. obs.). The vomer of "*Saniwa*" *feisti* is similar to that of *Varanus* (in contrast to *Heloderma* and *Lanthanotus*) in having a long straight lateral ridge on the anterior end, but differs from it in lacking the medial ridge.

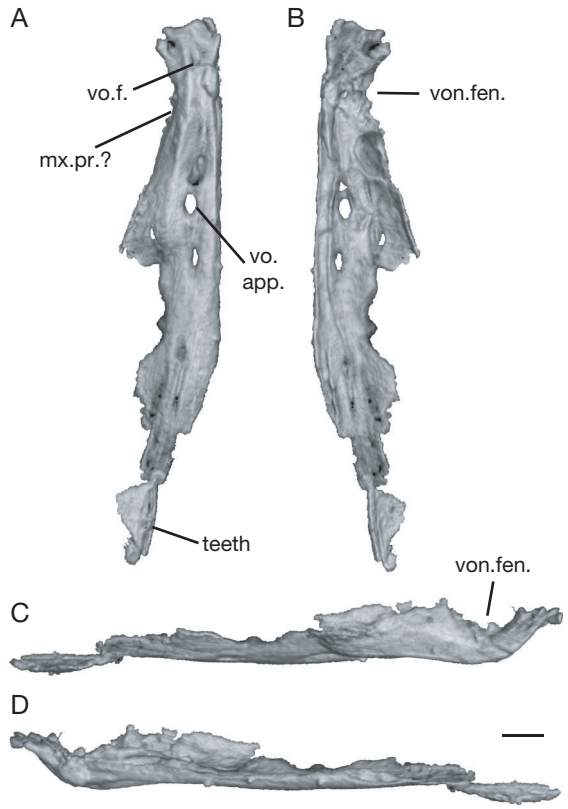

Fig. 8. — The vomer: **A**-**D**, partial right vomer segmented from CT scan of *Paranecrosaurus feisti* (Stritzke, 1983) n. comb. (Perner specimen) in ventral, dorsal, lateral, and medial views, respectively. Abbreviations: **mx.pr.**, maxillary process; **vo.ap.**, vomerine aperture; **vo.f.**, vomerine foramen; **von.fen.**, vomeronasal fenestra. Scale bar: 1 mm.

The vomer of "*Saniwa*" *feisti* is also like that of *Varanus* and extinct *Saniwa ensidens* USNM 2185 (KTS, pers. obs.) in having a series of ventral foramina. Similar foramina are found in *Heloderma*, but they are more laterally disposed. Unlike in *Varanus* and *Lanthanotus* (Gauthier *et al.* 2012, char. 220/1), the nerve that pierces them does not for the most part travel along a dorsal channel, except perhaps in the immediate vicinity of the lateral maxillary process. In this respect case it is more like *Heloderma*.

Vomerine teeth, as in "*Saniwa*" *feisti*, are rare in extant anguimorphs. They are sometimes present, and in the same position, only in *Pseudopus apodus* (Meszoely 1970). However, they were well developed in *Eosaniwa* (Rieppel *et al.* 2007). The relevant areas are poorly exposed or, apparently, broken in *Saniwa ensidens* USNM 2185 (KTS, pers. obs.).

Palatine

Description. It is the right element of the Pohl-Perner specimen that preserves the most anatomical detail (Figs 6; 9). The choanal groove is located at the anterior end between the maxillary and vomerine processes (Fig. 9A). Its margins are not distinct. The vomerine process is thick, at least at its base, and it extends at an angle of about 45° to the main body of the bone (Fig. 9C). Its tip is not preserved in any specimen.

The lateral articulation with the maxilla is best seen in SMF-ME 10954. The maxillary process of the palatine overlies the palatal shelf of the maxilla (Figs 3A, B; 4B), and its anterior end is at the 9th tooth position from the rear. The precise posterior extent is difficult to establish, but bone tissue not pertaining to the jugal and bearing a ridge that appears to be continuous with the maxillary process more anteriorly suggest it terminates below the 5th tooth from the rear (Fig. 3A, left side). Accordingly, it would extend over 5 tooth spaces. The ectopterygoid would have approached (but probably not touched) the palatine laterally.

The ventral surface bears an elongate, oval tooth patch (Fig. 9A) measuring 4.6 × 1.4 mm in maximum dimensions in the Pohl-Perner specimen. The teeth are short and conical and slightly posteriorly recurved. Much smaller tubercles interspersed with the emplaced teeth are conceivably incompletely formed replacement teeth, but this is difficult to test.

The posterior end of the palatine evinces a notch for the pterygoid and also has a short lateral process that would have extended along the lateral edge of the pterygoid (Fig. 9A, B). Posteromedially trending striations medial to the posterior half of the tooth patch (Fig. 6A) suggest a fibrous articulation with an anteromedial palatine process of the pterygoid, which, however, is not clearly preserved in any specimen.

Comparisons. The palatine articulation on the maxilla in "*Saniwa*" *feisti* is intermediate between the primitive condition exemplified by Anguidae, *Xenosaurus* and *Shinisaurus* and the derived condition in *Heloderma* and Varanidae (including *Saniwa ensidens* [Gilmore 1928]), in which the palatine is shifted so far posteriorly that it overlaps with the ectopterygoid (Pregill *et al.* 1986). Many mosasaurs also show the derived condition (Williston 1898). In this respect "*Saniwa*" *feisti* is probably similar to *Eosaniwa*, given the preserved position of the palatine relative to the posterior end of the maxilla (Rieppel *et al.* 2007). This character in "*Saniwa*" *feisti* is interesting insofar as it demonstrates that the backward (relative) shift of the palatine on the maxilla is not merely related to the foreshortening of the maxilla seen in *Heloderma* and Varanidae (Pregill *et al.* 1986) or lengthening of the snout as in *Eosaniwa*.

Palatine teeth are present, among extant anguimorphs, in Anguinae except for *Anguis* (Meszoely 1970), in *Lanthanotus* and in some *Heloderma horridum* (McDowell & Bogert 1954) but are absent in other taxa. However, they were previously more widespread, as shown by their occurrence in various Late Cretaceous taxa from Mongolia (Borsuk-Białynicka 1984; Gao & Norell 2000; Norell *et al.* 2007), *Eosaniwa* (Estes 1983; Rieppel *et al.* 2007) as well as extinct glyptosaurine anguids (Meszoely 1970; Sullivan 1979, 1986). More specifically, many of these taxa share the patch-like arrangement of the palatine teeth seen, albeit narrowly, in "*Saniwa*" *feisti*. A few palatine teeth also appear to be present in *Saniwa ensidens* USNM 2185 (KTS, pers. obs.; contra Gilmore 1922). These data show that palatine teeth were once widespread in Anguimorpha.

Maxilla

Description. The maxilla, bearing the remainder of the marginal teeth in the upper jaw, is a long element with a broad facial process (Figs 2; 5; 7; 10). On the left side of SMF-ME 10954, about 21 teeth or tooth positions are seen superficially; on the right side, there are apparently 23 teeth (Fig. 2). On the left side of the Pohl-Perner specimen (Fig. 6) there are around 22 tooth positions. The tooth count in SMF-ME A258 is apparently also 22 (Appendix 5). Thus, the maxilla holds about 22 teeth, and there is no indication of an ontogenetic increase in tooth count. No significant anterior or posterior portion of the maxilla lacks teeth.

The facial process of the maxilla curves upward, strongly marking the fenestra exonarina, which was located near the anterior end of the snout (Figs 2; 5; 7; 10). The narial fossa is nowhere well exposed. The CT-scan shows that the anterior alveolar foramen of the maxilla is located medial to the crista transversalis (Fig. 3C). The ventral border of the maxilla forms a dorsoventrally rounded, laterally projecting ridge in SMF-ME 10954 (Fig. 2). A similar, but weaker, ridge is present in the Pohl-Perner specimen (Fig. 5), but is absent in the holotype, except at the posterior end of the bone (Fig. 7).

There is a large number of labial foramina in all specimens, and these are divided into a discrete lower row and an elongate upper field concentrated in the lower half of the facial process. The foramina of the lower row, in the typical position for labial foramina, are larger. In HLMD-Me 13709 (left maxilla), there are about 8 foramina in the lower row, with the anteriormost one and posterior-most three somewhat larger than the others; a precise count cannot be given for the upper field (Fig. 7). In the Pohl-Perner specimen, there are 7 foramina in the lower row on the left side (whereby the first "foramen" is really a tight cluster of 3 individual openings) and 9 on the right side (of which the anteriormost and posterior-most are larger than the others); a precise number cannot be given for the upper field (Fig. 5). In SMF-ME 10954 there are 9 foramina in the lower row on the left side and 10 on the right side, whereby on both sides the posterior half of the foramina are larger than the anterior half; the upper field consists of about 4 foramina on the left and right (Fig. 2). The anterior foramina of the lower row are frequently accompanied by anteriorly trending grooves, whereas the posterior foramina are directed laterally; in the upper field, posteriorly directed grooves are more common. In the Pohl-Perner specimen, the foramina of the upper field are located between the osteoderms near the inferred scale boundaries (see Free osteoderms and scalation). CT scans show that the superior alveolar canal, which conveys the maxillary artery and superior alveolar nerve through the maxilla, giving off branches that pass through the labial foramina, is located at a dorsoventral level between the lower row and upper field of labial foramina in SMF-ME 10954. The canal opens posteriorly (superior alveolar foramen), at the level of the anterior margin of the orbit (Fig. 10B).

Dorsally, the facial process is strongly medially folded in SMF-ME 10954 and HLMD-Me 13709, forming a strong, oblique canthal ridge that demarcates an anterodorsally facing surface from the lateral surface of the facial process (Figs 2; 7). The ridge grows sharper posterodorsally (Fig. 7). It is less strongly expressed in SMNK-Me 1124 (Fig. 10). The anterodorsal surface is slightly depressed and bears a couple of small, posteriorly directed foramina close to the canthal ridge in SMF-ME 10954 (Fig. 2) and HLMD-Me 13709 (Fig. 7), whereas in SMNK-Me 1124 this surface is slightly convex (Fig. 10A); this may represent ontogenetic or more likely individual variation. In HLMD-Me 13709 there is a deep facet below the posterodorsal corner that is probably for the prefrontal (Fig. 7), but it seems the (incomplete) facet is weaker in SMNK-Me 1124 (Fig. 10A). The long, tapering posterior process is bordered dorsally by the jugal and lacrimal. Its dorsal edge is sharp posteriorly, but it was partly overlapped by the jugal anteriorly, forming a shallow, dorsolaterally facing facet (Fig. 2, right side; Fig. 5, left side).

The anterior end of the palatal shelf is dorsoventrally thin. Anteriorly it has a small medial projection with a dorsal facet for articulation with the vomer (Fig. 3A). The remaining thin portion of the palatal shelf might have been overlapped by the vomer (see Vomer). The remainder of the palatal shelf as far as the palatine articulation is thicker and rounded. A low nasolacrimal ridge, or "oblique ridge" of (Meszoely 1970), roughly parallel to the canthal ridge, extends anteroventrally along the medial surface of the facial process (Fig. 10B). It forms the dorsal boundary of the lacrimal duct, which is marked by the groove extending anteriorly and slightly ventrally from the lacrimal embayment. The palatine articulation

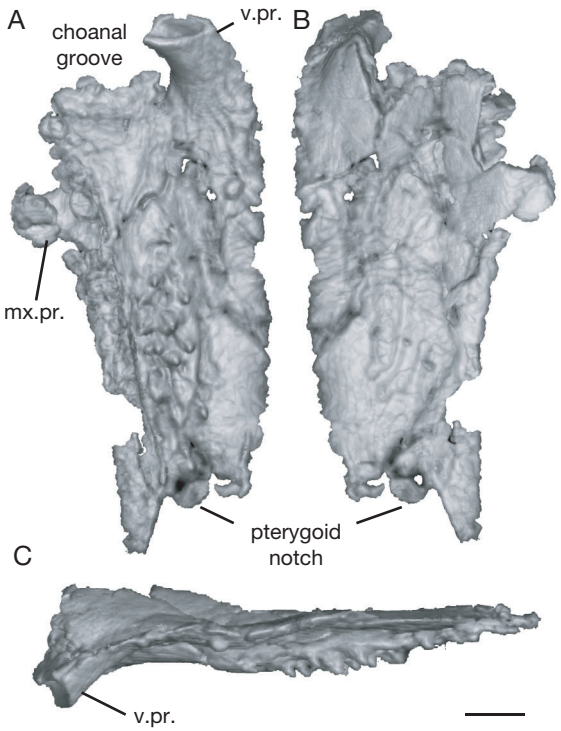

Fig. 9. — The palatine: **A**-**C**, partial right palatine segmented from CT scan of *Paranecrosaurus feisti* (Stritzke, 1983) n. comb. (Perner specimen) in ventral, dorsal, and medial views, respectively. Abbreviations: **mx.pr.**, maxillary process; **v.pr.**, vomerine process. Scale bar: 1 mm.

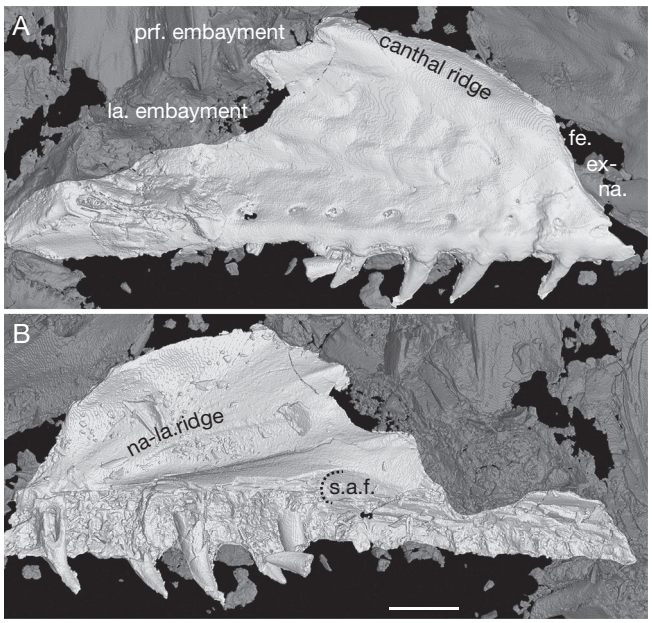

Fig. 10. — The maxilla: **A**, **B**, CT reconstruction of right maxilla of *Paranecrosaurus feisti* (Stritzke, 1983) n. comb. SMNK-Me 1124 (paratype) in lateral and medial views, respectively. Abbreviations: **fe.ex-na.**, fenestra exonarina; **la.embayment**, lacrimal embayment; **na-la.ridge**, nasolacrimal ridge; **prf.embayment**, prefrontal embayment; **s.a.f.**, superior alveolar foramen. Scale bar: 2 mm.

is located well behind the mid-point of the maxilla (Fig. 3B). Behind the palatine articulation the palatal edge is sharp and no longer projects medially beyond the tooth bases. The anterolateral process of the ectopterygoid (see Ectopterygoid) and the palatine therefore restricted the contribution of the maxilla to the suborbital fenestra, although it is was probably not totally excluded.

Comparisons. Given the shape of the facial process of the maxilla, the snout of "*Saniwa*" *feisti* would probably have had a moderately low profile. The anterior margin of the facial process clearly marks the posterior margin of the external nares. However, the snout of *Palaeovaranus cayluxi* was distinctly lower due to the lower angle of the anterior margin (see Zittel 1887-1890; de Fejérváry 1935; Georgalis 2017). The canthal ridge of both species (maxilla unknown in *Palaeovaranus* sp. from Quercy) would also have given the box-shaped cross-section. Indeed, the sharp medial fold giving rise to the canthal ridge is one of the most distinctive features of Palaeovaranidae (Georgalis *et al.* 2021). In contrast to Hoffstetter (1943: 134), we believe that the anterodorsally facing surface medial to the canthal crest did not support the nasals in *P. cayluxi*, any more than they do in "*Saniwa*" *feisti*. The fact that the anterodorsal surface rises dorsally at its medial edge in *P. cayluxi* suggests that the nasals may have been arched between the canthal crests, as seen in some *Anolis* Daudin, 1802. This arching was not obviously present in "*Saniwa*" *feisti*.

The nasolacrimal duct of squamates primitively arises as two separate ducts, each with its own opening (or "punctum") at the base of the orbit (Bellairs & Boyd 1947). The two ducts generally fuse, at least in Iguania, before passing through the lacrimal foramen between the lacrimal and prefrontal and entering the bony nasal capsule, at which point they run obliquely downward and open at the junction of the choanal groove and the duct of the vomeronasal organ (Hallermann 1994). The course of the nasolacrimal duct, as indicated by the sulcus in both "*Saniwa*" *feisti* and *Palaeovaranus cayluxi* (de Fejérváry 1935; Georgalis *et al.* 2021), is consistent with this primitive course. (On the number of ducts, see Lacrimal). The course of the nasolacrimal duct appears to be flatter in *P. cayluxi*, consistent with the generally lower skull profile. Conceivably the elongate depression found dorsal to the nasolacrimal ridge in specimens of *P. cayluxi* (e.g. MNHN SNB 1007; NHMW 2019/0048/0002, described by Georgalis *et al.* (Georgalis *et al.* 2021) housed part of the recessus lateralis and its surrounding paranasal cartilage (cf. Bernstein 1999).

The nasolacrimal ridge in *Paranecrosaurus feisti* n. comb. is thus formed dorsal to the lacrimal duct. In this sense it is similar to *Heloderma suspectum* Cope, 1869, where the ridge lies dorsal to the ductus nasolacrimalis and ventral to the lateral nasal gland and lateral recess (Bernstein 1999: fig. 6C, D). In the latter species a lateral margin of the parietotectal cartilage is in line with the ridge and extends within a short distance of it (Bernstein 1999: fig. 6D). In contrast, in a section of the scincid *Scelotes bipes* Linnaeus, 1766 the ductus nasolacrimalis is located dorsal to a medial projection of the facial process of the maxilla (Malan 1946: fig. 39) that presumably represents the nasolacrimal ridge. Thus, the ridge may not be homologous in all squamates.

Like *Palaeovaranus cayluxi* (Georgalis *et al.* 2021), "*Saniwa*" *feisti* appears to possess a deep facet on the medial surface of the posterodorsal corner of the facial process of the maxilla, although the anterior-most part of the facet cannot currently be studied in "*Saniwa*" *feisti*. Such a deep facet was not observed in other anguimorphs in which the relevant area could be examined. The medial surface of the facial process in "*Saniwa*" *feisti*, however, appears to lack the distinct facet for the nasal seen in *P. cayluxi* (Georgalis *et al.* 2021).

One of the striking features of the maxilla of "*Saniwa*" *feisti* is the large number of labial foramina, a median value of 9 for all countable maxillae. It is difficult to make detailed comparisons with *Palaeovaranus cayluxi* because figured maxillae are incomplete, although it is noteworthy that the fragment represented by NHMW 2019/0048/0002 alone has 5 (Georgalis *et al.* 2021: fig. 42A). In this respect "*Saniwa*" *feisti* is similar to *Varanus* (median of 8-9 foramina among examined species, depending on details of calculation), *Xenosaurus* (10.5) and *Heloderma* (8). The count is very high (around 14) in *Eosaniwa* as well (Rieppel *et al.* 2007: fig. 2.1). Among examined anguimorphs, these taxa had by far the highest counts.

A location of the anterior alveolar foramen medial to the crista transversalis is seen in both "*Saniwa*" *feisti* and *Palaeovaranus cayluxi* (Georgalis *et al.* 2021) as well as certain other anguimorph taxa (Smith & Gauthier 2013). This is a derived feature by comparison with lizard outgroups.

The facet for articulation of the vomer, as we interpret it in "*Saniwa*" *feisti*, is also present in *Palaeovaranus cayluxi* (Georgalis *et al.* 2021: fig. 42B) and numerous other anguimorphs.

Tooth count in "*Saniwa*" *feisti*, at >20, is high. Although the interpretation of ancestral maxillary tooth count in Anguimorpha depends on tree topology, Bhullar (Bhullar 2011) found values well below 20 in both hypotheses of broad-scale tree topology he examined. Indeed, in no taxon he examined did tooth count rise as high as 20. Counts well below 20 are also seen in Late Cretaceous anguimorphs from the Mongolia (Borsuk-Białynicka 1984; Gao & Norell 2000; Norell *et al.* 2007) and in primitive mosasauroids like *Russellosaurus* Polcyn & Bell, 2005. Maxillary tooth count is unknown in *Palaeovaranus cayluxi* and *Pa. giganteus*, but can likely be determined with CT scans in the latter. *Eosaniwa* shows an even higher tooth count of 38 (Rieppel *et al.* 2007). These observations raise the prospect that a high tooth count could be a synapomorphy of Palaeovaranidae and *Eosaniwa*. It is notable that *Provaranosaurus acutus* from the Paleocene of Wyoming also has >20 teeth in the maxilla (Gilmore 1942); the number is unknown but probably lower in *Pr. fatuus* Smith and Gauthier, 2013.

Prefrontal

Description. The prefrontal borders the orbit anteriorly. It is overlapped laterally by the maxilla, lacrimal and palpebral, the last of which is received by a small facet (Fig. 5A, right side). A well-developed canthal ridge is present that was continuous with that on the facial process of the maxilla and is laterally convex at the anterior corner of the orbit (Figs 2; 5; 7). Medial to the ridge, the dorsal surface is slightly depressed. The tapering anterior end of the bone inserted beneath the facial process of the maxilla, where it is indicated by the bulge it creates in SMF-ME 10954 (Fig. 2). The medial edge of the anterior end is exposed in HLMD-Me 13709 (Fig. 7), and because it extends anterior to the tip of the frontal, it is likely that contact between prefrontal and nasal excluded the maxilla from contact with the frontal. The long, narrow posterior process extends along the orbital margin of the frontal. The medial surface of the posterior process is also exposed in HLMD-Me 13709 (Fig. 7). It shows that the process is continued posteriorly behind the exposed dorsal edge by a tongue that inserted deeply beneath the frontal table and extended to mid-orbit (see also facet on frontal in Appendix 5C). The tongue is less well developed in SMF-ME 10954 (Fig. 2). The anterior portion of the prefrontal is hollowed out ventrally by the cartilaginous nasal capsule (Fig. 3A, left side; Fig. 6, right side). There is also a robust ventral process, with a rugose terminus, that would have inserted on the palatine or maxilla (Fig. 6).

Comparisons. The canthal ridge on the prefrontal of "*Saniwa*" *feisti* continues anteriorly beyond the palpebral articulation and is continuous with the ridge on the nasal process of the maxilla, a combination of feature not seen in extant anguimorphs. *Shinisaurus* comes perhaps closest, insofar as a canthal ridge is present, although in that taxon it is formed at the longitudinal suture between maxilla and prefrontal and is limited in extent, because the facial process of the maxilla is so short; in fact, the prefrontal achieves limited exposure at the posterior margin of the fenestra exonarina, a feature otherwise seen in *Heloderma* and Varanidae among extant anguimorphs. That exposure does not occur in "*Saniwa*" *feisti*. A similar canthal ridge is seen, however, in some mosasaurs, like *Russellosaurus* (Polcyn & Bell 2005: fig. 3J, P) and *Platecarpus ictericus* (Cope, 1871) (Russell 1967).

A very deep sulcus for the frontal process of the prefrontal, as in "*Saniwa*" *feisti*, is developed below the frontal table in *Shinisaurus*, *Elgaria multicarinata* Blainville, 1835 and *Pseudopus* Merrem, 1820, among examined anguimorphs. In *Xenosaurus grandis* (Gray, 1856), the sulcus is deep, but its posterior-most extent is visible dorsally, whereas in *X. platyceps* King & Thompson, 1968 the sulcus is shallow.

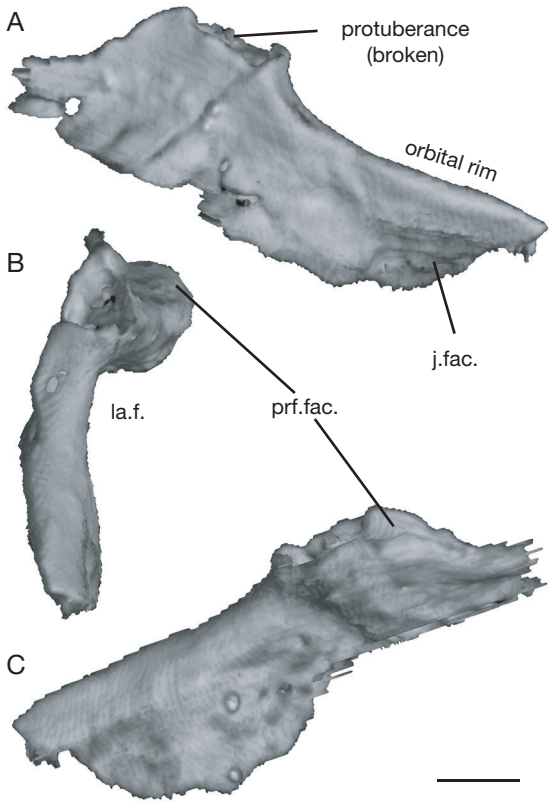

Fig. 11. — The lacrimal: **A**-**C**, partial left lacrimal segmented from CT scan of *Paranecrosaurus feisti* (Stritzke, 1983) n. comb. HLMD-Me 13709 (holotype) in lateral, dorsal, and medial views, respectively. Abbreviations: **j.fac.**, jugal facet; **la.f.**, lacrimal foramen. Scale bar: 1 mm.

Lacrimal

Description. The lacrimal is sutured dorsally to the prefrontal, anteriorly to the facial process of the maxilla, and posteroventrally to the jugal, forming part of the orbital rim. The lateral exposure of its suture to the jugal is an oblique line running anteroventrally (Figs 2; 5; 7). The bone attains considerable lateral exposure. The left lacrimal of SMF-ME 10954 (Fig. 2), both lacrimals of the Pohl-Perner specimen (Fig. 5), and probably the left lacrimal of HLMD-Me 13709 (Fig. 7) show a triangular, mediolaterally compressed eminence or boss that projected into the orbit. At least one small foramen pierces the lateral surface of the left lacrimal in these specimens.

The digitally segmented left lacrimal of HLMD-Me 13709 (Fig. 11) shows the orbital margin to be thicker than the ventral portion. In posterodorsal view the bone is comma-shaped, with a single embayment for the lacrimal duct(s) that did not wrap around the duct(s) ventrally (Fig. 11B). A shelf bounds the lacrimal duct(s) dorsally and additionally features a facet for articulation with the prefrontal (Fig. 11B, C).

Comparisons. The nasolacrimal duct in squamates primitively arises as a fusion of two separate ducts at the point where it enters the osseous nasal capsule (see Maxilla). Varanidae is unique among squamates in that the two ducts are separate throughout their length (Bellairs 1949). Curiously, in *Varanus* the larger duct that still runs between the prefrontal and lacrimal is short and wide and opens into the choanal groove posteriorly. In contrast, the smaller duct that pierces only the lacrimal (a derived condition) opens in the primitive position near the junction of the choanal groove and the duct of Jacobson's organ. The disposition of the foramina in *Ovoo* is like in *Varanus* (Norell *et al.* 2007). More curiously still, in *Saniwa ensidens* USNM 2185 (Gilmore 1922; KTS pers. obs.) *both* lacrimal foramina apparently pierce only the lacrimal, whereas in *Lanthanotus* both are located at the lacrimal-prefrontal suture (Rieppel 1980b), suggesting a certain evolutionary lability. In any case, two lacrimal foramina are clearly a synapomorphy of Varanidae (Pregill *et al.* 1986). The lacrimal foramen in "*Saniwa*" *feisti* is of the primitive, single kind; there is no evidence from osteology that the two ducts were separate within the osseous nasal capsule.

An eminence or boss like the one projecting into the orbit in "*Saniwa*" *feisti* is also seen in many *Varanus* (see Mertens 1942a; Rieppel 1980b) and *Saniwa ensidens* (Gilmore 1922; Rieppel & Grande 2007) and possibly some Late Cretaceous anguimorphs from Mongolia (e.g. *Proplatynotia*). Here, it is manifestly an elaboration of the orbital rim. A boss is absent, however, in *Heloderma* (Rieppel 1980b) and other Cretaceous Mongolian anguimorphs (Borsuk-Białynicka 1984) like *Gobiderma*. There is a weakly projecting (i.e., convex) structure of uncertain homology in *Lanthanotus* (KTS pers. obs.). The boss was illustrated incidentally by Bellairs (1949: figs 5F; 6) in *Varanus bengalensis* (Daudin, 1802), but its significance is obscure. Perhaps an explanation is to be sought in the conjunctiva.

Frontal

Description. The frontal is azygous, but anteriorly in all specimens a short median cleft indicates that fusion had not proceeded to completion (Figs 2; 5; Appendix 5). The frontal is broad posteriorly, where it contacts the parietal, and narrows between the orbits. The ratio of minimum frontal width to frontal length is 3.6 mm / 15.7 mm = 0.23 in SMF-ME 10954, 0.22 in HLMD-Me 13709, as much as 0.29 in the Pohl-Perner specimen, and 0.24 in SMNK-Me 1124. The ratio of maximum frontal width to frontal length is 9.9 mm / 15.7 mm = 0.63 in SMF-ME 10954 and as much as 0.69 in the Pohl-Perner specimen.

The frontal is arched anteroposteriorly. The orbital margins of the bone are slightly upturned, especially in the Pohl-Perner specimen and HLMD-Me 13709 (Figs 2; 5; 7), but very little in SMNK-Me 1124 (Appendix 5). The frontal is slightly restricted where the frontal is sutured to the prefrontals. The dorsal surface in SMF-ME 10954 is covered by eminences that probably are mere rugosities corresponding to epidermal scales (see Free osteoderms and scalation). In the larger specimens, apparently fused osteoderms are found along the entire dorsal surface between the orbital margins, and in the larger Pohl-Perner specimen rugosities are developed along the orbital margin, where unfused osteoderms (which have mostly slid off the lateral edge) attached (Fig. 5).

The anterior margin of the bone is triradiate, with a median spine and anterolateral spines. The subnasal lamina is partly exposed on the right side of SMF-ME 10954 (Fig. 2). On the ventral surface, there is a bilateral pair of excavations, probably for the olfactory chamber (see Bellairs 1949). The posterolateral corners of the frontal are sharp and are not as wide as the anterolateral corners of the parietal (Fig. 2). The frontal does not participate in the rounded, lateral-most corner of the skull roof, which is formed entirely by the parietal (see Parietal). The frontoparietal suture runs anterior to this corner, such that the postfrontal contact on the frontal is small. The frontoparietal suture is relatively straight, with no major curvature and only minor interdigitations in dorsal view. However, the Pohl-Perner specimen and the CT reconstruction of SMF-ME 10954 reveal that a small shelf of the frontal underlapped the parietal at the corner (Fig. 6).

On the ventral surface, the cristae cranii follow the margins of the orbits, approaching one another closely at mid-orbit and then diverging once again anteriorly (Figs 2B; 6). They are asymmetrical in cross-section at mid-orbit, the sharp apex directed more medially than ventrally. They are deeply incised by the tongue-like frontal process of the prefrontal (Appendix 5). They increase in height anteriorly and reach a maximum at the level of the ventral process of the prefrontal, i.e., at their anterior end. Anterior to the maximum, they decay abruptly. In the Pohl-Perner specimen (Fig. 6) and SMNK-Me 1124 (Appendix 5) the ventral surface is excavated bilaterally to roof the nasal capsule.

Comparisons. One of the noteworthy aspects of the frontal of "*Saniwa*" *feisti* is its narrowness, suggesting a laterally compressed head, which was recognized by McDowell & Bogert (1954) as a distinctive feature of *Shinisaurus*. The ratio of interorbital width to frontal length in "*Saniwa*" *feisti*, by comparison with *Palaeovaranus giganteus* (*c.* 0.32 in GMH 4139) and the large *Pa. cayluxi* (0.27, based on Augé 2005: fig. 189), is low. McDowell & Bogert (1954) suggested there may be an ontogenetic component to frontal constriction, with smaller individuals showing more constriction (a contention finding some corroboration in these data on "*Saniwa*" *feisti*), but they nevertheless thought Xenosauridae to have especially constricted frontals. Smith & Gauthier (2013) quantified these statements on frontal proportions, noting that in *Xenosaurus*, *Shinisaurus*, and *Provaranosaurus fatuus*

the ratio is ≤0.20, and in *Bahndwivici* it is 0.22. *Palaeovaranus* is most comparable to Gerrhonotinae (ratio *c.* 0.25), which also show constricted frontals (McDowell & Bogert 1954), whereas other anguids and *Lanthanotus* show a ratio of ≥0.40 (Smith & Gauthier 2013). *Saniwa ensidens* described by Rieppel and Grande (Rieppel & Grande 2007) shows a ratio of *c.* 0.23. Notably, Smith & Gauthier (2013) also used the narrowness of the frontals referred to *Pr. fatuus* to argue that it is related to *Shinisaurus*; if Palaeovaranidae also have a narrow, compressed skull, then this character would equally support a relationship of *Pr. fatuus* with Palaeovaranidae, as previously supposed (Estes 1983).

The frontal appears to have a weak hourglass shape in smaller specimens of "*Saniwa*" *feisti*, but it is essentially parallel-sided in larger specimens (Appendix 5) and in *Palaeovaranus cayluxi* (Augé 2005), as it is in *Eosaniwa* (Rieppel *et al.* 2007).

The frontal of *Palaeovaranus giganteus* is quite distinct from that of "*Saniwa*" *feisti* and later *Palaeovaranus*. It is covered with relatively broad, apically flat, rugose patches that appear to be fused osteoderms (KTS, pers. obs.). Although the patches in general probably corresponded to epidermal scales, to judge by the sulci developed between them, some of the smaller patches could have been enveloped under a single scale. These osteoderms are much broader and flatter than in "*Saniwa*" *feisti* and *Palaeovaranus* sp. from Quercy and presumably represent the primitive condition. CT reconstructions of *Eosaniwa* demonstrate the presence of an osteodermal crust (Rieppel *et al.* 2007), but the details of scale boundaries cannot be made out unequivocally.

Although the exact depth of the descending processes, or cristae cranii frontalis (de Fejérváry 1935), is unclear, the subolfactory process seen, for instance, in SMF-ME 10954 implies that they were better developed than in *Xenosaurus* or *Shinisaurus*. However, they were not so highly developed that they wrap beneath the olfactory lobes to contact each other, as in *Heloderma* and Varanidae (Pregill *et al.* 1986).

The frontal of *Eosaniwa* is paired (Rieppel *et al.* 2007). That of *Palaeovaranus giganteus*, however, is completely fused (contra Haubold 1977); Haubold (1977) and Estes (1983) did not recognize that the right lateral corner of the frontal in GMH 4139 is broken. Among Anguimorpha, fused frontals otherwise occur in *Xenosaurus*, *Pan-Shinisaurus* (McDowell & Bogert 1954), and Gerrhonotinae (Meszoely 1970) as well as in Mosasauria (Williston 1898; Russell 1967). Gauthier (1982) and Smith & Gauthier (2013) have documented that frontal fusion develops earlier in ontogeny in extant *Shinisaurus* than in species along its stem. Frontal fusion occurred relatively early in "*Saniwa*" *feisti* as well.

Palpebral

Description. The palpebral is a dorsoventrally thin, triradiate element, with a long, slightly curved posterolateral process that extended well past the midpoint of the orbit and a deeply concave posterior margin (Figs 2; 5; 7). The posterolateral process extends over the orbit and would presumably have been continuous with the canthal ridge of the maxilla and prefrontal anteriorly and the supratemporal arch posteriorly; the seeming medial curvature of the posterolateral process of the left element in SMF-ME 10954 is slightly exaggerated by displacement of its broken tip. A shorter posteromedial process is also present. The dorsal surface is smooth in SMF-ME 10954, and the only irregularities appear to be artifactual. In larger specimens, the palpebral is covered with small osteoderms that do not seem to be fused.

Comparisons. The palpebral of "*Saniwa*" *feisti* is similar to that of *Eosaniwa* (Rieppel *et al.* 2007), *Shinisaurus* (Conrad 2004), *Saniwa ensidens* (Gilmore 1922; Rieppel & Grande 2007), and *Varanus* (Mertens 1942a). In having a long, posterolateral process it is also reminiscent of the element identified as a palpebral in some mosasaurs (Camp 1942; Russell 1967). The posteromedial process in *Saniwa* and *Shinisaurus* appears slightly shorter and blunter than in "*Saniwa*" *feisti*, contributing to the less prominent concavity of the bone's posterior margin.

A palpebral is lacking in *Heloderma* (Gauthier *et al.* 2012), but this element was shown to be present, if highly reduced, in *Lanthanotus* (Maisano *et al.* 2002). In Anguidae and *Xenosaurus* the palpebral has the form of an isosceles triangle that is either broader (*Xenosaurus*) or narrower (Anguidae) but lacks a prominent posterolateral process and posterior concavity (Bhullar 2011).

BASAL UNIT

Pterygoid

Description. The element is best preserved in the Pohl-Perner specimen (Fig. 6). It possesses three main processes: an anterior palatine process, a lateral transverse process, and a posterior quadrate process. Extending onto the palatine process is an elongate, oval, nearly lenticular tooth patch measuring 2.3 × 6.9 mm in maximum dimensions on the right element in the Pohl-Perner specimen. The palatine process is poorly preserved in all specimens, so that the inferences derived from the palatine above are the best available data about its form. The left element of the Pohl-Perner specimen displays a small fragment of the edentulous anteromedial part of the palatine process, which is otherwise overlain by the mandible; that fragment gives a minimum length of the palatine process in the Pohl-Perner specimen of 8.1 mm, measured to the anterior base of the basipterygoid flange. The size and shape of the pyriform space cannot be determined.

Separated by a groove from the palatine process is the stout transverse process. It bears a strong, straight ventral ridge for the origin of m. pterygomandibularis (Oelrich 1956) and extends straight anterolaterally and bears on the anterior face of its distal end an anteriorly convex facet for the ectopterygoid (Fig. 6). Based on what may be an impression in the Pohl-Perner specimen (Fig. 6A, right element), it is probable that just dorsal to this facet there is an anterolateral extension of the transverse process that contributed to a firmer suture between the two elements. Between the two processes the ventral surface of the bone forms a fossa. At their junction, on the medial side of the bone, is a triangular, posteromedially directed flange that underlapped the basipterygoid process of the parabasisphenoid.

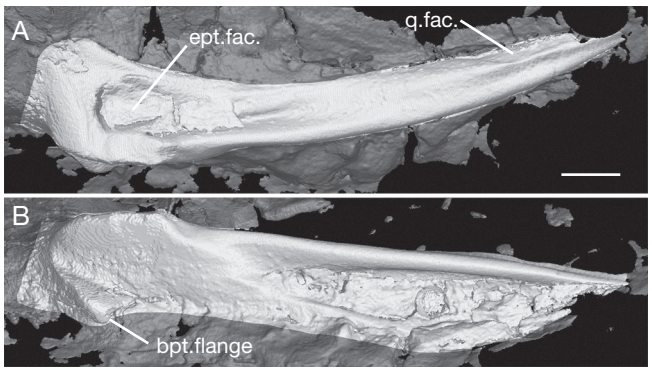

FIG. 12. — The pterygoid: **A**, **B**, CT reconstruction of quadrate process of right pterygoid of *Paranecrosaurus feisti* (Stritzke, 1983) n. comb. SMNK-Me 1124 (paratype) in dorsal and medial views, respectively. Abbreviations: **bpt.flange**, flange for basipterygoid process of parabasisphenoid; **ept.fac.**, epipterygoid facet; **q.fac.**, quadrate facet. Scale bar: 2 mm.

Dorsally at the base of the quadrate ramus is a deep facet for the epipterygoid (Fig. 12A), the center of which is located just behind the apex of the basipterygoid flange. The facet is continued posteriorly by a shallowing groove. The base of the quadrate process is thick and triangular in cross-section. Posteriorly, however, it becomes a vertically oriented blade with a flatter lateral surface (Figs 6A; 12A) and a deeply grooved medial surface (Fig. 12B). On the lateral face of the distal end of the quadrate process is a distinct facet for the quadrate (Fig. 12A). The quadrate process is longer than the palatine process (Fig. 6), about 10.5-10.7 mm in the Pohl-Perner specimen, measured to the posterior base of the basipterygoid flange.

Comparisons. Assuming the dorsal portion of the ectopterygoid process in "*Saniwa*" *feisti* did continue anterolaterally as a spine, the ectopterygoid facet may not have been markedly different from the same element in *Varanus* or many other anguimorphs.

Pterygoid teeth are more common in Anguimorpha than palatine teeth. They are also present in *Saniwa ensidens* USNM 2185 (contra Gilmore 1922). However, as on the palatine, it is noteworthy that not only were such teeth present, but they were also arranged in a patch. Such an arrangement is seen in extant *Pseudopus* (von Fejérváry-Lángh 1923; Klembara *et al.* 2010) but no other living anguimorph. Once again as with the palatine, tooth patches were once more common in Anguimorpha, being known from glyptosaurine anguids (Meszoely 1970; Sullivan 1979, 1986) and various late Cretaceous taxa from Mongolia (Borsuk-Białynicka 1984).

The deep, longitudinal, medial sulcus on the quadrate ramus is common in Anguimorpha but can show considerable interspecific variation even in closely related taxa, like *Varanus* spp. It should be noted that in "*Saniwa*" *feisti* it extends to the distal end of the ramus. Furthermore, a quadrate facet on the lateral face of the distal end occurs with some frequency in *Varanus*, *Heloderma*, and even *Lanthanotus* (KTS, pers. obs.). Pregill *et al.* (1986) noted the distinctive shape of the ventral (mandibular) condyle of the quadrate in *Heloderma* and Varanidae, but it is not clear that one can necessarily infer the one from the presence of the other.

A groove extending posteriorly from the epipterygoid fossa, as in "*Saniwa*" *feisti*, is also seen in *Saniwa ensidens* USNM 2185 (KTS, pers. obs.) and a number of other extant anguimorphs, such as *Elgaria multicarinata*, *Xenosaurus grandis* and juvenile *Shinisaurus*.

Ectopterygoid

Description. The bone is elongated and extends anterolaterally from its articulation with the transverse process of the pterygoid. The distal end of that articulation was forked, with a slender, apparently horizontally oriented dorsal tab and a thicker, rugose, apparently vertically oriented tab (Fig. 6A). There is a blunt projection on the posterior margin of the bone (Figs 5; 13), lateral to which the coronoid inserted when the jaw was closed. The neck and lateral portion of the ectopterygoid is preserved atop the mandible in SMF-ME 10954 and the Pohl-Perner specimen and is well exposed in superficial view (Fig. 2, right side; Fig. 5, left side). The lateral portion is enlarged and drawn out into an anterolateral process. That process forms a blunt tip dorsally, which is continued anteriorly by a short, non-exposed portion (Fig. 13A). Still, it probably did not extend far enough anteriorly to reach the palatine. The lateral surface of the bone, which would have articulated with the maxilla and jugal, is nearly flat anteriorly but shows a deep longitudinal invagination posteriorly (Fig. 13).

Comparisons. This element is broadly similar to the ectopterygoid referred to *Palaeovaranus cayluxi* by Augé (2005: fig. 193). Overall the forked ectopterygoid articulation on the transverse process of the pterygoid is similar to that of many anguimorphs. The lack of a posterolateral process of the ectopterygoid is a derived feature of "*Saniwa*" *feisti* (Smith 2009b; Gauthier *et al.* 2012) that it shares with Anguimorpha. In contrast, the blunt, posterior projection of the bone, lateral to which the coronoid inserted in the resting state, is uncommon in Anguimorpha and seems a remnant of the condition in Iguania. The rugosity on the tip of the ventral tab of the medial fork (together with the more delicate tip of the transverse process of the pterygoid) is also uncommon in Anguimorpha and suggests that the tendinous portion of m. pterygomandibularis that originated here was particularly strong.

Jugal

Description. The jugal forms the majority of the ventral orbital rim. Its anterior or suborbital ramus is sutured with the maxilla and lacrimal; its exposure is progressively restricted anteriorly by the facial process of the maxilla. Beneath the orbit it is thick (SMF-ME A258) and dorsoventrally broad and comes to a posteroventral angle (*c.* 90°) before the slender postorbital ramus rises toward the postorbital. This angle of the jugal is rounded and slightly more prominent in the larger HLMD-Me 13709, whereas in SMF-ME 10954 it is distinctly sharper. The exposed lateral surface of the suborbital ramus is weakly concave in cross-section, with a well-developed ventral rim. In the right jugal of SMF-ME 10954, a distinct row of eight small foramina penetrates the bone's lateral surface and would have

transmitted cutaneous branches of the maxillary nerve (Oelrich 1956); on the left side there are only two (widely separated) major foramina, with a field of smaller openings in between them. Small anteriorly to anteroventrally trending grooves extend from the foramina. The foramina can only been seen on the left side of HLMD-Me 13709 and are difficult to count even there, but it appears that there was a cluster of smaller foramina on the broadened area near the angle of the bone, supplemented by a large foramen higher up on the postorbital ramus (as in SMF-ME 10954). In the Pohl-Perner specimen, the left jugal shows only a cluster of about five foramina on the suborbital ramus and none on the postorbital ramus.

The bone is triangular in cross-section and shows a medial ridge that extends along most of its length and divides it into distinct surfaces (see Čerňanský *et al.* 2014 on this structure). One surface, the orbital face, is relatively broad, anteroposteriorly concave, and oblique. Near the posteroventral corner of the orbit it is pierced by a foramen. This face is gradually restricted anteriorly. Moving onto the postorbital ramus, the orbital face tapers strongly; it is pierced by a single foramen somewhat less than halfway up (*xz*510). The posteromedial face of the bone is excavated to form a fossa. This fossa follows the postorbital ramus longitudinally and near its dorsal extremity is quite shallow; it is pierced by a small foramen at the same level as that which pierces the orbital face (*xz*512). At the angle of the jugal, this fossa forms an anteriorly pointed, triangular depression whose anterodorsal margin, just beneath the bounding medial ridge of the jugal, is pierced by a single foramen (*xz*498). The fossa extends some distance anteriorly along the ventral margin of the bone, demarcating an area where the maxilla did not articulate. Anterior to this fossa, the medial ridge of the jugal bifurcates; the dorsal tine of the fork continues anteriorly as the suborbital margin, while the ventral tine runs to the ventral margin of the bone and the maxillary articulation. Between these tines there might be one or two small foramina (*xz*505). The ectopterygoid articulated there (see below).

Comparisons. The jugal in "*Saniwa*" *feisti* is similar to that in *Eosaniwa* (Rieppel *et al.* 2007) in being dorsoventrally broad beneath the orbit and having a well-developed posteroventral angle and a slender postorbital ramus. Indeed, the anterior ramus is even broader, and the angle more rounded, in *Eosaniwa* than in "*Saniwa*" *feisti*. A broad jugal was regarded as a distinctive feature of "shinisaurs" (including *Palaeovaranus*) by McDowell & Bogert (1954). Furthermore, the posterolateral fossa on the postorbital ramus, which in "*Saniwa*" *feisti* is expanded anteriorly to form an extensive region along the posteroventral margin of the jugal to which the maxilla was not applied, is primarily confined to the postorbital ramus in *Eosaniwa* (Rieppel *et al.* 2007: fig. 2.2); thus, the maxilla in *Eosaniwa* would have articulated along most of the suborbital ramus. The fossa in *P. giganteus* is intermediate between those in "*Saniwa*" *feisti* and *Eosaniwa* (KTS, pers. obs.) and close to the condition seen in *Xenosaurus* and *Heloderma*. The jugal in Varanidae further lacks any kind of projection or quadratojugal tubercle at the angle of the jugal (to which the quadratojugal ligament attaches that connects jugal and quadrate); the element is not described for *P. cayluxi*. The orbital face of the jugal, finally, is broader in "*Saniwa*" *feisti* and *P. giganteus* than in *Eosaniwa*, *Heloderma* and Varanidae, in which respect *Palaeovaranus* is also like *Shinisaurus* (Smith & Gauthier 2013).

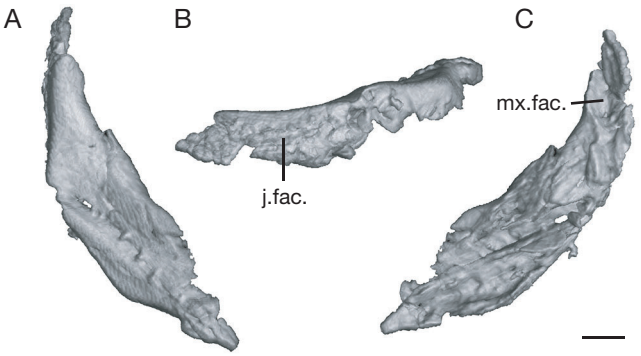

Fig. 13. — The ectopterygoid: **A**-**C**, partial left ectopterygoid segmented from CT scan of *Paranecrosaurus feisti* (Stritzke, 1983) n. comb. (Pohl specimen) in dorsal, lateral, and ventral views, respectively. Abbreviations: **j.fac.**, jugal facet; **mx.fac.**, maxillary facet. Scale bar: 1 mm.

Foramina on the posteromedial face of the postorbital ramus do not appear to be present in *Eosaniwa* (KTS, pers. obs.), although the bone in this area is multiply fractured, so small features might well go unnoticed. With more preparation, these foramina might be explored in *Palaeovaranus giganteus* GMH 4139. Laterally there is a cluster on the broad lateral face of the jugal near the angle in *Eosaniwa*, like in "*Saniwa*" *feisti*, and possibly also a foramen high up on postorbital ramus.

The jugals of "*Saniwa*" *feisti* and *Shinisaurus* are similar in having a long and deep posterior portion of the suborbital ramus that does not articulate with the maxilla. This morphology in both cases results from the anterior expansion of the posteromedial fossa and anterior displacement of the ectopterygoid contact. However, *Palaeovaranus giganteus* has a more primitive jugal, and that of *Eosaniwa*, while certainly not primitive, is not derived in the same way as the shinisaur-like jugal of "*Saniwa*" *feisti*.

Epipterygoid unit

Epipterygoid

Description. Much of the left epipterygoid is exposed on the left side in superficial view in SMF-ME 10954 (Fig. 2). The ventral portion of this rod-shaped element is exposed just inside the orbit. The surface appears to be broken near the base, but the articular surface with the epipterygoid fossa of the pterygoid is intact. The CT scan shows the epipterygoid to be broken and bent in the middle (beneath the postfrontal). The dorsal portion of the bone then continues toward the main body of the parietal, under whose mid-point it may have terminated. The bone is hollow, as shown by the Pohl-Perner specimen (Fig. 5A). Given the preserved orientation of the bone in the two specimens in which it can clearly be assessed, SMF-ME 10954 and the Pohl-Perner specimen, it is likely that the epipterygoid had a posterior component to its orientation.

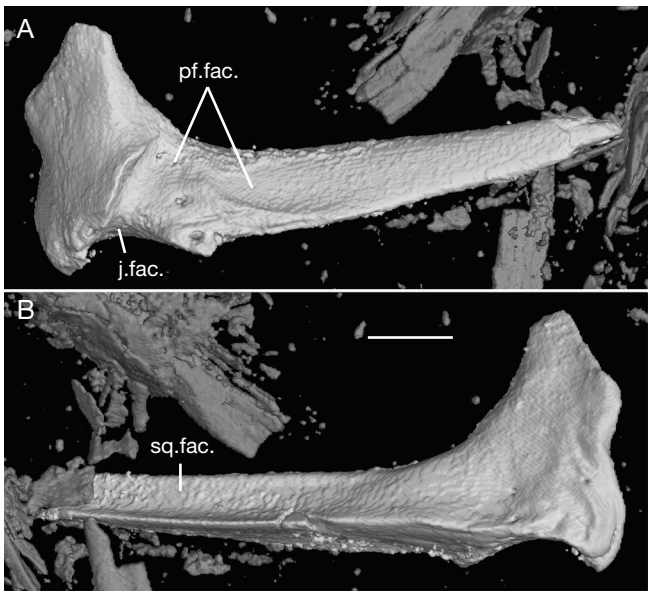

Fig. 14. — The postorbital: **A**, **B**, CT reconstruction of left postorbital of *Paranecrosaurus feisti* (Stritzke, 1983) n. comb. SMNK-Me 1124 (paratype) in dorsal and ventral views, respectively. Abbreviations: **j.fac.**, jugal facet; **pf.fac.**, postfrontal facet; **sq.fac.**, squamosal facet. Scale bar: 2 mm.

Parietal unit

Postfrontal

Description. The postfrontal is medially forked, embracing the frontoparietal suture laterally and ventrally. The anterior and posterior tines of the fork are of approximately equal length. The anterior tine approaches the posterior ramus of the prefrontal to within 5 mm in SMF-ME 10954 (Fig. 3A, left side); the posterior tine extends posteromedially, inserting in a posteriorly deepening notch in the parietal whose termination is visible in dorsal view (Fig. 2). The neck of the bone between the medial fork and the lateral processes has the shape of a dorsoventrally flattened oval in sagittal cross-section. The postfrontal is sutured laterally to the postorbital. A strong dorsolateral process of the former element terminates bluntly, forming (together with the postorbital) a boss at the posterodorsal corner of the orbital margin; the postorbital articulates along an arcuate suture on the posterior margin of this process. The concavity of the arc is better developed in HLMD-Me 13709 (Fig. 7) than in SMF-ME 10954 (Fig. 2). The postfrontal also extends a ventrolateral flange beneath the postorbital (Fig. 6, right side).

Comparisons. In terms of gross form the postfrontal of "*Saniwa*" *feisti* is most similar to that of *Palaeovaranus giganteus* (KTS, pers. obs.) and certain pan-iguanians from the Cretaceous of Mongolia, such as *Temujinia* and *Saichangurvel* (Gao & Norell 2000; Conrad & Norell 2007). Especially clear on the left side of SMF-ME 10954, the bone is transversely wide and anteroposteriorly narrow, with medial and lateral bifurcations. Unlike in those pan-iguanians, however, the lateral bifurcation is superficial only and does not extend vertically through the bone. As in some anguids, like *Celestus enneagrammus*, the postfrontal shallowly overlaps the postorbital, whereas in other anguids as well as *Xenosaurus platyceps* (where the postfrontal and postorbital are unfused), juvenile *Shinisaurus* and certain *Varanus* in which the postfrontal and postorbital fail to fuse (e.g. *V. niloticus* BSP 1959I466, left side; *V. semiremex* Peters, 1869 in Mertens 1942a: fig. 7) the posterior projection of lateral bifurcation does not form.

Postorbital

Description. The postorbital is a discrete, L-shaped element. Together with the postfrontal, it forms a small, flat table behind the orbit. The most clearly exposed example is the isolated left postorbital in the paratype, located at the juncture of the parabasisphenoid and right pterygoid (Appendix 5B, C). The arcuate articulation with the dorsolateral process of the postfrontal leaves a medially projecting shelf on the dorsal surface of the postorbital (Fig. 15A). On the exposed part of that shelf are two foramina in the paratype, one in HLMD-Me 13709 (Fig. 7, right side), and possibly one in SMF-ME 10954 (Fig. 4). At its anterior end the postorbital has two main processes (Fig. 15A): a short one that bends downward to contact the jugal and to achieve a short exposure on the orbital margin, and a longer one that projects medially to brace the postfrontal anteriorly (see also Fig. 6). The posterior process of the bone is long and tapering; it does not reach the level of the anterior tip of the supratemporal or the posterior end of the parietal table. Its ventral surface is grooved where it apparently overlapped the squamosal (Fig. 15B). The jugal and squamosal were apparently widely separated in life. The postorbital is well separated from the margins of the parietal, indicating normal development of a supratemporal fenestra.

Comparisons. In contrast to "*Saniwa*" *feisti*, the postorbital and postfrontal are fused in most *Varanus* and in adult *Shinisaurus* (Conrad 2004; Gauthier *et al.* 2012). Gauthier *et al.* (2012) interpreted the postorbital as absent in *Heloderma* and in *Lanthanotus*, rather than fused to the postfrontal. The two elements are separate in the pan-shinisaur *Bahndwivici* (Conrad 2006a). Postfrontal and postorbital fusion is interspecifically variable in *Xenosaurus* (Bhullar 2011) and intraspecifically variable in *Saniwa ensidens* (Gilmore 1922, 1928; Rieppel & Grande 2007); *Varanus* shows both inter- and intraspecific variation (Gilmore 1928; Mertens 1942a) and even bilateral variation within a single individual, with one side showing fusion, the other side not (KTS, pers. obs. on *V. niloticus* Linnaeus, 1766 BSP 1959I466).

The ventral process of the postorbital beneath the postfrontal in "*Saniwa*" *feisti* is somewhat more anteromedially extensive than in many Anguidae, juvenile *Shinisaurus* and adult *Varanus* in which these elements fail to fuse (e.g. *V. niloticus* BSP 1959I466, left side).

Parietal

Description. The main body of the parietal is trapezoidal, narrower posteriorly, and extends a pair of long supratemporal processes posterolaterally (Figs 2; 5; 7). The dorsal surface of the parietal, like that of the frontal, is covered with osteoderms

anteriorly (see Free osteoderms and scalation), which also are best developed in the central portion of the bone and disappear along the margins of the supratemporal fenestra. The parietal foramen (Smith *et al.* 2018b) is not quite circular, measuring *c.* 0.8 mm in length and somewhat less in width in SMF-ME 10954. In that specimen it is located *c.* 2 mm posterior to the frontoparietal suture; in all specimens it is fully enclosed in the parietal. In SMF-ME 10954 a bilateral pair of artifactual holes punctures the bone near its posterior end; these holes approach one another anteriorly as depressions. The median pillar between them probably indicates the anterior extent of the ascending process of the synotic tectum.

The supratemporal fossa is deeply concave and faces dorsolaterally, and the adductor musculature therefore had a dorsal origin over almost all of the parietal. However, the lateral edges of the parietal table project dorsolaterally over the fossae. The supratemporal processes are triradiate in cross-section, with anterodorsal, posterodorsal, and (presumably) ventral faces. The processes arch gently ventrally at their distal extremity. The posterodorsal surfaces of the processes are formed by the projection of a horizontal lamina from their ventral margin, forming discrete attachment surfaces for the nuchal musculature.

Comparisons. The dorsal origin of the adductor musculature on the parietal is a character shared with *Shinisaurus* and Varanidae as well as with extinct *Palaeovaranus* from Quercy and *P. giganteus*. The parietal is poorly known in *Eosaniwa* (Rieppel *et al.* 2007). Unlike in *Palaeovaranus* from Quercy, however, the adductor crests in "*Saniwa*" *feisti* do not meet one another on the midline to form a sagittal crest. The parietal table is trapezoidal rather than triangular, as in the parietal referred to "*Necrosaurus eucarinatus*" from Quercy (Augé 2005). The parietal table in those taxa with a sagittal crest in adults typically undergoes a transformation from trapezoidal to V-shaped to Y-shaped (e.g. de Queiroz 1987; Lang 1989), and a similar transformation has been suggested for *Palaeovaranus* sp. (Georgalis *et al.* 2021). However, "*Saniwa*" *feisti* is not substantially smaller than *Palaeovaranus* spp. from Quercy with a sagittal crest, and there is no tendency seen in the known ontogenetic trajectory for increased restriction of the parietal table. Thus, a trapezoidal table is not simply the morphology of a non-terminal semaphoront but an adult feature.

The triangular cross-sectional shape of the supratemporal processes, with a broad posterodorsal surface for attachment of the nuchal musculature, is unusual for a species with dorsal attachment of the jaw adductor musculature. The nuchal fossa is frequently obliterated by backward extension of the parietal table. Modern examples include Varanidae, but some adult *Shinisaurus* (e.g. FMNH 215541) come close to the morphology seen in "*Saniwa*" *feisti*. The supratemporal processes are poorly known in *Palaeovaranus cayluxi* (Rage 1978; Georgalis *et al.* 2021). A posterodorsal surface is absent in the holotype parietal of *Palaeovaranus* sp. (Georgalis *et al.* 2021). However, this additional surface is present in *P. giganteus* (KTS, pers. obs.).

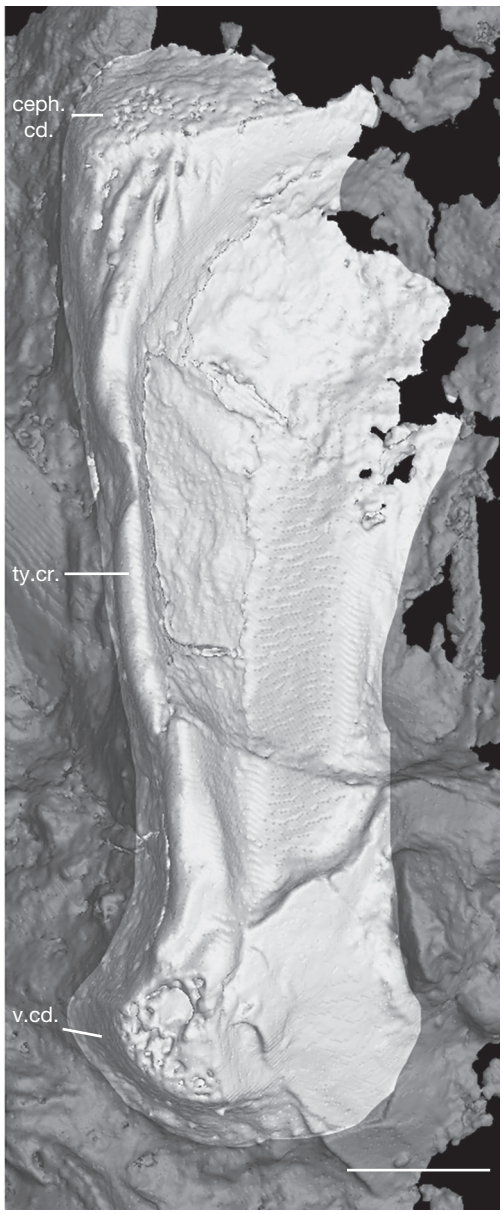

FIG. 15. — The quadrate. CT reconstruction of left quadrate of *Paranecrosaurus feisti* (Stritzke, 1983) n. comb. SMNK-Me 1124 (paratype) in lateral view. Abbreviations: **ceph.cd.**, cephalic condyle; **ty.cr.**, tympanic crest; **v.cd.**, ventral condyle. Scale bar: 2 mm.

Supratemporal

Description. This element lies between the squamosal and supratemporal process (Figs 2; 7). It is mediolaterally relatively thick. The lateral edge is bevelled (Fig. 7), probably for the squamosal. Between this articulation and the medial margin is a dorsal shelf that overhung part of the supratemporal fossa. This shelf decays rather abruptly anteriorly, such that the bone becomes a dorsoventrally oriented blade. The anterior tip does not quite, or just barely reaches the level of anterior end of the parietal recess. At its posterior end the supratemporal appears to bear a small, hooklike process that would have wrapped around the distal end of the supratemporal process, separating it from the squamosal and quadrate.

Comparisons. A strong posterodorsal shelf on the supratemporal is seen in some extant *Varanus* (e.g. *V. gouldii* (Gray, 1838)), but it appears to be absent in *Saniwa ensidens* (Rieppel & Grande 2007: fig. 4.1) and *Lanthanotus*. It is also absent in *Shinisaurus* and examined anguids, where close apposition of the squamosal and supratemporal process of the parietal greatly restricts dorsal exposure of the supratemporal. In *Xenosaurus grandis* there is a slight posterodorsal shelf of the supratemporal, although the primary increase in attachment area in that taxon is achieved by medial expansion of the squamosal; the slight expansion of the supratemporal is entirely ventral to the squamosal expansion.

Squamosal

Description. The squamosal is a dorsally arched, bow-shaped element (Appendix 5C overlying right pterygoid; Figs 2; 7). Posteriorly the squamosal is hooked, tapering to a blunt, rounded, anteroventrally directed tip that would have been joined to the quadrate just lateral to its cephalic condyle. Together with the postorbital it would have formed a strong crest and contributed to a box-like skull construction, also consistent with the strong canthal ridge on the maxilla and prefrontal and the elongate posterolateral process of the palpebral.

Comparisons. The squamosal in "*Saniwa*" *feisti* approximates the "hockey stick" shape of Robinson (Robinson 1967). The curvature is similar to that seen in *Palaeovaranus giganteus* (KTS, pers. obs.).

Quadrate unit

Quadrate

Description. The least distorted example is the isolated left element from SMNK-Me 1124 (Fig. 15; Appendix 5), but the bone remains in articulation with the mandible on the left side of SMF-ME 10954 (Fig. 2). The thick posterior crest – the main shaft of the bone – arches posterodorsally and somewhat medially, growing in thickness and ending in the cephalic condyle, whose hemispherical dorsal surface in SMF-ME 10954 is rugose and "unfinished" but in HLMD-Me 13709 is "finished". This condyle rises slightly anteriorly where it joins a virtually horizontal shelf with sharp margins (Fig. 15). In SMNK-Me 1124 this surface is "finished". Its lateral corner is a strongly rugose, and the tympanic crest extends nearly straight ventrally to join the lateral aspect of the ventral condyle. A depression appears to be developed on the posterior face of the lateral concha in SMF-ME 10954 and SMNK-Me 1124, just medial to the tympanic crest, but it is the product of breakage. A medial crest of the quadrate is present along the entire height of the bone (*xy*115 ff.; Fig. 3A), although it appears to diminish in prominence ventrally, which can be seen at mid-height and is not impacted by the crack running through the base of the right quadrate in the Pohl-Perner specimen (Fig. 6). On the posterior face of the bone, just dorsal to the ventral condyle on the medial aspect of the posterior crest, there appears to be a small depression (Fig. 3A, right element), possibly for medial collateral ligament (Oelrich 1956). The morphology of the glenoid fossa of the articular (see Articular *s.s.*) suggests that the medial half of the ventral condyle was narrower but longer than the lateral half.

Comparisons. The quadrate of "*Saniwa*" *feisti* is highly similar to the referred quadrate of *Palaeovaranus cayluxi* (Augé 2005) in the tall, straight tympanic crest, and apparently in the width of the lateral conch as well, to judge by the portion folded backward over the shaft in the Pohl-Perner specimen (Fig. 5B). Further similarities are: the presence of a pit above the medial half of the ventral condyle for the medial collateral ligament, which is particularly well developed in *P. cayluxi*; the relatively large quadrate foramen (KTS, pers. obs.) for the anterior tympanic vein and an anastomotic branch of the posterior condylar artery (Oelrich 1956); and the subtriangular shape of the cephalic condyle in dorsal view (KTS, pers. obs.). Only the posterior crest in "*Saniwa*" *feisti* appears to be more strongly arched, so that the cephalic condyle is more strongly posteriorly shifted with respect to the ventral condyle. A further, highly distinctive feature of the quadrate of *P. cayluxi* is the sharp, arcuate crest on the anterior face whose curvature is opposite to that of the posterior crest (Augé 2005: fig. 200), which might be associated with m. adductor mandibulae externus et medius (Oelrich 1956); a highly similar crest is seen in *Eosaniwa* (KTS pers. obs.). A similar but less sharp arcuate crest is seen in many *Varanus*, although its curvature is opposite, running parallel to the medial curve of the posterior crest, and in *Lanthanotus*, although in the latter taxon it seems to occur as a ridge between a displaced lateral and medial halves of the bone. A similar crest also occurs in certain anguids (e.g. *Pseudopus*) and in *Heloderma* (weakly in *H. suspectum*), but not in *Shinisaurus*, *Xenosaurus* or other anguids.

Occipital segment

Parabasisphenoid

Description. The parabasisphenoid is partially preserved in SMNK-Me 1124 (Fig. 16C, D) and the Pohl-Perner specimen (Fig. 16E, F). The basipterygoid processes are massive, expanding at the pterygoid articulation to more than twice the width of the neck. The distal margin is overall convex in ventral aspect but near the anterior end shows a notch (Fig. 16C). The dorsal surface of the processes, however, is hollowed out (Fig. 16D). The parasphenoid rostrum is narrow, dorsoventrally compressed, and parallel-sided, as far as it is preserved. There is a weak longitudinal groove on the ventral surface (Fig. 16C). The dorsal surface evinces a pair of longitudinal ridges that divide the surface into three weak grooves (Fig. 16D); the lateral ones probably received the trabeculae, facets for which can be discerned dorsally at the base of the rostrum in the Pohl-Perner specimen (Fig. 16F), and the median one may have supported the interorbital septum.

The ventral surface of the bone has sharp lateral margins (Fig. 16E). The bone bears a pair of elongate posterolateral processes that ascend the anterior aspect of the spheno-occipital tubercles and contribute to their tip. The paired internal carotid arteries entered the posterior opening of the Vidian canal in the posterior third of the bone but was fully enclosed by the parabasisphenoid alone. The palatine branch of the arteries

exited through the anterior opening of the Vidian canal at the base of the parasphenoid rostrum (Fig. 16F). Just medial to them are the bases of the paired trabecular cartilages. The intracranial branch of the arteries cannot clearly be made out in the sella turcica, nor is the dorsum sella well preserved.

Comparisons. Lizards are characterised by a tropibasic skull, in which the trabeculae are fused anteriorly between the orbits to form a trabecula communis. It is unusual for there to be paired grooves on the parasphenoid rostrum. The rostrum is highly reduced in Varanidae and *Heloderma* (Gauthier *et al.* 2012), and even in *Shinisaurus* is it much shorter than in "*Saniwa*" *feisti*. In no other examined anguimorph or iguanian was such a pair of grooves observed. Because the rostrum in SMNK-Me 1124 is incomplete, however, it is not clear what the significance of this observation is.

The position of the posterior opening of the Vidian canal appears similar to that of *Varanus* and mosasaurs but unlike *Heloderma* (Rieppel & Zaher 2000a).

Basioccipital

Description. Part of the basioccipital can be segmented from the CT scan of the Pohl-Perner specimen (Fig. 16E, F). The spheno-occipital tubercles (or basal tubera), on which m. longus capitis insert (Rieppel & Zaher 2000a), were strong and posteroventrolaterally directed (Fig. 16C). In SMNK-Me 1124 the left member shows a smooth apophyseal calcifications. The spheno-occipital tubercles (basal tubera) were clearly situated behind level of the basisphenoid-basioccipital suture. The ventral surface is divided into paired fossae by a median ridge. Two small foramina may be present near the midline adjacent to the basisphenoid-basioccipital suture, although it cannot be excluded that these are artifactual.

Comparisons. Unlike in Varanidae and mosasaurs, the spheno-occipital tubercles are located anteriorly, and processes of the basisphenoid run up them (Rieppel & Zaher 2000a; Gauthier *et al.* 2012). In *Heloderma*, in contrast, like "*Saniwa*" *feisti*, the tubercles are located posteriorly, and basisphenoid processes are present in juveniles (where the braincase is not fused).

Prootic

Description. Parts of the prootic can be segmented from the CT scans of HLMD-Me 13709 (Fig. 16A). There is a prominent trigeminal notch bounded by a strong ventral process and a dorsal alar process; a distinct supratrigeminal process could not be identified. It is not clear to what extent a crista alaris was developed. The crista prootica is a strong and presumably anteroventromedially trending (Fig. 6). The opening for the facial nerve (VII) could not clearly be discerned, however.

Comparisons. A reduced supratrigeminal process is common to Anguimorpha (Norell & Gao 1997). A large projecting crista alaris (of membranous origin) of the alar process of the prootic is characteristic of *Varanus* (Rieppel & Zaher 2000a). While there is no evidence for the crista alaris in "*Saniwa*" *feisti*, it is noteworthy that the distal extremity of the alar process evinces no grooves or ridges or other structures that might indicate a closer articulation with the descensus parietalis or epipterygoid.

Oto-occipital

Description. Parts of the oto-occipital (fused exoccipital and opisthotic; Evans 2008) can be segmented from the CT scan of the Pohl-Perner specimen (Fig. 16E). A crista tuberalis extends dorsally from the position of the spheno-occipital tubercle (which, however, cannot be distinguished here). Immediately posterior to the base of the crista is the large vagus foramen for the combined vagus (X) and accessory (XI) cranial nerves (Watkinson 1906). Ventral to this larger foramen are two separate foramina for the hypoglossal (XII), one anterior and one posterior (Fig. 16G). These openings are all located close to the foramen magnum (Fig. 16E). The condylar portion of the exoccipital is labelled "eo" in Figure 16G.

Comparisons. In Varanidae and *Heloderma* the hypoglossal foramina merge with the vagus foramen, forming one large opening (Lee 1997; Conrad 2008). This derived feature is lacking in "*Saniwa*" *feisti*.

Supraoccipital

Description. Parts of the supraoccipital can be segmented from the CT scan of HLMD-Me 13709 (Fig. 16B). The bone appears to be hexagonal in shape. A strong mid-sagittal crest runs down the dorsal surface on the midline. A notch on the posterior midline marks the foramen magnum. Details of the bony labyrinth cannot be discerned.

Comparisons. A sharp median keel of the supraoccipital was not observed in extant Varanidae or *Heloderma*. In the former, a ridge sometimes develops anteriorly near the base of the processus ascendans, but it is neither sharp nor posteriorly extensive. In *Lanthanotus*, in contrast, a long, rounded median ridge is present.

MANDIBLE

Dentary

Description. The dentary makes up a little more than half the length from the symphysis to the articular fossa (Figs 2; 6; 7). Except at its anterior extremity, the ventral border is nearly straight. On the ventrolateral margin is an elongate, planated surface that begins a few teeth from the anterior end of the bone and terminates at about the dentary's mid-point; it probably marks the insertion of m. genioglossus (Oelrich 1956). The dorsal border of the dentary is slightly concave, so that the jaw increases uniformly in depth posteriorly.

The lateral surface of the dentary is weakly convex and is pierced by a row of mental foramina. On the right side of SMF-ME 10954 seven foramina are visible; eight are present on the left dentary. A similar number is present in the left dentary of HLMD-Me 13709. A smaller number, about five to six on each side, is present in the Pohl-Perner specimen. About seven foramina are present in the left dentary of SMNK-Me 1124 (Appendix 5B, C). In HLMD-Me 13709, the Pohl-Perner specimen and possibly SMF-ME 10954 the posterior-most foramen is distinctly enlarged; this is not the case in SMNK-Me 1124.

A strong, anteriorly trending groove attends each foramen in SMF-ME 10954, but these are poorly developed in HLMD-Me 13709. The foramina are sometimes arrayed with fairly regular spacing (e.g. left dentary of SMF-ME 10954) but can also be irregular (the large gap between foramina 4 and 5 in the right dentary of SMF-ME 10954 (Fig. 3) is conceivably related to the lower number of foramina on this side compared to the left).

The posterolateral margin of the dentary is notched, exposing part of the surangular and angular. A U-shaped buckling of the dentary running a short distance anterior to this notch in SMF-ME 10954 (Fig. 2) and HLMD-Me 13709 (Fig. 7) indicates the anterior, tapering extremity of the combined prearticular and surangular medial to the lateral wall of the dentary, as seen in SMNK-Me 1124 (Fig. 17C). That extremity extends well anterior to the last tooth. There is a smaller notch dorsally for the anterolateral process of the coronoid, so that the posterior end of the dentary was essentially three-pronged.

A ventromedially directed shelf is present along the whole of the tooth row (Fig. 3). It is strong anteriorly and in the middle of the dentary, nearly as wide as the base of a tooth, but its width diminishes posteriorly. Note, however, that in the character of Gauthier *et al.* (2012), this ventromedially directed "shelf" is not considered a subdental shelf, which must be horizontal (or with a parapet); only anteriorly in "*Saniwa*" *feisti* would there be a moderate shelf in their sense (character 217/1). It is also more rounded anteriorly than posteriorly. Additionally, there is a very weakly developed subdental gutter along the anterior quarter of the dentary. The Meckelian groove becomes progressively restricted anteriorly as a result of the ventrally sloping subdental shelf. As a result, it rotates ventrally, and in the anterior *c*. 40% of the tooth row it is entirely ventral (Appendix 5C). The symphysis is well developed, and on its medial face is an arcuate fossa marking the insertion of the interdental ligament (Fig. 3).

An accurate tooth count could not be obtained but almost certainly exceeded 17 and probably 20 (Fig. 3). Given the posterior margin of the bone, the dentary tooth row probably terminated in front of the maxillary one.

Comparisons. As in the maxilla, the high number of mental foramina in the dentary, with a mode of about 7, is noteworthy. Such a count was commonly observed in extant *Varanus* spp. but not in other anguimorphs, except *Xenosaurus* and some *Heloderma*. Fewer mental foramina were illustrated by Hünermann (1978) for a probable palaeovaranid he described as "indet. Varanoid", which has five. Comparison with *Palaeovaranus* from Quercy is not possible for want of sufficiently complete material. At least some mosasaurs, however, also have an even larger number of mental foramina (e.g. 9 in the right dentary of *Clidastes propython* ANSP 10193; KTS pers. obs.).

Enlargement of the posterior-most mental foramen was indicated as a synapomorphy of Varanoidea (and also of Mosasauridae) by Gauthier *et al.* (2012). In three of four specimens of "*Saniwa*" *feisti* this is also the case, as it is in a specimen referred to *Palaeovaranus giganteus* (Augé 2005: fig. 197a). However, in an illustrated specimen of *P. cayluxi* (Augé 2005: fig. 186a) it does not appear to be the case.

A distinct fossa for m. genioglossus, as in "*Saniwa*" *feisti*, has also been observed in certain fossil iguanians (Wellstead 1982; Smith 2011). K. K. Smith (1986) notes that m. genioglossus, most of which inserts in the lower part of the tongue (Schwenk 1988), causes tongue protrusion in *Varanus*. Tongue protrusion functions in gustation as well as in prey prehension and ingestion in squamates (e.g. Smith 1986; Schwenk 1988), and it is not yet clear what, if anything, can be inferred from the presence of a well-developed fossa for m. genioglossus.

The dentary tooth count of *Palaeovaranus giganteus* GMH XLI-203 (Kuhn 1940) is around 22-23 (KTS, pers. obs.). That specimen is slightly older than the holotypes of both *eucarinatus* and *giganteus* (it comes from Grube Cecilie (Ce) LXI, whereas the types come from CeIII and IV (see Haubold 1990)), but at present there is no reason not to accept the referral. With a length of nearly 4 cm, it suggests that *P. giganteus*, as its name suggests, could obtain a large size. Such a high tooth count is unusual for the extant anguimorphs that have been surveyed (Gauthier *et al.* 2012; Smith & Gauthier 2013) as well as mosasaurs (e.g. *Clidastes propython* ANSP 10193). A relatively high tooth count was notably also found in the maxilla (see Maxilla). In contrast, the most complete dentaries of *P. cayluxi* have only 13 teeth (Augé 2005).

Splenial

Description. The splenial is a long element, extending anteriorly well past the dentary mid-point to reach roughly the mid-point of the fossa for m. genioglossus (Fig. 6). Thus, it probably rotated ventrally with the Meckelian groove. It has the overall shape of an obtuse triangle, with a very long anterior and short posterior process (Fig. 17A). Its dorsal margin bears a laterally directed (into the mandible) shelf posteriorly that articulated on the undersurface of the subdental shelf of the dentary. The splenial shelf is interrupted to form the ventral margin of the anterior inferior alveolar foramen (which was bordered dorsally by the dentary); a small anterior prong probably projected anteriorly over the foramen. The splenial shelf picks up again, but weaker, anterior to the foramen, and it decays rapidly anteriorly. Posteroventral to the anterior inferior alveolar foramen is the anterior mylohyoid foramen, which is fully enclosed in the splenial. The ventral margin bears a weak, longitudinal facet for the dentary that merges posteriorly, behind the anterior mylohyoid foramen, with the angular facet. The latter is much deeper than the dentary facet and dorsoventrally and anteroposteriorly extensive.

The height of the bone increases posteriorly toward the posterior end of the tooth row, ascending toward the coronoid (Fig. 17A). From its apex, the bone tapers posteriorly. The ventral margin curves slightly dorsally. In SMF-ME 10954 the posterior process appears to be notched, with a strong, posteroventral prong, the angular and posterior mylohyoid foramen located above the prong (Fig. 3D). However, following the slices carefully, it appears that the structure in question is the prearticular, and the "foramen" a canal within it.

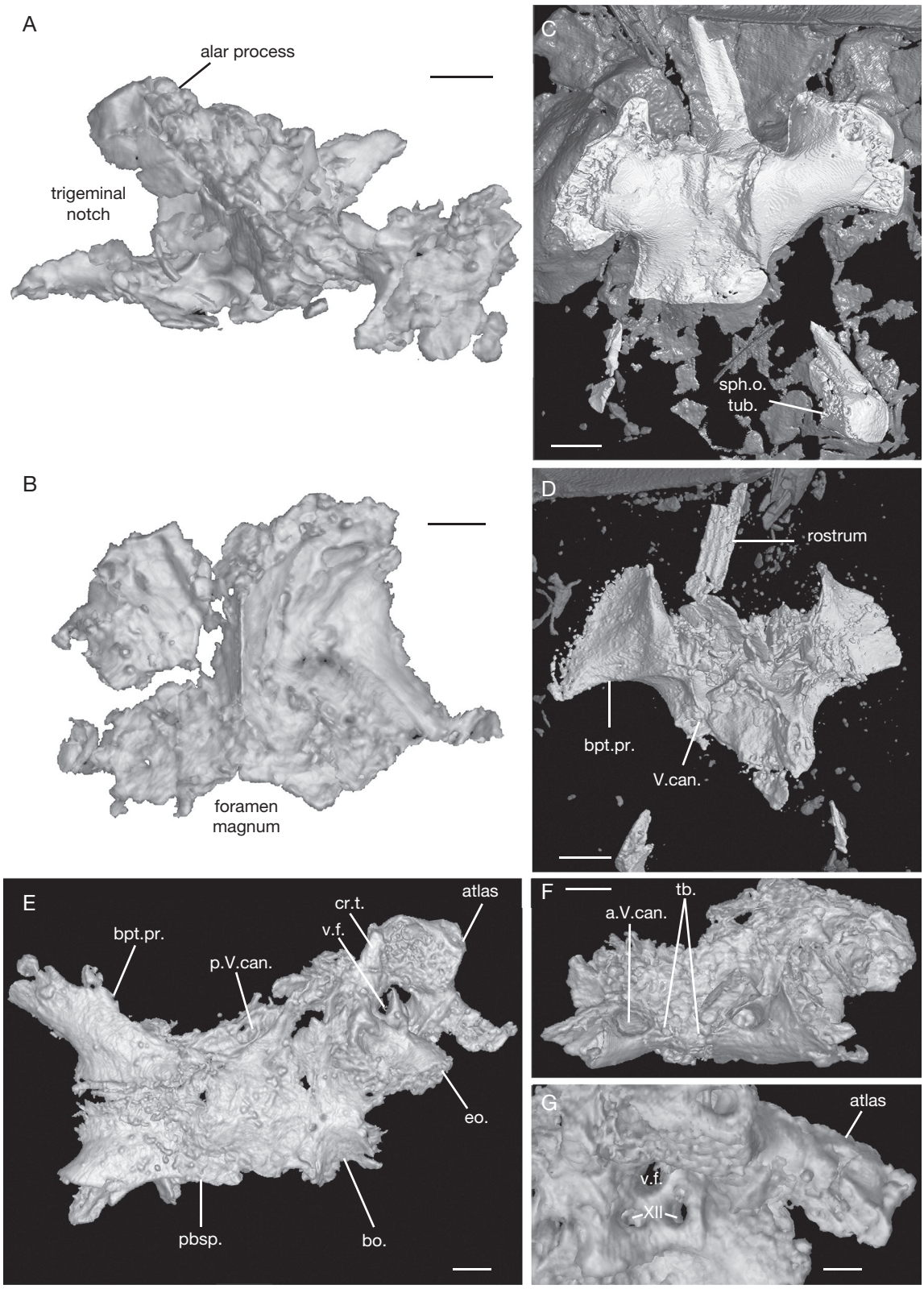

Fig. 16. — Braincase elements: **A**, partial left prootic segmented from CT scan of *Paranecrosaurus feisti* (Stritzke, 1983) n. comb. HLMD-Me 13709 (holotype) in lateral view; **B**, partial supraoccipital segmented from CT scan of *Paranecrosaurus feisti* n. comb. HLMD-Me 13709 (holotype) in dorsal view; **C**, **D**, partial parabasisphenoid segmented from CT scan of *Paranecrosaurus feisti* n. comb. SMNK-Me 1124 (paratype) in ventral and dorsal views, respectively (different threshold settings to maximize visibility); **E**, **F**, articulated portions of the parabasisphenoid, basioccipital and left oto-occipital in the Pohl-Perner specimen in left lateral and anterior views, respectively; **G**, close-up of left oto-occipital region of the Pohl-Perner specimen in posteroventrolateral view. Abbreviations: **a.V.can.**, anterior opening of Vidian canal; **bo.**, basioccipital; **bpt.pr.**, basipterygoid process; **cr.t.**, crista tuberalis; **eo.**, exoccipital portion of oto-occipital; **pbsp**., parabasisphenoid; **p.V.can.**, posterior opening of Vidian canal; **sph.o.tub.**, spheno-occipital tubercle; **tb.**, facets for trabeculae; **v.f.**, vagus foramen (for cranial nerves X+XI); **XII**, foramina for cranial nerve XII. Scale bars: A, B, E, F, 1 mm; C, D, 2 mm; G, 0.5 mm.

Comparisons. A posteriorly shortened splenial with a posterior notch into which the angular inserts is clearly seen in *Varanus* as well as *Heloderma* and Anguinae and, to a limited extent, in basal alethinophidian snakes and *Lanthanotus*. It is also seen in at least some basal mosasauroids like *Haasiasaurus* Polcyn, Tchernov & Jacobs, 2003. It is absent in other squamates. This feature contributes to an intramandibular hinge (e.g. Pregill *et al.* 1986; Lee 1997; Rieppel & Zaher 2000b), and its plesiomorphic absence in "*Saniwa*" *feisti* is therefore noteworthy. There remains a long splenial-angular overlap, as in *Varanus* (Rieppel & Zaher 2000b).

The lateral (internal to mandible) crest of the splenial that wraps dorsally over the angular occurs in *Varanus* and Anguinae, but not at all, or only to a limited extent, in *Shinisaurus*, *Heloderma*, *Xenosaurus* and other Anguidae. The conditions in *Lanthanotus*, primitive snakes, and mosasaurs are not comparable due to the development of a strong intramandibular joint.

Coronoid

Description. The coronoid sits atop the anterior end of the surangular (Figs 3; 17). Its apex, the coronoid process, is triangular, with an oblique anterior and a vertical posterior margin. The process is more delicate and pointed in SMF-ME 10954 (Fig. 3) than in SMNK-Me 1124 (Fig. 17C). The coronoid process is thus located well behind the posterior end of the dentary. Its posterolateral surface bears a fossa in which the adductor mandibulae inserted. The bone has an extensive, nearly horizontal anterior process that rests on the surangular, for which a facet is developed. An anteromedial process is almost lacking, but it must have been weakly forked anteriorly, for a short anterolateral process is present that is received by a facet on the dentary (Fig. 17B; see also Dentary). The ventral margin of the bone is undulose in lateral aspect but rises posteriorly to bypass the anterior surangular foramen dorsally. The ventromedial process runs posteroventrally and is marked by a sharp medial ridge (Fig. 2). A small flange of bone extends posteriorly along the medial surface of the surangular and so bounds the mandibular fossa anteriorly. Moreover, in the Pohl-Perner specimen, where the lateral (internal) surface of the ventromedial process is visible on the right side, the distal end is bifurcated (Fig. 6) and would have wrapped around the mandibular fossa.

Comparisons. The coronoid of "*Saniwa*" *feisti* shows some degree of reduced articulation with the dentary and postdentary bones. It is especially similar to that of *Varanus*, and to a lesser extent *Heloderma*, in having a long, nearly horizontal, weakly bifurcated anterior portion. In contrast, the coronoid process in most other extant anguimorphs has a triangular lateral profile, with steep anterior and posterior margins. That of *Lanthanotus* is highly autapomorphic and difficult to compare.

On the other hand, the degree of overlap of the coronoid with other bones of the mandible is greater than in extant Varanidae or *Heloderma*. In particular, the anterolateral process overlaps the dentary more significantly even than in *Varanus* and terminates anterior of the posterior end of the dentary. Furthermore, "*Saniwa*" *feisti* – like *Palaeovaranus cayluxi*, to judge by the articular facet present on MNHN QU 17173 (KTS pers. obs.) – retains a significant, if delicate, posteromedial process that wrapped around the anterior end of the Meckelian fossa. This process is a primitive feature retained in *Varanus* and *Heloderma* but reduced in *Lanthanotus* and absent in described Mosasauroidea.

Angular

Description. The angular forms the ventral border of most of the posterior half of the mandible (Fig. 6). Its articulation anteriorly with the dentary and splenial is not easily inferred. On the medial surface of the mandible it inserts deeply into the splenial (see Splenial), but it may have achieved greater exposure posteriorly, where the posterior process of the splenial curves upward. Its lateral surface bears a distinct facet for the posteroventral process of the dentary (Fig. 6). Its ventral margin is thicker, but acute, so that a "pinched" wedge of the angular formed the major part of the ventral margin of the mandible at this point. The posterior mylohyoid foramen is difficult to make out but appears to traverse the angular obliquely in slices *xz*552-556. Posteriorly, the angular tapers. Its sharp posterior tip coincides with the surangular-prearticular suture (Fig. 6), or nearly so (Appendix 5B).

Comparisons. The "pinched" morphology of the angular becomes much more exaggerated in *Varanus* and *Heloderma* as well as Anguinae, coincident with the development of a splenial prong. It is conceivable that the evolution of a more highly "pinched" angular, with a well-developed facet not only ventrolaterally for the dentary but also ventromedially for the splenial prong, was a necessary change that permitted the evolution of a well-developed intramandibular hinge between angular and splenial, which is well-documented in alethinophidian snakes, *Lanthanotus* and mosasauroids (Rieppel & Zaher 2000b). The isolation of the prong on the angular creates a small but distinct facet, as seen in the isolated angular of *Varanus* and *Heloderma* and CT reconstructions of both (KTS, pers. obs.). Further transformation would involve deepening of this facet and making it horizontal as well as the development of a synovial capsule.

The anterior inferior alveolar foramen in "*Saniwa*" *feisti* is located far posteriorly in the mandible by comparison with most anguimorphs. In this respect it approaches Varanidae, *Heloderma* and *Anniella*, where the foramen is generally located beneath the ultimate tooth, or more posteriorly. The position is somewhat variable, however, in *Varanus*, with the middle of the foramen located beneath the penultimate tooth in *V. gouldii*.

Prearticular

Description. The prearticular is not completely fused to the surangular even in the largest specimen, SMNK-Me 1124 (Appendix 5B). Its anterior process overlaps extensively with the dentary (Fig. 17C). Here it was braced medially by the angular. Its anterior tip forms the ventral margin of the mandibular foramen, through which nerves of the man-

dibular ramus of the trigeminal nerve and the mandibular artery and vein pass (Bhullar & Smith 2008). Throughout its posterior extent it is sutured dorsally to the surangular. Its medial surface protrudes, forming an elongate ridge that forms the medial border of the mandibular fossa. The fossa, however, is highly restricted in mediolateral extent; indeed, it appears to have been little more than a narrow groove for the Meckelian cartilage (Figs 5; 17C). Posteriorly, it wraps ventrally around the articular *s.s.* and extends as a retroarticular process. As a whole, the process is directed slightly medially. The medial margin of that process extends somewhat posteromedially (Fig. 5); in contrast, the lateral margin extends at first posteriorly, before curving medially. Thus, at first it expands slightly posteriorly, producing a weak neck at its base. On the left mandible of SMF-ME 10954, beginning anteriorly near the posterior end of the mandibular fossa, is a prominent, longitudinal ventromedial fossa that extends posteriorly onto the retroarticular process (Fig. 3A). Conceivably this fossa received a part of m. pterygomandibularis.

Comparisons. As noted above (see Dentary), the prearticular of "*Saniwa*" *feisti* extends some distance anteriorly deep to the dentary (see Rieppel & Zaher 2000b for comparisons in Anguimorpha), more specifically well surpassing the ultimate dentary tooth, unlike in *Heloderma*, Varanidae, mosasaurs and snakes. This implies that the connection between dentary and post-dentary bones was as not highly restricted as in those taxa. At the same time, simply the fact that in two of the four specimens the angular-prearticular-surangular complex is shifted ventrally in death suggests that there was a degree of mobility built into the dentary/post-dentary articulation by the nature of the connective tissues, because such displacement is not see in other lizards from Messel (e.g. Smith 2009b).

The mandibular fossa is highly restricted in many extant anguimorphs, including Varanidae, *Heloderma* and many Anguidae. In contrast, that of "*Saniwa*" *feisti* and *Palaeovaranus cayluxi* (MNHN 17173) is like *Shinisaurus* in being widely open.

The posterior surangular foramen in *Palaeovaranus cayluxi* is located at about the same dorsoventral level as in "*Saniwa*" *feisti* but more posteriorly.

The medial edge of the retroarticular process of "*Saniwa*" *feisti* maybe slightly rotated slightly ventrally, as in *Palaeovaranus cayluxi*, but it is not comparable to the condition in mosasaurs (deBraga & Carroll 1993). In *Eosaniwa* the orientation of the process appears to be similar to that in *Palaeovaranus*, although the dorsal surface is divided by a curious longitudinal ridge (Rieppel *et al.* 2007: fig. 2.1), possibly separating muscle insertions (such as m. pterygomandibularis and m. depressor mandibularis, or parts thereof).

Surangular

Description. The surangular is widely exposed posterolaterally on the jaw (Figs 2; 6; 7; Appendix 5B, C). Medially its anterior tip meets the prearticular, forming the posterodorsal margin of the mandibular foramen (Fig. 17C). It is overlapped dorsally by the coronoid and laterally by the dentary.

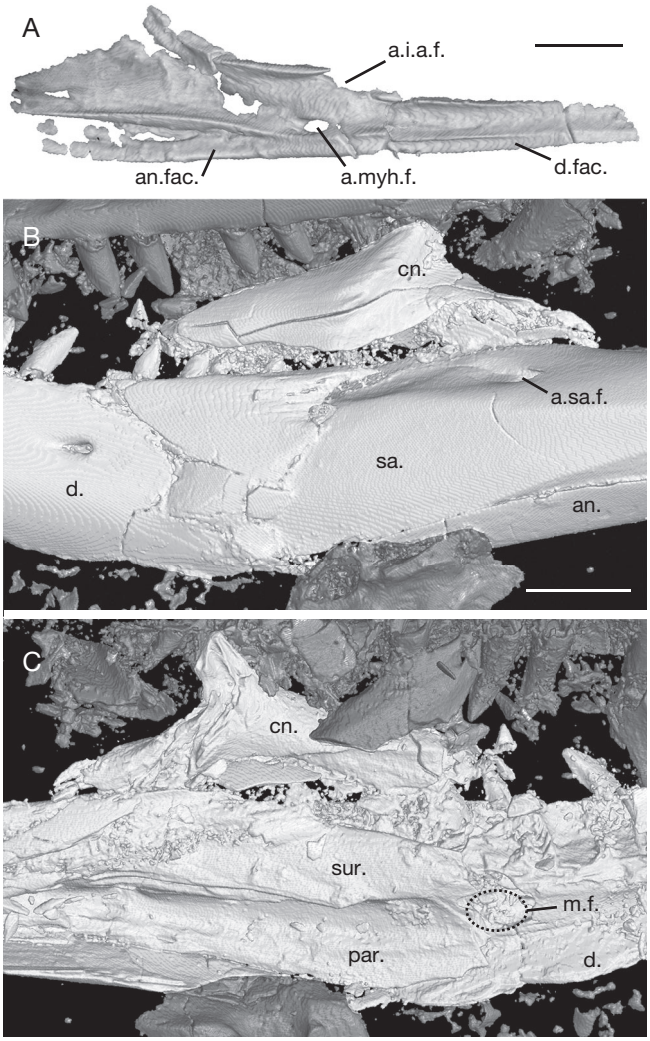

Fig. 17. — The mandible: **A**, partial right splenial segmented from CT scan of *Paranecrosaurus feisti* (Stritzke, 1983) n. comb. (Perner specimen) in medial view; **B**, **C**, middle portion of left mandible from CT scan of *Paranecrosaurus feisti* n. comb. SMNK-Me 1124 (paratype) in lateral and medial views, respectively. Abbreviations: **a.i.a.f.**, anterior inferior alveolar foramen; **a.myh.f.**, anterior mylohyoid foramen; **an.**, angular; **an.fac.**, angular facet; **a.sa.f.**, anterior surangular foramen; **cn.**, coronoid; **d.**, dentary; **d.fac.**, dentary facet; **m.f.**, mandibular foramen; **par.**, prearticular; **sa.**, surangular. Scale bars: A, 2 mm; B, 4 mm.

The articulation with the dentary is a tight scarf joint; there is no sharp-margined facet on the surangular that would suggest a loose connection (Figs 2; 6). Thus, an intramandibular hinge as in *Varanus* can safely be ruled out. The lateral face is smooth and relatively flat (Fig. 7). The anterior surangular foramen pierces the surangular on its dorsolateral face posterior to the coronoid process and is accompanied by a short, anterior groove (Fig. 17B; see also CT-scan of SMF-ME 10954, *xz*573 ff.). The posterior surangular foramen pierces the bone near its posterior margin, just anterior to the glenoid fossa in HLMD-Me 13709 (Fig. 7) and somewhat more anteriorly in SMNK-Me 1124 (Appendix 5B, C). The dorsal edge of the surangular is relatively sharp in HLMD-Me 13709 (Fig. 7), but more rounded in SMNK-Me 1124 (Appendix 5B, C). A tapering posterior process, terminating in a point, extends posteriorly beyond the glenoid fossa along the lateral face of the retroarticular process

(Fig. 7). The medial margin of the surangular, bounding the mandibular fossa dorsolaterally, is broadly rounded in cross-section (Appendix 5B, C). Along its ventral margin it appears to be grooved, probably for the Meckelian cartilage.

Comparisons. It was suggested that the absence of an anterior surangular foramen is a feature uniting *Eosaniwa* and certain other terrestrial taxa with mosasaurs (Rieppel *et al.* 2007: 768), which Conrad (2008: 124) clarified is not "distinct". Re-examination of the CT reconstruction of *Eosaniwa* shows an anterior surangular foramen to be present in this species (*xz*276 ff.). Russell (1967: 52) described a foramen in approximately the correct position (but partly obscured by the coronoid) in his general osteology of American mosasaurs.

Articular s.s.

Description. The endochondral articular bone is only clearly visible in the Pohl-Perner specimen (Fig. 5). It is dorsally and somewhat posteriorly directed and generally concave, except for a longitudinal ridge that divided the glenoid fossa into medial and lateral moieties.

Comparisons. A longitudinal ridge dividing the glenoid into medial and lateral parts is widespread in squamates.

MARGINAL DENTITION

Dentition

Description. For tooth counts, see Premaxilla, Maxilla and Dentary.

All teeth are unicuspid (Figs 2; 3A; 4; 6; 7; Appendix 5). The crowns of fully emplaced anterior and middle teeth are strongly recurved. The degree of curvature decreases posteriorly, such that the last 6 or so teeth in the maxilla of SMF-ME 10954 are vertical (Fig. 3). In the Pohl-Perner specimen, curvature is more pronounced, with only the third tooth from the end effectively straight (Fig. 6). Most teeth are relatively high-crowned and are tallest in the middle of the tooth row. However, those of the premaxilla are distinctly smaller than the anterior maxillary teeth. Anteriorly on the maxilla, the teeth are slender, and mesial and distal carinae, if present at all, are very weak (the distal carina is visible on the fourth tooth of the right side in SMF-ME 10954). Toward and beyond the middle of the maxilla, the bases of the teeth become broader, most prominently in the Pohl-Perner specimen (Fig. 6). Posteriorly, the crowns appear to acquire a lenticular cross-section, with strong carinae mesially and (less so) distally. The posterior-most teeth are short-crowned and stumpy, and the last two or three teeth are very small, less than half the height of middle maxillary teeth (Fig. 3).

Labially, the surfaces are generally smooth. One tooth in SMF-ME 10954, the 11th on the left side, evinces two weak, labial, longitudinal grooves, which are shallower and wider than typical infoldings observed in Varanoidea, and a single such groove is present on the 14th tooth (Fig. 2). Infoldings are more distinct on the lingual surface. In the Pohl-Perner specimen it is the middle teeth of the left maxilla that show the greatest number of infoldings, up to 7 per tooth on the lingual surface (Fig. 6). The infoldings are relatively short and probably did not reach the level of the jaw parapet. X-radiographs of SMF-ME 10954 show that the pulp cavity was not notably restricted by the infoldings (Fig. 4), although the caveat must be borne in mind that this is the smallest specimen, where infoldings conceivably were not as well developed. Most telling are X-radiographs taken at a high angle (>30°) to the perpendicular, i.e., those in which the teeth are viewed more apically.

Resorption pits are lacking. On the left maxilla of SMF-ME 10954, the teeth in spaces 3, 4, 6, 9, 12, 14, 17, and 19 are either missing or incompletely emplaced; in the Pohl-Perner specimen (left maxilla) it is 3, 5, 7, 10, 12, 14, 16, 19, and 21. Thus, teeth were replaced in alternating waves (Edmund 1960). Replacement teeth are best preserved on the left maxilla of the Pohl-Perner specimen. The teeth are developed distolingual to the shaft of the tooth they are to replace. At the base of teeth 8-9, there appear to be 3-4 replacement teeth (excluding the larger tooth tip broken from the dentary). These replacement teeth cannot pertain to the dentary, because the bases of the dentary teeth are located dorsal to the palatal shelf of the maxilla, nor can they pertain to more distal maxillary teeth, which have replacement teeth associated with them already. Thus, here it seems that up to two waves of replacement teeth were present simultaneously adjacent to the emplaced tooth. However, given the exceptional preservation of the maxilla and the fact that only here can this detail be made out, it remains uncertain. There is no evidence that the replacement teeth were held at an angle other than vertical.

Comparison. The teeth are similar in form to those of *Palaeovaranus giganteus*. In at least some specimens referred to *P. cayluxi*, the teeth begin to acquire a more lenticular cross-section, a feature convergent on Varanidae (Bhullar & Smith 2008). In combination with the increased number of tooth infoldings in *P. cayluxi* (see below), it is understandable that early authors saw close similarities to *Varanus* or even included *P. cayluxi* in that genus (e.g. de Fejérváry 1918, 1935).

The lack of resorption pits is noteworthy given the large number of tooth positions in maxilla and dentary seen in X-radiographs and CT scans. The same is true of material of *Palaeovaranus* from Quercy (Augé 2005; Georgalis *et al.* 2021). To be sure, caution is warranted in fossils. For instance, Smith and Gauthier (Smith & Gauthier 2013) found little evidence of resorption pits in *Entomophontes incrustatus*, a species they interpreted as a stem xenosaur. Nevertheless, the consistency of this pattern in preserved material supports our interpretation that it is not artifactual. A lack of resorption pits is a feature exclusively found in Serpentes, *Heloderma* and Varanidae amongst extant squamates (Rieppel 1978). If the evidence presented above for more than one replacement tooth wave associated with a single tooth locus is accurate, this would further strengthen the similarity in dentition to Serpentes, *Heloderma* and Varanidae (Rieppel 1978).

The infoldings present in "*Saniwa*" *feisti* are not nearly as well developed as in *Heloderma*, *Lanthanotus* and especially *Varanus*, where they are extremely numerous, involve also

the dentine, and constrict the pulp cavity (Rieppel 1978; Kearney & Rieppel 2006; Maxwell *et al.* 2011), a morphology called plicidentine. Infoldings otherwise appear only rarely in Squamata (Meszoely 1970; Kearney & Rieppel 2006; Smith & Gauthier 2013). Augé (2005: 278) described "plicidentine" in *Palaeovaranus cayluxi*, and indeed the longitudinal striations ("sillons longitudinaux" of Rage 1978: 206, fig. 3Bi) are more numerous and better developed in this species than in "*Saniwa*" *feisti*. Infoldings could not be sought in the *P. giganteus* type material, but a referred dentary, GMH XLI/203 (Haubold 1977), has a few (no more than three) infoldings on each tooth. In *Eosaniwa* infoldings are present but not very numerous (cf. Rieppel *et al.* 2007; Caldwell 2012: 21). In the left maxilla thirty-three tooth positions are preserved; an "infolding formula" for these teeth, giving the number of infoldings per tooth, with dashes for missing teeth, is roughly –7—·???–5·—3–·–4—·—3–0·———·–0– (dots separate blocks of five teeth). Infoldings are thus concentrated anteriorly and decrease in abundance posteriorly. Smith & Gauthier (2013) observed a similar pattern in *Provaranosaurus fatuus*, a pan-shinisaur. If the development of infoldings is an adaptation for preventing the breaking-off of teeth in taxa that take larger, active prey, it is reasonable that infoldings should be best developed toward the anterior end of the jaws. Infoldings of any kind are absent in Serpentes (Rieppel 1978).

Hyoid apparatus

Ceratobranchial I

Description. The first ceratobranchial is the only ossified element (Cope 1892), and although calcified cartilage is known from some Messel lizards (e.g. Smith 2009b), no other parts of the hyoid apparatus could be discerned in any specimen. The element is best seen on the left side in SMF-ME 10954 (Figs 2; 4). It is a very thin element, <0.5 mm in diameter and *c.* 13.7 mm long. It is hollow, broken in several places and wrapped around the retroarticular process (Fig. 4), extending anteriorly to run parallel to the quadrate ramus of the pterygoid and underlie the quadrate (Figs 3A; 4). The anterior end is expanded and ball-like, suggesting a well-developed, synovial articulation for the basihyoid and perhaps hyoid cornu (sensu Romer 1956), or "anterior process" (Smith 1986). The posterior end is also expanded for articulation with the epibranchial.

Comparisons. K. K. Smith (1986) noted in *Varanus* the unusual length of the anterior process, ceratohyal and ceratobranchial and the unusual mobility between the anterior process and ceratohyal and between the ceratohyal, basihyoid, and ceratobranchial. Opposing muscular action on the former junction shifts the basihyoid with respect to the ceratohyal and produces gular expansion, which is important in a number of behaviors like hissing, drinking, pharyngeal packing, swallowing large prey, etc. (Smith 1986: 282-283). These cartilaginous structures are not preserved, so the most important part of the gular expansion mechanism in *Varanus* cannot be evaluated. However, the ball-like terminus of the ceratobranchial at the basihyoid may suggest a special link.

Postcranial axial skeleton

Vertebrae

Description. The vertebrae are procoelous. The presacral series in SMF-ME 10954 appears to consist of 29 vertebrae (Appendix 2; Fig. 18). (The penultimate vertebra, in the interpretation followed here, is poorly preserved, but it cannot be ruled out that this vertebra does not exist and there were only 28 presacrals.) In HLMD-Me 13709, a count is difficult due to poor preservation of the neural spines and non-exposure of the rib connections, but there appear to be 29 presacrals in this specimen as well (Appendix 4). In the Pohl-Perner specimen, however, there are only 28 presacrals (Appendix 3).

The morphology of the ribs and their attachments constitute the primary basis for recognizing distinct regions in the squamate vertebral column (Hoffstetter & Gasc 1969). In particular, the first vertebra connected to the sternum by a ventral, cartilaginous (inscriptional) rib is usually considered the first sternal vertebra. This vertebra is also the first dorsal vertebra (a more inclusive category including abdominal and lumbar vertebrae). Anteriorly, in SMF-ME 10954, the 6th vertebra retains a short, thick rib (Fig. 18, top); assuming the next two vertebrae, bearing long ribs, did not attach to the sternum, as in most other squamate clades, including *Varanus* (e.g. Schachner *et al.* 2014) and *Lanthanotus* (Rieppel 1980a), then there would be eight cervicals under the usual definition (Romer 1956; Hoffstetter & Gasc 1969), followed by 21 dorsals. Clearly, specimens in which the sternal attachments are preserved (e.g. Smith 2009b) are desirable to confirm this deduction. (Gauthier *et al.* (2012) used a different definition, which in our phylogenetic analysis facilitates comparison with extant taxa; see character 304.) Two sacral vertebrae succeed these, then the caudal series, which is only preserved in its entirety in SMF-ME 10954 (Appendices 1; 2). There are 82 caudal vertebrae: 16.5 vertebrae on the proximal segment, 5.5 on the counterpart (SMF-ME 10954b), and 60 more distally.

Little is discernible of the atlas. In SMF-ME 10954 part of the left atlantal neural arch is visible (Fig. 2A). This element is thick and flat-topped distally, but it tapers as it arches ventrally to a stout neck. In the Pohl-Perner specimen the segmented left neural arch is seen to connect with the stout pedicel (*sensu* Jandzík & Bartík 2004). There is a small lateral bump, suggesting a weak transverse process, on the posterolateral face of the pedicel (Fig. 16E). The articular surface for the axis is visible as a rugose surface that appears to be fairly medially directed. The atlantal intercentrum is seen in ventral view in the Pohl-Perner specimen (Fig. 6). It is wing-shaped, with lateral processes. The anterior margin appears to be notched. A posteroventrally directed protuberance is present at its posterior end.

The axis is poorly exposed in all specimens. It appears to have a sagittal crest that rises posteriorly into a strong neural spine. A ventral projection can be seen (most clearly in the CT scan) at the posterior end that extends a short distance beneath the centrum of the 3rd cervical (Appendix 3B). Digital segmentation reveals that its terminus is anteroposteriorly elongate, but it was not possible to determine whether the

structure comprises hypapophysis, 3rd intercentrum, or both, nor whether the intercentrum is fused to the base of the vertebra or hypapophysis. The remaining cervical vertebrae are shorter than the axis (Appendix 3B). The extent of development of hypapophyses or intercentra in the neck is unclear. The anterior-most vertebrae in SMNK-Me 1124, which are associated with the shoulder girdle, have flat ventral surfaces (Appendix 5).

The dorsal vertebrae evince gradual morphological transitions along the column (Appendices 3-5). Anteriorly, they have nearly parallel anterior and posterior margins; although the tips are directed slightly posteriorly, each spine is nearly vertical in orientation, nearly square in lateral aspect, and scarcely overhangs the neural arch of the succeeding vertebra. The tips of the spines are flat and horizontal, with rounded corners; they are very long, and their dorsal edges make up a large fraction of total neural arch length. By the 9th dorsal (17th presacral), they are distinctly more posteriorly oriented and more strongly overlap successive neural arches. Furthermore, their anterior margins have an even stronger posterior orientation than the posterior margins, leading to a distal tapering of the neural spine. The last two or three presacral vertebrae have reduced neural spines, but there is otherwise no obvious progressive variation neural spine length in the dorsal series. In SMF-ME 10954, the tips of the neural spines are rugose and poorly formed, indicating skeletal immaturity; in SMNK-Me 1124, in contrast, they are smooth, well formed, and apparently fully ossified. Where a glimpse of the anterior end of the neural arch can be gleaned in SMF-ME 10954 (Fig. 18), there is no evidence of even a rudimentary zygosphene.

The dorsal vertebrae grow in length posteriorly in the column (Appendix 3B), except perhaps for the last one or two presacrals, which may be shorter again. Their ventral surface is weakly convex in cross-section and triangular in shape, expanding anteriorly as the subcentral ridges extend anterolaterally toward the paradiapophyses. Posteriorly the centra also become wider, and the ridges extend further laterally. Subcentral foramina could not be discerned in the Pohl-Perner specimen (the only one clearly showing the vertebrae in ventral view), but since the vertebrae are covered with ventral osteoderms, this observation should be taken with caution.

The articulation between cotyle and condyle is seen as an arcuate suture in ventral view (Appendix 3B). Although it appears that the condyle had a distinct neck at the anterior end of the dorsal series in SMNK-Me 1124 (Appendix 5A), this may be artifactual, since a distinct neck is lacking everywhere in the Pohl-Perner specimen (Appendix 4B). The ventral margin of the condyle is sharp-edged, and the condyle apparently faced posterodorsally. The cotyle is frequently marked by a more or less exaggerated lip, even in apparently undistorted vertebrae (e.g. behind the gut contents of the Pohl-Perner specimen), suggesting this is a valid feature.

Anteriorly, the paradiapophyses project strongly laterally, well beyond the anterior terminus of the subcentral ridge (Appendix 3). However, they become increasingly less prominent posteriorly. The dorsoventral extent of their articular surface also diminishes posteriorly, about by approximately the 21st presacral vertebra in the Pohl-Perner specimen they are essentially hemispherical.

The sacrals vertebrae are distinctly shorter than the ultimate presacral (Fig. 18). The transverse process of the first sacral projects laterally. Its distal end is flared and appears to be strongly U-shaped (posteriorly emarginate) in sagittal section, and the dorsal limb of the U is much shorter than the ventral limb (compare Fig. 18; Appendix 3B). The transverse process of the second sacral projects laterally and slightly anteriorly. It is a flat tab that tapers slightly distally in the well-preserved Pohl-Perner specimen (Appendix 3B) but has a posterior kink, probably artifactual, in SMF-ME 10954 (Fig. 18).

The caudal vertebrae are entirely without autotomy planes, even in SMF-ME 10954 (Appendices 1; 2). Anteriorly they are robust, but in the distal two-thirds of the tail length they are very slender. At first they increase slightly in length before reaching a plateau in the middle third of the tail. The first five caudals retain a strongly posterodorsally projecting neural spine with a flat, approximately horizontal tip whose length is nearly half of the neural arch length. Thereafter, they become rapidly reduced in prominence and are ever more strongly inclined, until they are confined to the posterior end of the neural arch. The spine is weak and posteriorly directed; a sharp, mid-sagittal keel extends anteriorly from the spine. Distally in the tail, no more neural spines can be discerned, and the vertebrae appear cylindrical. Similarly, distinct pre- and postzygapophyses disappear.

The transverse processes of the proximal caudals are robust (Appendix 3B). On the first caudal, its anterior margin extends more or less laterally, whereas its posterior margin curves somewhat posteriorly; the anterior margin is also shorter than the posterior one, so that the process as a whole appears to curve posteriorly. In the Pohl-Perner specimen, the ventral surface of the transverse process bears a groove or possibly foramen (Appendix 3B), but in SMF-ME 10954 the dorsal surface of the same is flat and smooth (Fig. 18). More posterior transverse processes project essentially laterally in SMF-ME 10954 (Fig. 19), where as in the Pohl-Perner specimen the second and third caudals still retain slightly posteriorly deflected transverse processes (Appendix 3B). The transverse processes are slightly anteriorly displaced from a position at mid-length throughout most of the caudal series where they are present (Appendices 1-3). They disappear distally in the tail, which together with the lack of a neural spine (see above) implies that the tail had a rounded cross-section.

Starting on the third caudal a weak but sharp mid-sagittal keel is developed on the ventral surface of the centrum (Appendix 3B). At first, it is developed along most of the length of the centrum, but on more distal vertebrae it becomes restricted to the anterior portion. The first caudal lacks a hemal arch, but probably on the second and certainly on the third caudal a pair of weak facets is developed on the posterior margin of the centrum confluent with the intervertebral suture. In this position the pedicels of the hemal arch are also more prominent, projecting distinctly below the condyle, and they are accompanied by sharp ridges that run anteriorly, parallel to and just overlapping the mid-sagittal keel. The implied

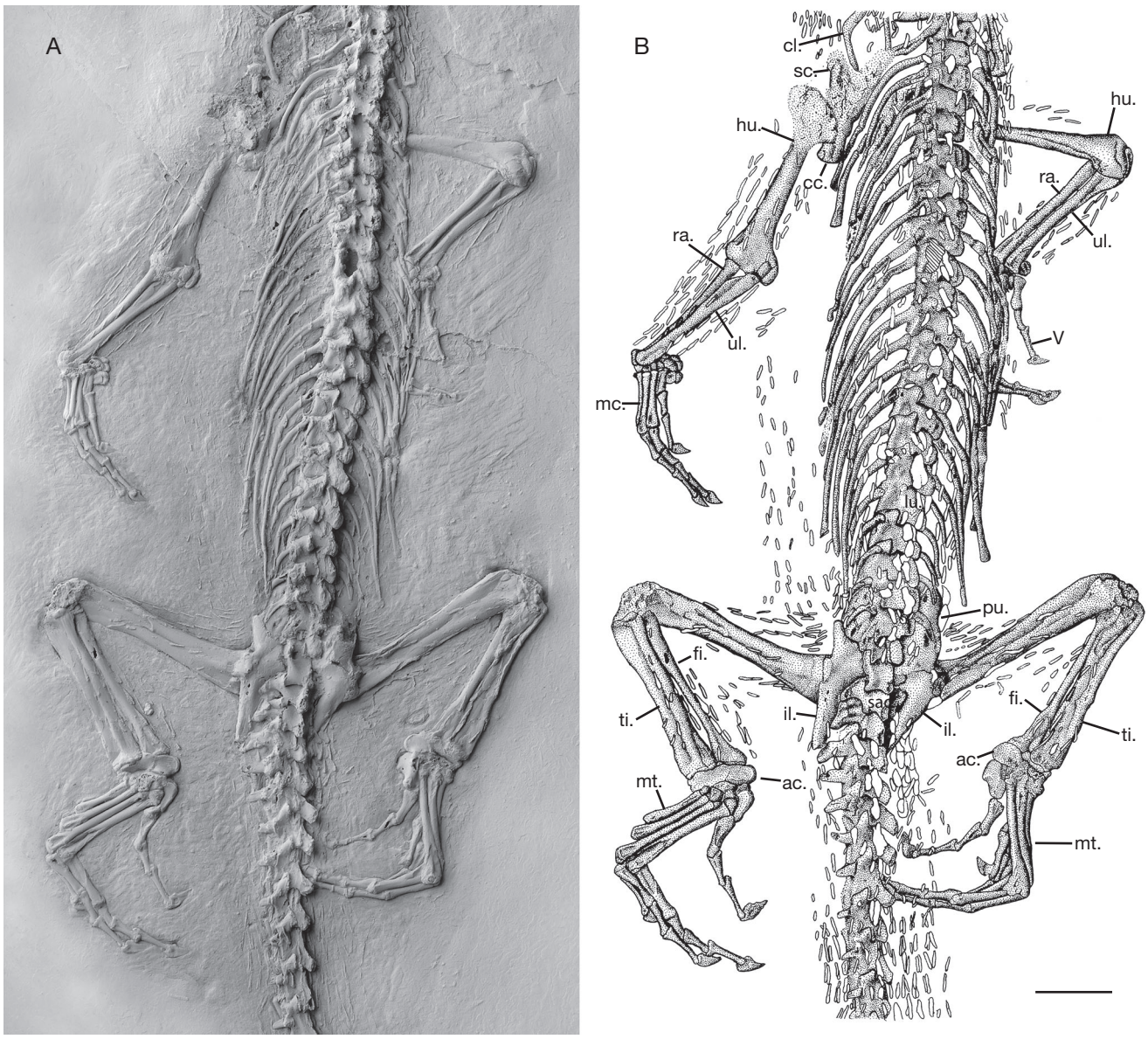

Fig. 18. — The torso: **A**, **B**, photograph and interpretive drawing, respectively, of torso and limbs of *Paranecrosaurus feisti* (Stritzke, 1983) n. comb. SMF-ME 10954 in dorsal view. Specimen coated with ammonium chloride in photograph. Osteoderms are unshaded. Abbreviations: **ac.**, astragalocalcaneum; **cc.**, coracoid; **cl.**, clavicle; **fi.**, fibula; **hu.**, humerus; **il.**, ilium; **lu.**, first lumbar vertebra; **mc.**, metacarpals; **mt.**, metatarsals; **pu.**, pubis; **ra.**, radius; **sac.**, first sacral vertebra; **sc.**, scapula; **ti.**, tibia; **ul.**, ulna; **V**, digit 5 (manus). Scale bar: 10 mm.

hemal arch of the third caudal may be visible to the right of the suture in the Pohl-Perner specimen, and it appears to be relatively short. Hemal arch length increases at first, so that by the 8th caudal it equals the length of the centrum. On proximal caudals it was probably Y-shaped, with a strong median process. More distally in the tail, the hemal arches rapidly diminish in size and are reduced to very slender, V-shaped structures. They seem to disappear in the distal tail.

Comparisons. Stritzke (1983) gave a number of at least 27 presacral vertebrae in the holotype, HLMD-Me 13709, but remarked that a precise count could not be given at the time. We consistently count 28-29 presacrals, depending on the specimen.

Gauthier *et al.* (2012: character 465/1) provided an important criterion for the recognition of hypapophyses in the cervical vertebrae, namely the presence of both fore and aft margins (separate from the intercentrum articulation). In this precise sense cervical hypapophyses are present in Varanidae (Hoffstetter 1943) but not Helodermatidae. They are also present in *Palaeovaranus cayluxi* (Augé 2005) and many mosasaurs, such as *Plotosaurus bennisoni* (Camp 1942), *Clidastes propython* ANSP 10193, and *Platecarpus tympaniticus* ANSP 8559.

Kuhn (1940: pl. 4) illustrated the mid-dorsal neural spines of *Palaeovaranus giganteus* as being square in lateral aspect and strongly abutting on one another, forming a continuous dorsal crest. Examination of the specimen (GMH 4139) shows this interpretation to be somewhat inaccurate. The neural spines do

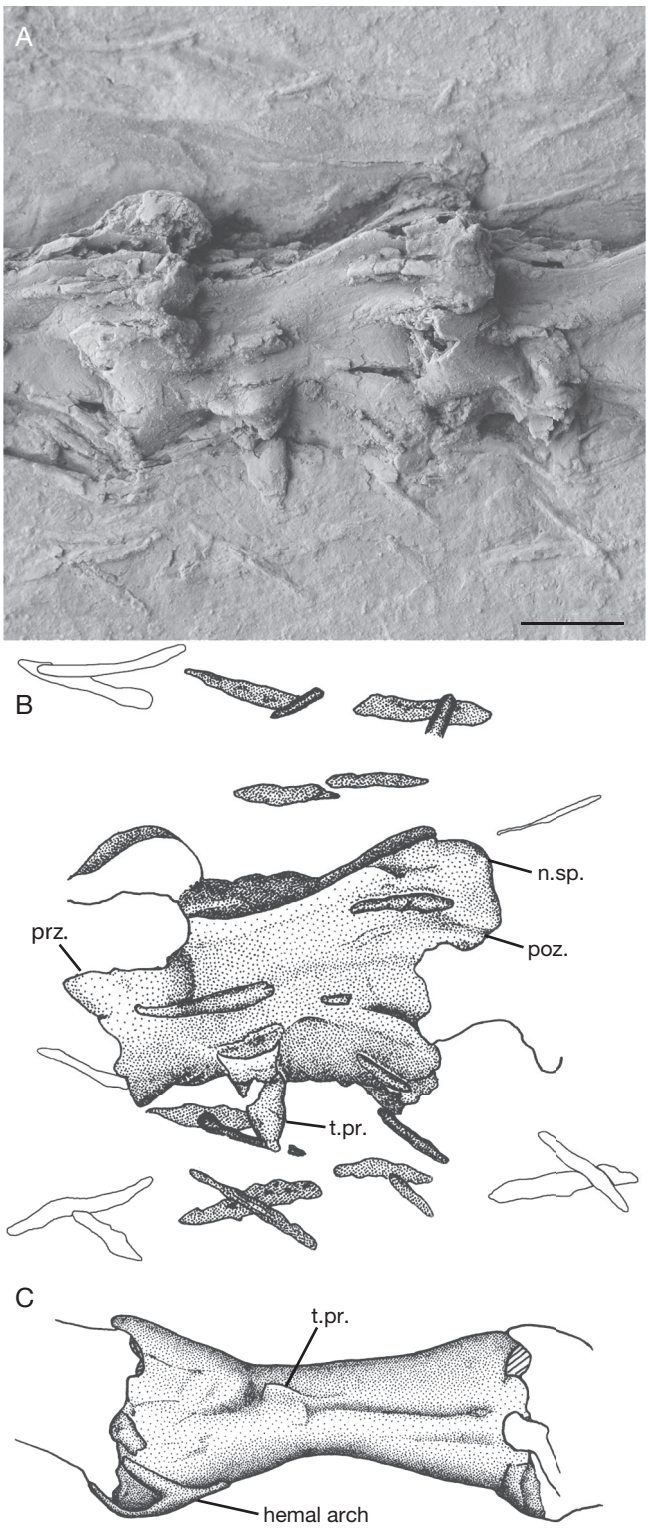

Fig. 19. — Caudal vertebrae of *Paranecrosaurus feisti* (Stritzke, 1983) n. comb. SMF-ME 10954: **A**, **B**, photograph (specimen coated in ammonium chloride) and interpretive drawing, respectively, of proximal caudal vertebra (C11) in left dorsolateral views. Note criss-crossing of osteoderms, with dorsal ones overlying ventral ones. **C**, Middle caudal vertebra (C46) in left ventrolateral view. Abbreviations: **n.sp.**, neural spine; **poz.**, postzygapophysis; **prz.**, prezygapophysis; **t.pr.**, transverse process. Scale bar: 2 mm.

not abut, at least posteriorly. Additionally, tendons appear to be preserved near the apex of the spines. As these tendons run anteroposteriorly and are difficult to distinguish from the bone on the basis of color, they give the impression of a continuous dorsal crest. The tendons appear to arise from the middle of the neural spine on its dorsolateral edge and run anteriorly, forming distinct rods by the time they reach the anterior edge of the spine. Given their site of origin and extension, it seems likely that they represent the tendons of m. spinalis capitis (Tsuihiji 2005). The preservation of tendinous material is not altogether surprising at Geiseltal, where the preservation of muscle tissue, epidermal scales, and even blood corpuscules (Voigt 1988) has previously been documented.

Free ribs

Description. The first rib is apparent in X-radiographs of SMF-ME 10954 on the left side of the 4th cervical (Fig. 4). It is short and slender, scarcely more robust than the ossified ceratobranchial. The rib on the 5th cervical is more robust, and that on the 6th cervical more robust still. The rib on the 6th cervical, in particular, has a sigmoidal shape in three dimensions (Fig. 18), and an expanded terminus (Appendix 2, right rib). Abruptly on the 7th presacral vertebra the rib is very much longer, but also more slender. It as well as succeeding ribs have expanded tips, suggesting that they articulated with a ventral, cartilaginous element. The last dorsal rib with a clearly expanded tip, in SMF-ME 10954, is that on the 19th presacral vertebra (11th dorsal). On the left side of this specimen, especially, there is a clear distinction between the expanded tip of the rib on the 19th vertebra and that on the 20th (Fig. 18; Appendix 2). Thus, the last 10 presacral vertebrae may have lacked articulated ventral, cartilaginous (inscriptional) ribs.

The rib on the 22nd presacral vertebra is distinctly shorter than (about one-third the length of) that on the preceding vertebra (Fig. 18; Appendix 2). This change in length marks the beginning of the abdominal series (Smith & Buchy 2008), which thus comprises 7 vertebrae. Ribs could not be distinguished on the penultimate presacral vertebra; the synapophyseal region is not well exposed here, but ribs also are absent in the X-radiograph (Appendix 2), whereas they are clear on preceding vertebrae. Ribs are also absent on the well-preserved ultimate presacral (Fig. 18). It appears, then, that the last two presacral vertebrae lacked even short "abdominal" ribs and could be described as "lumbar" vertebrae (reviewed in Smith & Buchy 2008).

The ribs of the dorsal series up to that on the 19th presacral vertebra (i.e., pre-abdominal) show a weak, uniform curvature.

Inscriptional ribs, the cartilaginous ventral ribs that may or may not attach to the sternum (Etheridge 1965; Hoffstetter & Gasc 1969), are partly preserved in the Pohl-Perner specimen (Appendix 3). Long inscriptional ribs arc anteriorly from the distal ends of the dorsal ribs associated with presacral vertebrae 14 and 15. The association with vertebrae is reasonably clear on the right side, and we assume that the two such long, anteriorly trending inscriptional ribs on the left side are the contralateral homologs of the same. Somewhat more anteri-

orly on the right side only a single rod of cartilage could be identified, suggesting the possibility that vertebrae 14 and 15 attached to a xiphisternum that in turn attached to the posterior end of the sternum; given the state of preservation, this must remain speculative. Unfortunately, inscriptional ribs associated with more anterior vertebrae could not clearly be identified, although as stated in the discussion of vertebral counts (see Vertebrae), we assume that the first presacral vertebra attached to the sternum by a cartilaginous rib was the 9th. This suggests that long cartilaginous ribs trending toward the sternum (whether or not they actually reached it) were associated with large number (7) of dorsal vertebrae.

Comparisons. The general shape of the dorsal ribs – long, with low curvature – suggests the thorax (sensu Thompson & Withers 1997) of "*Saniwa*" *feisti* may have been tall and possibly somewhat compressed.

Smith & Buchy (2008) examined and reviewed the number of posterior presacral vertebrae in various anguimorphs which lack ribs. They found two lumbar vertebrae to be common in *Heloderma*, whereas usually only one lumbar is present in *Lanthanotus* and *Varanus*. Other anguimorphs usually showed one lumbar but occasionally two.

Smith & Buchy (2008) also examined the number of posterior presacral vertebrae with distinctly short or absent ribs. With 7 abdominal vertebrae (those posterior vertebrae with very short or absent ribs), "*Saniwa*" *feisti* has more than all other extant anguimorphs except *Shinisaurus*, which has 8.

The apparently high number of inscriptional ribs that attached to the sternum exceeds the number in all examined extant anguimorphs, particularly Varanidae (see Gauthier *et al.* 2012).

Pectoral appendage

Clavicle

Description. In all three articulated specimens, the bone has rotated posteriorly around its medial process. The element is a slender, bent rod, the bend dividing it into dorsal and medial rami (Figs 4; 20; 21; Appendices 1; 4). The angle between the two is *c.* 117-120°. The medial ramus is longer, constituting about two-thirds of the total length of the bone. At the angle, the clavicle is slightly expanded, forming a projection that is small in SMF-ME 10954 (Appendix 2) and prominent in the Pohl-Perner specimen (Appendix 3A). It tapers towards its medial and especially dorsal ends. In the Pohl-Perner specimen the medial end appears somewhat expanded (Fig. 21). If this feature is not artifactual, it might indicate a particularly well-developed m. sternohyoideus (see Smith 1986: fig. 4). The details of its connections with other elements of the pectoral girdle are not known.

Comparisons. The clavicle is not expanded ventromedially at its articulation with the interclavicle, as it is in *Shinisaurus* (KTS pers. obs.) and *Lanthanotus* (Rieppel 1980a: fig. 5). The dorsal and medial rami of the clavicle in *Shinisaurus* meet one another at an angle of *c.* 115° (viewed perpendicular to the plane that includes both rami), whereas in "*Saniwa*" *feisti* the subtended angle is slightly larger.

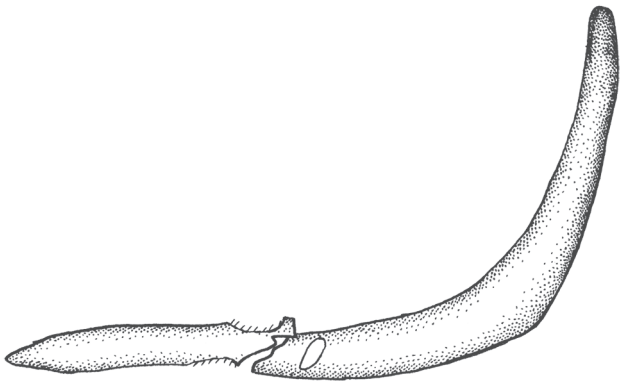

Fig. 20. — Left clavicle of *Paranecrosaurus feisti* (Stritzke, 1983) n. comb. SMF-ME 10954, in approximately anterior view. Dorsal is to top. Scale bar: 2 mm.

The dorsal and medial rami of the clavicle are subequal in length in *Shinisaurus* and *Heloderma*. In *Lanthanotus* (Rieppel 1980a) and *Varanus* the dorsal ramus is only half as long as the medial ramus, similar to, but more extreme than, the configuration of the clavicle in "*Saniwa*" *feisti*.

The angle of the clavicle in "*Saniwa*" *feisti*, though slightly expanded, is not drawn out into a strong process like in (some) *Shinisaurus* and *Eosaniwa*. Conrad (2006b) suggested that this process, first described in *Shinisaurus* by McDowell & Bogert (1954: 24), is calcified cartilage or tendon; in the adult specimens examined for this study (UF 71623, SMF PH 91, 93, 94) the fingerlike process is distinct and clearly osseous. A process of this form is absent in *Lanthanotus* (McDowell & Bogert 1954; Rieppel 1980a).

Interclavicle

Description. The interclavicle is an arrow-shaped element (Figs 4; 21). All processes of the element are slender, more slender even than the clavicle, and of approximately constant diameter. There is a distinct anterior process in SMF-ME 10965 (Fig. 4), but it is much smaller in the Pohl-Perner specimen, assuming its tip is not hidden behind osteoderms (Fig. 21). The longer lateral processes extend posterolaterally at an angle of *c.* 45° near their base in SMF-ME 10954, curving slightly posteriorly; in the Pohl-Perner specimen the angle is *c.* 61°, and the process is not curved; there is no reason to suspect that this difference is artifactual. The posterior process is the longest of the processes, although its precise posterior extent is uncertain. The ratio of posterior to lateral process length is 1.56 in SMF-ME 10954 and 1.55 in the Pohl-Perner specimen.

Comparisons. Estes *et al.* (1988) stated that Xenosauridae (including *Shinisaurus*) is derived in lacking an anterior process of the interclavicle. While this is approximately true in *Xenosaurus*, *Shinisaurus* has a well-developed anterior process (Conrad 2006b), more so than "*Saniwa*" *feisti*. Thus, a reduced anterior process should be considered autapomorphic of *Xenosaurus*. The anterior process also appears to be lacking

in *Lanthanotus* (Rieppel 1980a: fig. 5A). McDowell & Bogert (1954: 24) mistakenly believed (based on radiographs) that *Lanthanotus* lacks the transverse processes of the interclavicle; Rieppel (1980a: fig. 5A) clearly shows them to be present.

Scapulocoracoid

Description. Although portions of this compound element are preserved in all four illustrated specimens, it is by far the most clearly visible in the Pohl-Perner specimen, where the scapula and coracoid are indistinguishably fused (Fig. 21). The dorsally located scapula expands strongly dorsally while curving slightly anteriorly (Figs 4; 21). X-radiographs show that the anterior margin also curves posteriorly near its tip, though not so strongly as the posterior margin (Fig. 4). On its posterior margin above the glenoid cavity is a tuberosity (Fig. 21). A scapular fenestra is absent. However, a deep scapulocoracoid fenestra divides scapula from coracoid anteriorly. The coracoid is fan-shaped and has both primary and secondary fenestrae. A prominent, anteriorly directed protuberance appears to be present at the anteroventral corner of the coracoid (Fig. 4). Remains of epicoracoid or suprascapular cartilage could not be discerned. The glenoid cavity is bounded dorsally and ventrally by strong ledges on the scapula and coracoid, respectively (Fig. 21). The cavity appears angular in dorsoventral cross-section.

Comparisons. The configuration of the scapulocoracoid of "*Saniwa*" *feisti*, with scapulocoracoid and primary and secondary coracoid fenestrae, is like in *Varanus*. *Heloderma* lacks coracoid fenestrae (Lécuru 1968a), whereas *Shinisaurus* and *Lanthanotus* have only the primary coracoid fenestra (Rieppel 1980a; Conrad 2006b).

Sternum

Description. Portions of the sternum, which consists of calcified cartilage, appear to be preserved in the Pohl-Perner specimen (Fig. 21). Details of its shape or rib attachments, however, cannot be discerned.

Humerus

Description. The "twisting" of the distal with respect to the proximal end of the humerus that is commonly observed in squamates is not especially prominent in "*Saniwa*" *feisti*, as seen in the left humerus of the Pohl-Perner specimen (Appendix 3B). Except for the pectoralis tuberosity, the proximal part of the humerus is best seen in the Pohl-Perner specimen (see Appendix 3A for dorsal view of right humerus, and Appendix 3B for ventral view of left humerus). The epiphyseal line extends roughly transversely, but near the posterior end curves distally and near the anterior end proximally through the deltoid tuberosity. The epiphysis includes the oval head of the humerus as well as the latissimus tuberosity and part of the deltoid tuberosity. On the ventral surface of the proximal part of the humerus is a broad concavity bounded anteriorly by a strong pectoral tuberosity (Appendix 5D), as in lizards generally. The shaft is relatively slender.

The distal end of the bone is slightly ventrally curved. On the anterior margin of this end there is a sharp supinator crest that grows in prominence toward the ectepicondyle (Appendix 5A). An ectepicondylar foramen is present (Appendices 1; 2; 5). The entepicondylar process is not especially prominent and has a rounded proximal margin (Appendix 2, left humerus; Appendix 3B) to which the flexor muscles attached. On the ventral surface of the distal end is a prominent fossa (which we may call the *supratrochlear fossa*), as in lizards generally. The articular surface for the ulna and radius was covered in calcified cartilage and is well marked by a lip. The trochleus for the ulna is slightly impressed relative to the distal extent of the entepicondyle. The capitellum or radial condyle is oval and also appears to be surpassed in length distally by the ectepicondyle (Appendix 3A).

In squamates the brachial nerve enters the humerus on its proximodorsal surface, traverses the bone through the medullar cavity, and exits again on the ventral surface through a foramen in a fossa just proximal to the ulnar and radial condyles (Lécuru 1968b). Neither foramen could clearly be identified in the specimens.

Comparisons. Smith (2009a) pointed out that in Varanidae and *Heloderma* the distal foramen for the brachial nerve tends to be very small or appears to be absent in the usual position. It would therefore be of some interest to establish the occurrence of the distal foramen in "*Saniwa*" *feisti*.

Radius and ulna

Description. The radius and ulna are preserved in all three articulated specimens. The ulna is on the whole slightly bowed dorsally (Appendix 4, left ulna). The ulna has a prominent epiphysis, the olecranon process, for the insertion of the triceps (Appendices 1-4). It does not appear to have been fused in any specimen. There is no indication of an ulnar patella (Romer 1956). The proximal part of the ulna in HLMD-Me 13709 evinces a prominent dorsal expansion that encompasses also the olecranon and gives it a convex dorsal margin in anterior and posterior views (Appendix 4, left ulna). The expansion is much less prominent in SMF-ME 10954 (Appendix 2, left ulna). The medial surface of the proximal end is best seen in HLMD-Me 13709; it has a deep artifactual impression marked by partly broken margins. Part of the radial facet on the anterior face of the ulna may be seen here. The posterior surface, best seen in SMF-ME 10954, also evinces a deep impression (Appendix 1, left ulna); although a similar impression is present in some extant *Varanus* (e.g. *V. griseus*), it cannot be ruled out that this feature is an artifact, especially given the presence in this young specimen of impressions in unexpected places of other long bones. The ulna tapers distally to a point somewhat beyond mid-length. It then expands slightly toward its distal end, where there is a prominent, ball-shaped epiphysis (Appendix 3B left ulna).

The radius is slightly shorter and less robust than the ulna (Appendix 2, right radius). It is a spindle-shaped element, slightly expanded at both ends. Its distal end, presumably an epiphysis, appears to have wrapped around the proximoventral

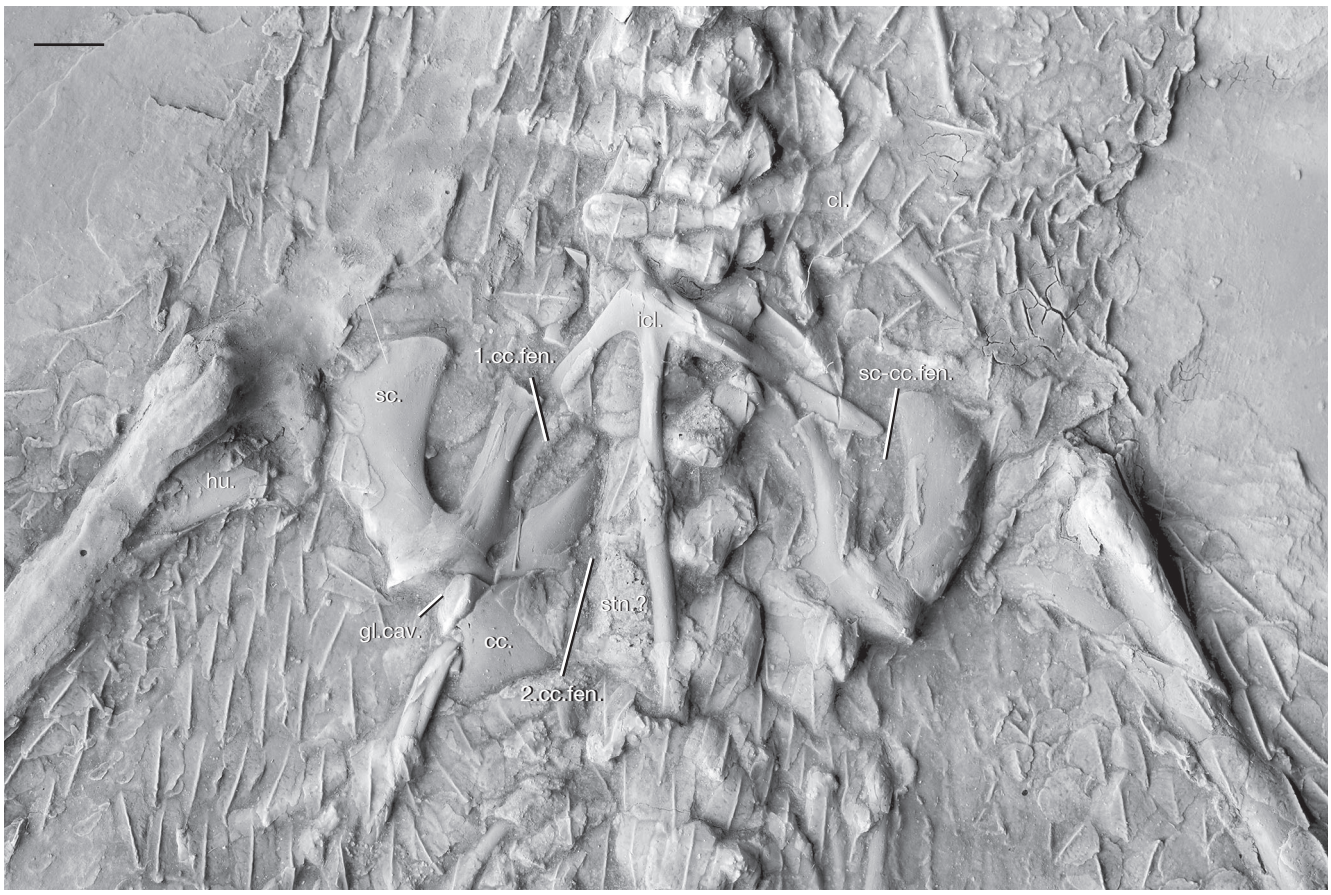

FIG. 21. — Pectoral girdle of *Paranecrosaurus feisti* (Stritzke, 1983) n. comb. (Perner specimen) in ventral view. Abbreviations: **1.cc.fen.**, first coracoid fenestra; **2.cc.fen.**, second coracoid fenestra; **cc.**, coracoid; **cl.**, clavicle; **gl.cav.**, glenoid cavity; **hu.**, humerus; **icl.**, interclavicle; **sc.**, scapula; **sc-cc.fen.**, scapulocoracoid fenestra; **stn.**, sternum. Scale bar: 10 mm.

surface of the radiale (Appendix 3B left radius), as in many other squamates (Renous-Lécuru 1973).

Comparisons. A posterior ulnar fossa is found on the proximal end of that bone in some *Varanus* (e.g. *V. griseus*) but is absent in *Heloderma*. A dorsal convexity of the proximal end of ulna is found in *Heloderma* but not examined in *Varanus*.

Carpus and manus

Description. The manus is completely preserved in the articulated specimens (Appendices 1-4), but only a part of the left manus, with digits I-IV seen in ventral (palmar) view, is preserved in SMNK-Me 1124 (Appendix 5A). In SMF-ME 10954 (Fig. 22A, B) and HLMD-Me 13709 (Fig. 22C) the left hand is preserved in preaxial view (slightly inclined dorsally and ventrally, respectively), and the right hand is largely obscured by the thorax. In the Pohl-Perner specimen both hands are seen in more or less dorsal view on the counterpart, but the right wrist is somewhat telescoped and the elements displaced (Appendix 3B).

There is no evidence of an intermedium. The radiale appears nearly triangular in dorsal view with a vertical postaxial margin (Appendix 3B left hand). The centrale is almost the mirror image of the radiale, but its rounded postaxial corner is stronger. The ulnare appears as a cup-shaped element, with a concave proximal surface into which the ulna inserted and a thick hemispherical distal surface. Distal carpals 2-4 are visible proximal to metacarpals II-IV, respectively. Distal carpal 2 is block-shaped with a rounded distal margin. Distal carpal 3 is wedge-shaped, with a narrow proximal and wide distal margin. Distal carpal 4 has a concave preaxial margin where it articulated on distal carpal 3, a flat distal margin, and a smoothly rounded proximo-postaxial surface. An edge of a distal carpal 1 is probably visible just preaxial to distal carpal 2, but it is disarticulated from metacarpal I and from the radiale. The postaxial elements – pisiform (sesamoid of the m. extensor carpi ulnaris tendon; Landsmeer 1984) and distal carpal 5 – could not clearly be identified, given the preservation, although there are elements preserved in this position in the left hand of SMF-ME 10954 (Fig. 22A, B; some may be the obscured phalanges of digit I). An ovoid structure preserved on the palmar side of the distal end of the left ulna in HLMD-Me 13709 is potentially the pisiform (Fig. 22C).

There are five digits supported by five metacarpals. Metacarpal III is the longest, followed in order of decreasing length by IV, II, V, and I (Appendix 3B left hand). Thin proximal epiphyses are seen on the metacarpals of SMF-ME 10954 (Fig. 22A, B). The proximal articulations of metacarpals III and IV appear

to be flat but shallowly inclined, whereas that of metacarpal V appears to be angulated (Fig. 22A-C), although the articular surface may be confined to the more preaxial portion. The metacarpals, particularly metacarpals III-IV, have a rounded but asymmetrical cross-section, rising postaxially to a ridge that decays abruptly (Appendix 3B left hand). The distal ends are preaxially-postaxially expanded with flat dorsal surfaces; the unfused epiphyses form a kind of cap that wraps around the distal end. The ventral surface of the distal end is concave, with ventrally projecting preaxial and postaxial margins (Fig. 22C).

The phalangeal formula is 2-3-4-5-3. Unlike the metacarpals, the pre-terminal phalanges tend to have broader proximal than distal ends (Fig. 22). They taper distally, reaching a minimum width in the distal half, before expanding again slightly at the terminus. They tend to be half-moon-shaped in cross-section, with a semicircular dorsal and nearly flat ventral surface, at least in the middle. On these elements it is the ventral surface of both proximal and distal ends that is concave, with ventrally projecting preaxial and postaxial margins (Fig. 22C) to which digital flexors attached. The concave proximal articular surface is divided by a dorsoventral keel into preaxial and postaxial moities and frequently bears a projection beneath the distal articular surface of the preceding element. The penultimate phalanges are all longer than the antepenultimate ones, especially on digits IV and V. Distal epiphyses of the phalanges appear to be fused.

Proximally, the ungual phalanges wrap around the distal ends of the penultimate phalanges (Fig. 22; Appendix 3). The thin dorsal edge is convex, bulging especially prominently near the base, and the thick ventral edge is concave. The degree of convexity/concavity is greater in the larger specimens than in SMF-ME 10954. Prominent plantar tubercles are developed on the ventral surface near the base.

No clear evidence of sesamoids was discovered ventral to the distal ends of the metacarpals or dorsal to the distal ends of the penultimate phalanges (Gauthier *et al.* 2012: characters 541 and 547).

Pelvic appendage

Ilium

Description. The ilium is only exposed in medial or dorsomedial view (Figs 18; 23; Appendix 4). Anteroventrally it evinces an arcuate suture with the pubis that leaves it a strong, anteroventral process, and ventromedially it has a slightly shorter suture with the ischium. The acetabulum is not exposed in any specimen. The iliac blade is moderately deep. At its anterior end is a prominent preacetabular process (*sensu* Snyder 1954) for the ilio-pubic ligament, on which various muscles terminate (Romer 1922); the process, however, does not overhang (or only barely overhangs) the ventral, acetabular portion of the ilium. The iliac blade diminishes gradually in height posteriorly and terminates bluntly. Its dorsal edge is notably thin in HLMD-Me 13709 (Appendix 4). It extends as far posteriorly as the middle of the first caudal vertebra (Fig. 18). On its medial surface is a weak, elongate prominence over which the sacral vertebrae inserted; posteriorly this surface is weakly striated.

Comparisons. The well-developed preacetabular process of "*Saniwa*" *feisti* is similar to that of *Varanus*. The process is absent in *Shinisaurus* (Conrad 2006b), *Lanthanotus* (Rieppel 1980a) and *Heloderma*.

Pubis

Description. The pubis is best seen in the Pohl-Perner specimen. From its suture with the ilium the pubis runs anteriorly and, presumably, ventrally. The foramen for the obturator nerve extends anteroventrally through the base of the pubis (Fig. 23A). The medial margin of the pubis curves very gently toward the contralateral element (Fig. 23B), suggesting that the thyroid fenestra ("pelvic fenestra" of Gauthier *et al.* 1988), through which m. puboischio-femoralis internus passes from the internal surfaces of the pubis (and ischium), was U-shaped anteriorly. The pectineal tubercle, to which the other end of the ilio-pubic ligament attaches (Romer 1922), is developed at the lateral edge of a prominent, triangular expansion of the pubis. The tubercle is anterolaterally directed and located roughly halfway between the pubic symphysis and the acetabulum, or slightly more distally. It is capped by an apophysis. Distally the pubis narrows toward the symphysis, which, however, is not clearly visible in any specimen.

Comparisons. The pectineal tubercle is located closer to the acetabulum in *Shinisaurus* (Conrad 2006b) and *Lanthanotus* (Rieppel 1980a) than in "*Saniwa*" *feisti* or *Varanus*. The tubercle is virtually absent in *Heloderma*.

Ischium

Description. The ischium is only clearly seen in the Pohl-Perner specimen. This is a broad, fan-shaped, medially and (presumably) ventrally directed element (Fig. 23B). The anteriorly directed process along the medial edge divided the thyroid fenestra posteriorly and joined its counterpart in a very long ischiadic symphysis. There is no evidence bearing on persistent cartilage at the symphysis, nor of an anteromedian cartilaginous process or a hypoischium. On the posterior margin, directed away from the symphysis, is a prominent ischiadic tubercle ("tuber ischii" of Romer 1922), to which the ilio-ischiadic ligament, running down from the tip of the iliac blade, and m. ischio-caudalis attach (Romer 1922). The neck of the ischium, between the acetabular and fan-shaped medial portions, is approximately as wide as that of the pubis. The ventral edge of the acetabulum can be seen in the Pohl-Perner specimen.

Comparisons. The broad fan-shape is unusual in anguimorphs but similar to that of *Iguana* Laurenti, 1768 and approached by *Shinisaurus* (Conrad 2006b).

Femur

Description. The femur has a sigmoidal form (most apparent in Appendix 3), with the proximal end turned anteriorly and the distal end posteriorly. The head of the femur is ovoid, rounded in transverse and horizontal section, and produced

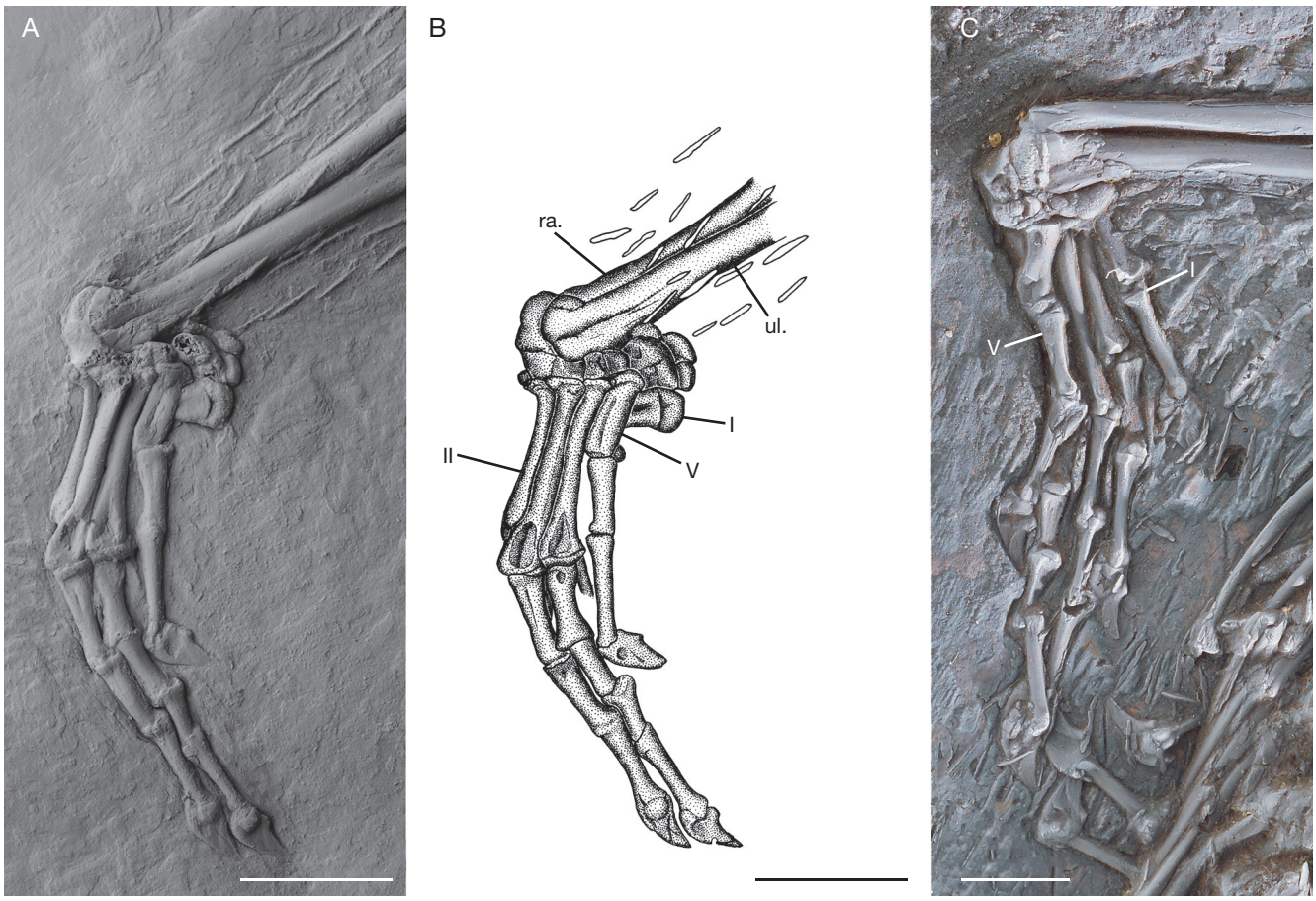

Fig. 22. — The carpus and manus: **A**, **B**, photograph and interpretive drawing, respectively, of left manus of *Paranecrosaurus feisti* (Stritzke, 1983) n. comb. SMF-ME 10954, in roughly postaxial view; **C**, photograph of *Paranecrosaurus feisti* n. comb. HLMD-Me 13709 (holotype) in roughly postaxial view. Specimens coated with ammonium chloride in photographs. Abbreviations: **I**, **II**, and **V**, metacarpals one, two, and five; **ra.**, radius; **ul.**, ulna. Scale bars: 5 mm.

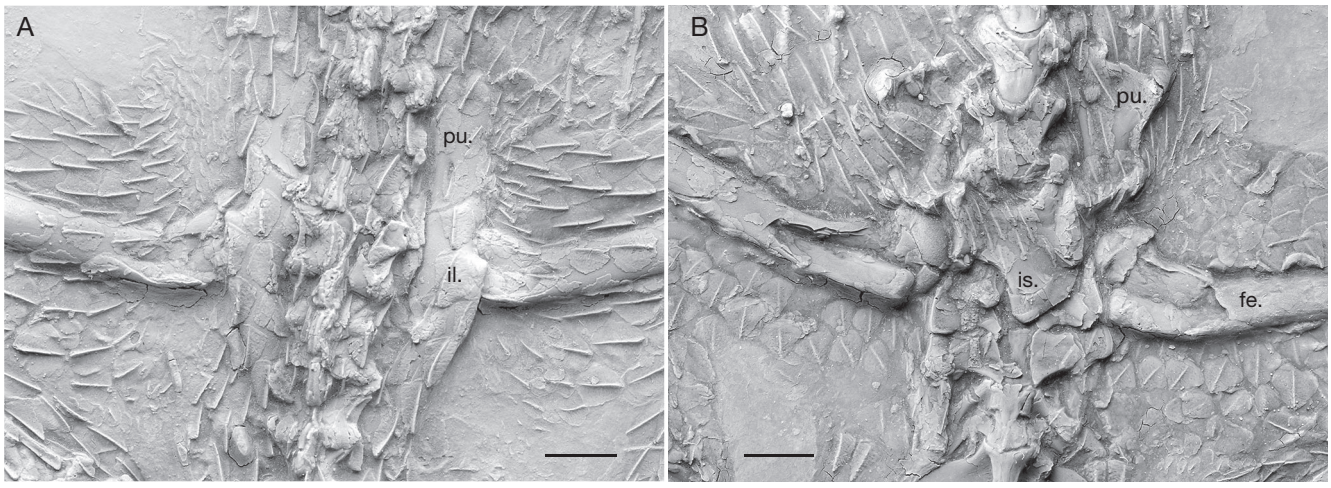

Fig. 23. — Pelvic girdle of *Paranecrosaurus feisti* (Stritzke, 1983) n. comb. **A**, photograph of Pohl specimen in dorsal view; **B**, photograph of Perner specimen in ventral view. Abbreviations: **fe.**, femur; **il.**, ilium; **is.**, ischium; **pu.**, pubis. Scale bars: 5 mm.

anteriorly (Fig. 23B). In SMF-ME 10954 there is on the dorsal surface of the left femur a longitudinal ridge, noteworthy because it is continuous distally with a longitudinal groove of artifactual nature (Fig. 18). On the anterodorsal face of this ridge is a weak impression, which could represent the insertion site for m. pubo-ischio-femoralis internus (Romer 1922), as appears to be the case in some taxa (e.g. *Varanus griseus*). There is a prominent internal trochanter, which continues

distally as a pronounced ridge for some distance and which in the Pohl-Perner specimen has an epiphysis that runs down the same ridge (Fig. 23B). The distal end of the femur is not well exposed in any specimen. On the anterior surface of the anterior condyle is a small, elongate fossa running nearly perpendicular to the shaft (Appendix 3B right femur) in which the collateral ligament of the tibia probably inserted. On the posterior surface of the posterior condyle is another small, elongate fossa running parallel to the shaft (Appendix 3A left femur) in which the collateral ligament of the fibula probably inserted. The right femur of HLMD-Me 13709 appears to have rotated forward, and on the ventral surface of the distal end, the popiteal space between the condyles, in which various ligaments insert (Haines 1942), though crushed, can be made out (Appendix 4).

Comparisons. Lydekker (1888a: 280) in referring a femur to "*Placosaurus margariticeps*" noted that it is relatively longer than in *Varanus*. This was hinted at earlier (Lydekker 1888b), but no explicit reason given for dissimilarity.

The right femur that Filhol (1877) referred to *Palaeovaranus cayluxi*, reassigned by Georgalis (2017) to *Palaeovaranus* sp., shows a similar degree of sigmoidal curvature and rotation of the distal with respect to the proximal end. However, the bump for the insertion of m. pubo-ischio-femoralis is stronger.

Tibia and fibula

Description. The tibia and fibula are poorly preserved in HLMD-Me 13709 (Appendix 4). There is no clear evidence of ossifications of the tendons, meniscus, and ligaments that were recently surveyed by Gauthier *et al.* (2012); the small, elliptical body at the medial side of the proximal left tibia in SMF-ME 10954 is probably a part of the epiphysis. The tibia, as usual, is the stouter of the two. Its proximal portion appears to have been subtriangular in cross-section, with a posterior cavity (Appendix 4, right tibia). The cnemial crest for insertion of m. quadruceps femoris is seen in profile in the other two articulated specimens, but it is not prominent (Fig. 18; Appendix 3). On the medial surface of the proximal end of the left tibia in SMF-ME 10954, below the elliptical body noted above, are some striations which probably mark the ligament associated with the fibular articulation (see Haines 1942). The distal end of the tibia is scarcely expanded with respect to the shaft and appears to be slightly notched, wrapping around the astragalus (Fig. 24A, B). In SMF-ME 10954 the distal epiphysis is not fused.

The fibula, as usual, is slender. Its proximal end, retaining a distinct epiphysis in SMF-ME 10954, has a flattened posterior surface and is slightly expanded with respect to the shaft (Fig. 18, left fibula). The expansion of the distal end is more prominent, especially on the posterior side. The dorsal exposure of the articulation with the calcaneum is nearly straight (Fig. 24A, B).

Comparisons. On the proportions of the lower leg, to which the tibia and fibula principally contribute, see Locomotion and habitat.

Tarsus and pes

Description. The proximal elements are the astragalus and calcaneum (Fig. 24). In SMF-ME 10954, these elements are incompletely fused, with a distinct suture line still visible, on the left side (Fig. 24A, B), but the X-radiographs suggest complete fusion on the right (Appendix 2). Damage makes it impossible to determine in HLMD-Me 13709. They appear to be fully fused in the Pohl-Perner specimen (Appendix 3). Although in SMF-ME 10954 it appears superficially that there is no notch separating the tibial and fibular articulations (Fig. 24A, B), a detailed examination both of that specimen and of the holotype suggests instead that there was a narrow notch. First, in SMF-ME 10954 the edge of the tibial articulation does not extend postaxially to the preserved end of the tibia, but rather it curves toward the proximal margin and disappears beneath the tibia (Fig. 24A, B). The dorsal surface of the astragalus appears to curve ventrally into a notch, bounded postaxially by the preaxial shelf of the fibular articulation. Second, in HLMD-Me 13709, although the tibial articulation is poorly preserved, the region adjacent to that fibular shelf also suggests a distinct separation of the two. Thus, we believe that a moderately deep, narrow notch separated the tibial and fibular articulations and that the apparent absence of a notch on the left side of SMF-ME 10954 is an artifact induced by crushing upward of the posterior margin of the tibia. The astragalus appears to be somewhat proximodistally shorter than the calcaneum. The distal articulations of the astragalus are poorly exposed. The suture between astragalus and calcaneum runs, in the left foot of SMF-ME 10954, proximodistally from the middle of the fibular articulation. The dorsal surface of the calcaneum is slightly saddle-shaped, concave along the proximodistal axis and convex along the preaxial-postaxial axis. Virtually the entire postaxial margin of the calcaneum is expanded into a broad, rounded *crural process* ("calcaneal tuber" or "talus" of Rieppel & Grande 2007), to which Romer (1956: 392) believed the "lateral elements of the crural musculature" attached. The crural process bears a thin, well-formed apophysis. In the Pohl-Perner specimen the crural process is even larger, squared off, and bears a thicker apophysis (Appendix 3A left foot). In ventral view most of the astragalocalcaneum is flat, but preaxially there is a large ventral protuberance of unknown significance (Appendix 3B right foot).

The distal tarsal series contains at least two and possibly three elements. The largest is distal tarsal 4, in dorsal view a L-shaped element whose outer surfaces articulate proximally with the calcaneum and, to a lesser extent, the astragalus and postaxially with the metatarsal V (Fig. 24). At the angle of the L its dorsal surface appears to bear a groove. In ventral view distal tarsal 4 is U-shaped, open proximally (Appendix 3B both feet). The limbs of the U insert into shallow notches on the distal edge of the astragalocalcaneum. Nestled inflexibly in the angle of the L in dorsal view is the much smaller distal tarsal 3 (Fig. 24). In the left tarsus of both SMF-ME 10954 and HLMD-Me 13709 there is a distinct element preaxial to distal tarsal 3 and separate from (the diaphysis of) metatarsal I. This element is somewhat smaller than distal tarsal 3.

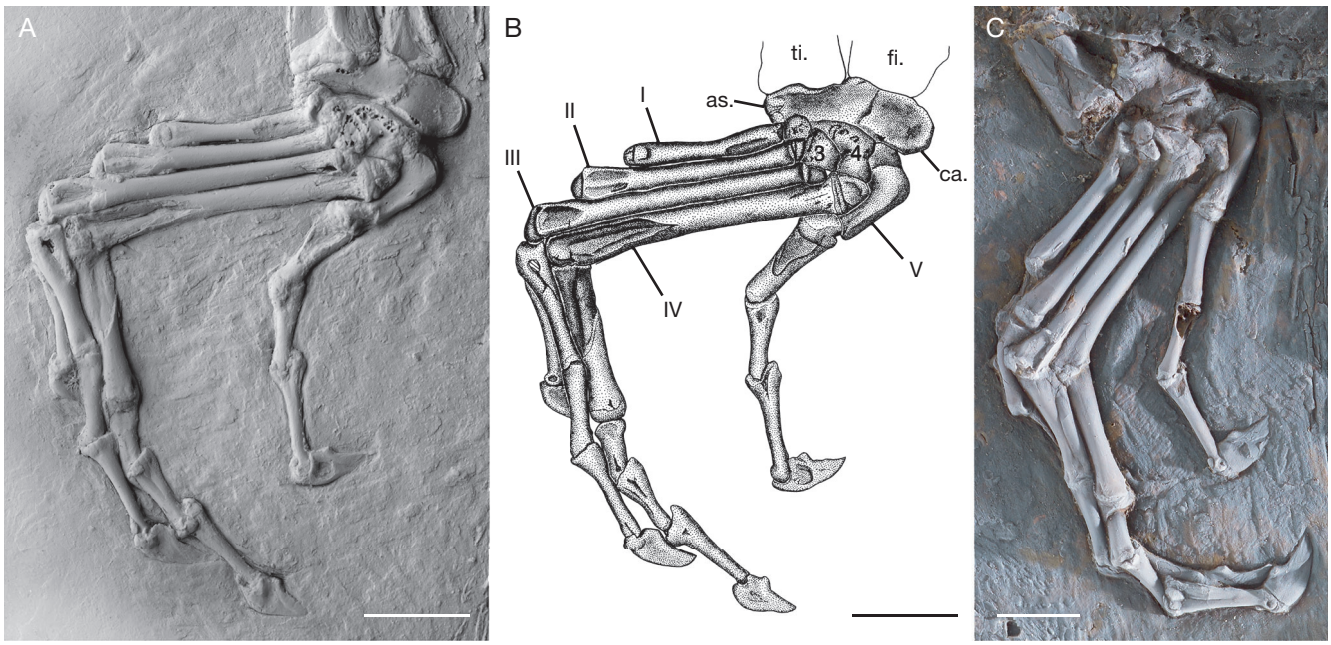

FIG. 24. — The tarsus and pes: **A**, **B**, photograph and interpretive drawing, respectively, of left pes of *Paranecrosaurus feisti* (Stritzke, 1983) n. comb. SMF-ME 10954, in roughly dorsal view; **C**, photograph of *Paranecrosaurus feisti* n. comb. HLMD-Me 13709 (holotype) in roughly dorsal view. Specimens coated with ammonium chloride in photographs. Abbreviations: **I-V**, metatarsals one through five; **3-4**, distal tarsals three and four; **as.**, astragalus; **ca.**, calcaneum; **fi.**, fibula; **ti.**, tibia. Scale bars: 5 mm.

In HLMD-Me 13709 it is clearly rounded in outline and has a "finished" dorsal appearance (Fig. 24C). Most likely this is the displaced proximal epiphysis of metatarsal I rather than distal tarsal 2, which is unknown in extant squamates (Romer 1956). A sesamoid can also be entertained (Gauthier *et al.* 2012: character 562). Evans & Barbadillo (1998) encountered a similar problem in the interpretation of *Scandensia ciervensis*.

There are five digits supported by five metatarsals with staggered proximal ends. Metatarsal IV is the longest in absolute terms (although it does not extend so far distally), followed in order of decreasing length by III, II, I, and V (Fig. 24). Unlike on the metacarpals, the unfused proximal epiphyses of metatarsals I-IV are highly angular. Metatarsal V is relatively long. As in most squamates (Gauthier *et al.* 1988), it is hooked. It has an extensive preaxial articulation on distal tarsal IV and apparently was separated from the astragalus in the resting state. Its proximal end bears a prominent ventral (plantar) tubercle (Appendix 3B right foot). In other morphological respects, including the greater robustness of the unguals, the metatarsals and phalanges are similar to the homologous elements of the hand (see Carpus and manus). The phalangeal formula is the primitive one, 2-3-4-5-4 (contra Stritzke 1983). No clear evidence of sesamoids was discovered ventral to the distal ends of the metatarsals or dorsal to the distal ends of the penultimate phalanges (Gauthier *et al.* 2012: characters 565 and 596).

Comparisons. A strong, flange-like crural process of the calcaneum, like in "*Saniwa*" *feisti*, is also present in *Varanus* and *Saniwa ensidens* (Rieppel & Grande 2007) but smaller in *Heloderma* and absent in *Lanthanotus* (Rieppel 1980a: fig. 10). The preaxial shelf of the fibular articulation on the astragalus is strong in *Varanus* but weak in *Heloderma*.

SYSTEMATIC PALAEONTOLOGY

PHYLOGENETIC RELATIONSHIPS

In MP and BI analyses without molecular data (Fig. 25A and C, respectively), a core necrosaur clade (bootstrap 0.65 in MP, posterior probability 0.69 in BI) comprising "*Saniwa*" *feisti* and a monophyletic *Palaeovaranus* (*cayluxi* + sp. Quercy) forms the sister-group to a clade (bootstrap 0.83 in MP, posterior probability 1.0 in BI) comprised of the Mongolian Cretaceous taxa (*Gobiderma* Borsuk-Białynicka, 1984, *Aiolosaurus* Gao & Norell, 2000, *Estesia*), Helodermatidae and Varanidae. In the strict consensus, *Eosaniwa* is either in a polytomy with the core necrosaur clade (MP) or is the immediate sister-group to the core necrosaur clade (BI). For the first time in a pure morphological analysis, two of the Mongolian Cretaceous taxa (*Aiolosaurus* and *Estesia*) form successive outgroups to Varanidae (posterior probability 0.92 in BI for both clades) to the exclusion of Helodermatidae. Only *Gobiderma* is falls outside of Varanoidea (synonym of Helodermatidae + Varanidae), which has a posterior probability of 0.95 in BI. Notably, in combined analyses of molecules and morphology (Reeder *et al.* 2015; this study) the Mongolia Cretaceous taxa are often determined to be outgroups to Varanidae. The remaining anguimorphs (*Shinisaurus*, *Xenosaurus* and Anguidae, which the extinct glyptosaurines on the stem of crown Anguidae) effectively form a polytomy with the putative varanoid clade.

When molecular data are included, both MP and BI analyses (Fig. 25B and D, respectively) produce a clade comprising *Eosaniwa* and the core necrosaurs, albeit with low support (bootstrap <0.50 in MP, posterior probability 0.67 in BI). That clade, in turn, is the sister-group (with low support) to a clade comprising the Mongolian Cretaceous taxa and crown

TABLE 3. — Unambiguous morphological synapomorphies of selected clades examined in this study. Potential autapomorphies of "*Saniwa*" *feisti* Stritzke, 1983 are very numerous but ambiguous (deltran only) due to missing data in other members of Palaeovaranidae.

Clade	Character	State change	Description
Eosaniwa Haubold, 1977 + "core necrosaurs" ("*Saniwa*" *feisti* Stritzke, 1983, *Palaeovaranus* (Zittel, 1887-1890)	75	2 → 3	Maxilla facial process length rises to >56% of maxilla length
	97	0 → 1	Jugal suborbital ramus becomes deep
	124	1 → 0	Quadrate-pterygoid overlap becomes extensive
	149	1 → 0	Vomerine teeth present
	269	0 → 1	Maxillary tooth count rises to 16-27
	270	1 → 2	Dentary tooth count rises to 21-35
"core necrosaurs" ("*Saniwa*" *feisti*, *Palaeovaranus*)	74	0 → 1	Maxillary anterior alveolar foramen shifts behind crista transversalis
	77	1 → 2	Maxilla facial process apical surface faces anterodorsally
Palaeovaranus	58	0 → 1	Parietal sagittal crest present
	59	0 → 2	Parietal nuchal fossa overgrown by parietal (nearly) to midline

Varanidae, as in previous combined analyses (Hsiang *et al.* 2015; Reeder *et al.* 2015). As in molecular analyses in general, the BI combined analysis produced a monophyletic Neoanguimorpha (posterior probability 0.77; and for *Xenosaurus* + Anguidae, 1.0), but support for Paleoanguimorpha (*Shinisaurus* + Varanidae, including extinct taxa) was especially low.

In no analysis did we find support for a union of "*Saniwa*" *feisti*, *Palaeovaranus* and *Eosaniwa*, or of any part thereof, with Mosasauria, which always fell outside Anguimorpha, and sometimes outside of Squamata. Given that the analysis relied heavily on the matrix of Gauthier *et al.* (2012), this result is not surprising.

There are many ways in which "*Saniwa*" *feisti* differs from *Palaeovaranus* spp. and *Eosaniwa*, but it is often impossible to infer unambiguously at which level apomorphies are diagnostic, because species other than "*Saniwa*" *feisti* are highly incomplete. Unambiguous morphological synapomorphies (under both acctran and deltran models of character evolution), as inferred from combined morphological and molecular analyses, for the clade (*Eosaniwa*, "*Saniwa*" *feisti*, *Palaeovaranus*), for core necrosaurs ("*Saniwa*" *feisti*, *Palaeovaranus*) and for *Palaeovaranus* (*cayluxi* and sp. Quercy) are given in Table 3.

Conrad *et al.*'s (2011b) combined, but not pure morphological, phylogenetic analysis produced a clade comprised of *Palaeovaranus* and "*Saniwa*" *feisti*. *Eosaniwa* was found not to be related to this clade.

We specifically avoided detailed comparisons or analysis of *Palaeovaranus giganteus* from Geiseltal, as this species will be the subject of a later paper. In some ways, such as osteodermal covering, it is more primitive than the species examined here, so it would not be surprising if its tentative attribution to *Palaeovaranus* (Georgalis 2017), consistent with previous attribution to *Necrosaurus* (e.g. Estes 1983), will have to be revisited.

REVISED TAXONOMY

We found support for a core necrosaur clade ("*Saniwa*" *feisti*, *Palaeovaranus* from Quercy) and, in most analyses, including both combined analyses, for a union of this clade with *Eosaniwa*. Therefore we revise the nomenclature of these taxa.

Order SQUAMATA Oppel, 1811

Infraorder ANGUIMORPHA Fürbringer, 1900

COMMENTS

Fürbringer's (1900a) "Beitrag zur Systematik und Genealogie der Reptilien" was apparently extracted, repaginated, and published separately from his "Zur vergleichenden Anatomie des Brustschulterapparates und der Schultermuskeln" (Fürbringer 1900b). With the exception of a small, new introduction to the extract, the works appear to be identical, and although we do not know the precise dates of publication, it seems likely that "Zur vergleichenden Anatomie" precedes the "Beitrag", in which case the former is the proper work to cite (as is usually done).

Family PALAEOVARANIDAE Georgalis, 2017

INCLUDED GENERA. — *Eosaniwa* Haubold, 1977, *Palaeovaranus* von Zittel, 1887-1890, *Paranecrosaurus* n. gen.

EMENDED DIAGNOSIS. — Anguimorph lizards showing the following synapomorphies: maxilla facial process >56% length of maxilla; jugal suborbital ramus deep; quadrate pterygoid overlap extensive; vomerine teeth present; maxillary tooth count >20; and dentary tooth count >20. Additionally, where known: ethmoidal nerve exits through external naris (anterior premaxillary foramina absent); premaxillary nasal process extends more than half-way to frontal; nares not retracted; posterior extension of medial flange of septomaxilla long; both pterygoid and palatine teeth present; palatine-maxillary articulation posteriorly displaced but (probably) not reaching ectopterygoid; and splenial anterior extent *c.* 2/3 of dentary tooth row; at least 5 sternal ribs; scales of torso homogeneous; strongly keeled, oval to rhomboidal, non-imbricate osteoderms present in dorsum, venter, and tail; and ventral scales roughly same size as adjacent laterals.

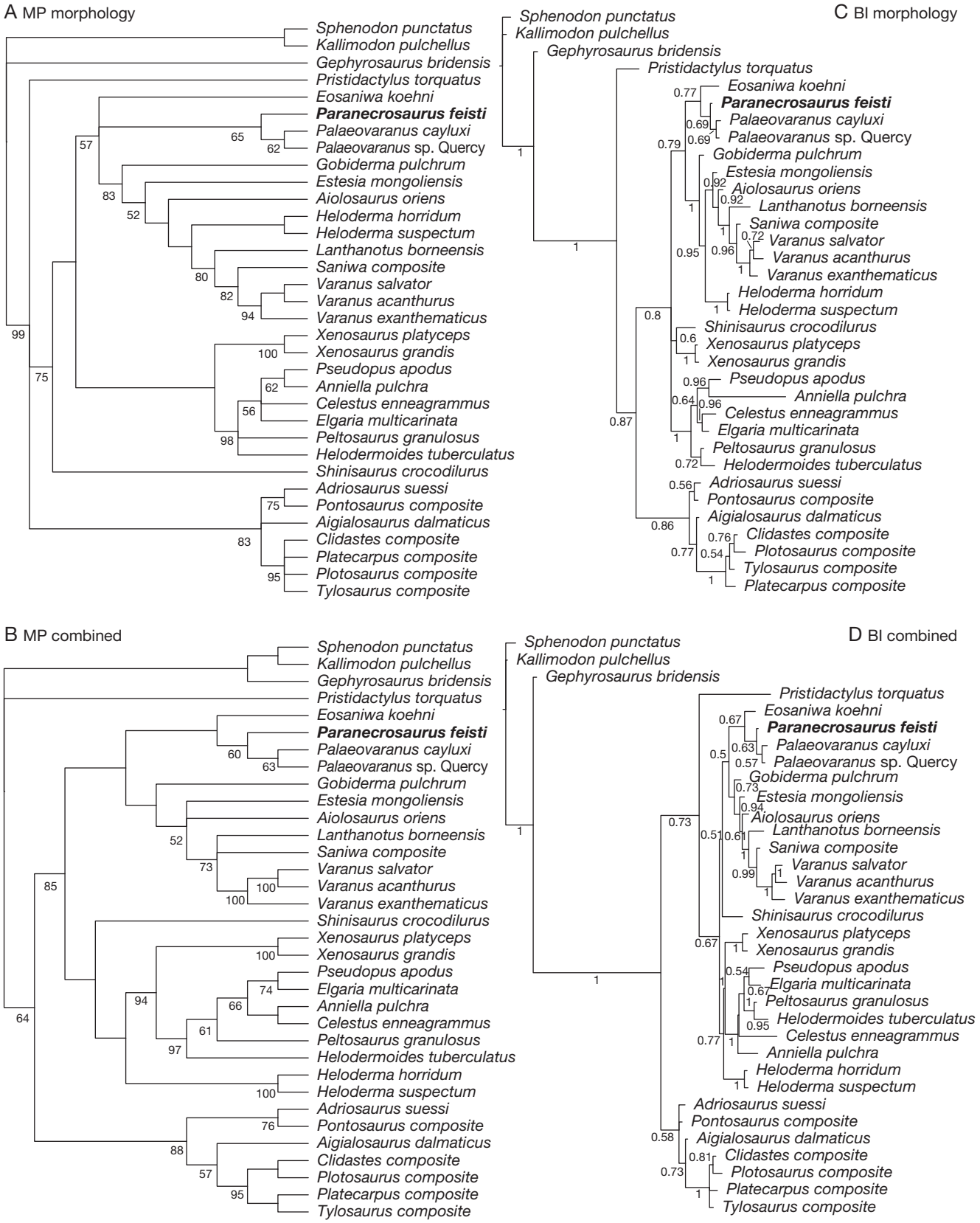

FIG. 25. — Phylogenetic relationships of *Paranecrosaurus feisti* (Stritzke, 1983) n. comb.: **A**, MP analysis of morphology only; **B**, MP analysis of combined data; **C**, BI analysis of morphology only; **D**, BI analysis of combined data. For MP analyses, bootstrap values are shown next to branch (when >50%). For BI analyses, posterior probability is shown next to branch.

Comments
Georgalis (2017) critically reviewed the historical literature on the name *Necrosaurus* and determined that the earliest publications using this name did not make it available in the sense of the International Code of Zoological Nomenclature. The earliest available name is *Palaeovaranus* von Zittel, 1887-1890 (1887-1890), and the corresponding family-level name is Palaeovaranidae Georgalis, 2017. That author only recognized *Palaeovaranus* as a member of the family, not the many other taxa that were assigned to Necrosauridae over the years (Estes 1983; Borsuk-Białynicka 1984; Nessov 1985). Accordingly, his diagnosis of the genus was equivalent to that of the family. Augé's (2005: 276) diagnosis of *Palaeovaranus* comprised the following features: fairly large to large size, ornamented oval osteoderms (tending to disappear in larger species, i.e., *P. cayluxi* – though this presumably refers to the fusion with dermal skull bones, not on body), dorsal origin of jaw adductor musculature on the parietal, parietal without processus descendans at the base of the supratemporal processes, medial crest of facial process of maxilla with an articular facet. Remaining features cited by Estes (1983) he relegated to plesiomorphy.

As noted in the introduction, there is considerable precedent for Stritzke's (1983) reference of "*Saniwa*" *feisti* to Varanidae. The reasons he gave (p. 503-504) were as follows: supratemporal fossa open, premaxilla and parietal azygous, teeth subpleurodont, palatines separated, neural spines of the dorsal and anterior caudal vertebrae tall, and trunk/tail ratio <1. We note that many of these features are plesiomorphic for Anguimorpha.

Until the publication of *Eosaniwa koehni* by Haubold (1977), the squamation of *Palaeovaranus* was a reasonably construed as a unique apomorphy of that taxon. However, *Eosaniwa* shows well-developed, oval, keeled osteoderms (e.g. Rieppel *et al.* 2007) that may have impinged on one another proximodistally (Haubold 1977). The distinctive sculpturing of these osteoderms – consisting of moderately strong ridges that run, on average, perpendicular to the keel and occasionally anastomose to enclose little hollows in which foramina are frequently located – is conceivably derived from something like the weak sculpturing seen in "*Saniwa*" *feisti*. Thus, there is now little known in *Palaeovaranus* osteoderms that could be viewed as autapomorphy.

Genus *Paranecrosaurus* n. gen.

urn:lsid:zoobank.org:act:5FAA51E8-B1A5-4584-AB00-FD6C557DCD1D

Type species. — *Saniwa feisti* Stritzke, 1983.

Etymology. — The eponymous taxon name *Necrosaurus*, originally applied to the species now known as *Palaeovaranus cayluxi*, is widely known. The prefix, *para* (Gr.) means "near".

Distribution and range. — Known only from type area, Middle Messel Formation, early-middle Eocene of Messel, Germany.

Emended diagnosis. — Palaeovaranid with the following combination of characters: nearly all scales keeled; head scales smaller than body scales; two paired, longitudinal rows of enlarged nuchal scales; caudal autotomy planes lacking; two transverse rows of scales per caudal vertebra; parietal nuchal fossa wide and broadly exposed dorsally; lacrimal boss present; supratemporal shelf partly closes supratemporal fenestra from behind; pterygoid teeth arranged as patch; posterior-most mental foramen of dentary enlarged; tooth bases expanded; posterior (secondary) coracoid emargination present; and pectineal tubercle of pubis about equal distance between pubic symphysis and acetabulum. Differs from *Eosaniwa*, among other features, in the shorter snout; narrow, constricted, fused frontals; lower maxillary tooth count; more robust anterior tip of dentary; relatively longer humerus (probably longer limbs overall); less expanded retroarticular process; and smaller size. Differs from *Palaeovaranus cayluxi* and *Palaeovaranus* sp., among other features, in the higher tooth count and lower number of infoldings per tooth (plicidentine poorly developed), tooth crowns not strongly lenticular, the absence of a sagittal crest on the parietal, and the present of broadly exposed nuchal fossae.

Paranecrosaurus feisti (Stritzke, 1983) n. comb.
(Figs 1-24; Appendices 1-11)

Saniwa feisti Stritzke, 1983: 498. — Augé 2005: 263.

"*Saniwa*" *feisti* Rage & Augé 1993: 203. — Rieppel *et al.* 2007: 768. — Conrad *et al.* 2011b: 36.

Necrosaurus feisti – Smith *et al.* 2018c: 139.

Holotype. — HLMD-Me 13709, Specimen A in Stritzke (1983): nearly complete skeleton preserved in mostly dorsal view (Appendix 4).

Paratype. — Specimen B in Stritzke (1983), the part of which is now SMNK-Me 1124: partial, partially disarticulated skeleton (Appendix 5).

Referred specimens. — SMF-ME 10954: complete skeleton preserved in dorsal view (Appendices 1; 2); the Pohl-Perner specimen: nearly complete skeleton (Appendix 3).

Distribution and range. — As for genus.

Diagnosis. — As for genus.

Comments
Keller & Schaal (1988), amongst others (e.g. Georgalis 2017), have already cast doubt on the original referral of this species to *Saniwa* and suggested that the species pertained to a separate genus that they named "Genus B". Smith *et al.* (2018c), in a book completed before publication of Georgalis (2017), referred to the species as "*Necrosaurus feisti*". It has not yet formally been transferred (using the term "n. comb." or similar).

AUTECOLOGY OF *PARANECROSAURUS FEISTI* N. COMB.

Locomotion and habitat
Preliminary data visualization using histograms demonstrated that *Paranecrosaurus feisti* n. comb. diverges in its body proportions from the *Varanus* spp. in the extant dataset.

The SVL ratio of *P. feisti* n. comb. is at the low end (presumably due to its short neck), whereas its head length and especially width ratios fall outside the distribution of extant species. Head width, notably, is the least well-constrained variable in *P. feisti* n. comb. Both forelimb lengths fall outside the upper end of the distribution of extant species, as does lower hind limb length.

PCA with and without *Paranecrosaurus feisti* n. comb. produced quite different results, but for the purposes of this study equally uninformative. Without *P. feisti* n. comb., only two PCs had a variance >1, and these two accounted for over 86% of the total variance. With *P. feisti* n. comb., only two PCs had a variance >1, and they accounted for over 85% of the total variance. In the latter analysis, *P. feisti* n. comb. plots well outside the 95% confidence ellipses of the two *Varanus* ecomorphs with sufficient sample size (plots of PC1-PC2, PC1-PC3, and PC2-PC3), suggesting it occupies a distinct region of morphospace.

On the other hand, the LDA as applied to the training dataset (modern *Varanus*), when used to predict the autecology of *Paranecrosaurus feisti* n. comb., gave unambiguous results. The fossil species is predicted to be a "widely foraging" animal with a posterior probability near 1.0. Other categories had a negligible ($<1 \times 10^5$) posterior probability. Because the sample size of observations (species) is relatively low (only 2×) compared to the number of predictor variables, the results should be taken with caution. Still, long limbs, especially the distal units of the long limbs, are considered to be an adaptation for rapid locomotion (and hence covering large distance in a short time) in mammals (Hildebrand & Goslow 1998), and our result is therefore consistent with the very long limbs, and especially the long distal units, in *P. feisti* n. comb.. That *P. feisti* n. comb. is not predicted to have been semiaquatic is consistent with the apparently rounded tail, whereas the tail is frequently (but not always) laterally compressed in semiaquatic *Varanus* (Mertens 1942c).

Christian & Garland (1996) noted that in *Varanus*, which rely on stamina rather than sprinting, the fore- and hindlimbs are more similar in size. In particular, the hindlimb/forelimb length ratio was normally around 1.35 or less, slightly lower in smaller monitors and slightly higher in larger monitors. Measured as in Thompson & Withers (1997) we find that extant *Varanus* have a mean ratio of 1.36 (standard deviation 0.07), and *Paranecrosaurus feisti* n. comb., at 1.38, is a little above the mean and well within the distribution. We also find that the hindlimb/forelimb length ratio is weakly positively correlated with body size (here measured as thorax length), and that *P. feisti* n. comb. has a ratio like *Varanus* of similar size. In contrast, iguanians (other than chameleons), the faunivores among which are mostly ambush predators, tend to have higher ratios (Garland unpubl., *in* Christian & Garland 1996).

While it must be born in mind that *Paranecrosaurus feisti* n. comb. is not in the crown of Varanidae, much less of *Varanus*, and in some features (like its shorter neck and especially long limbs) it falls outside the morphologies seen today in *Varanus* (based on data given in Mertens 1942b), these results are consistent with the interpretation of a widely foraging predator. In African monitors, the behavior of some species varies during the year, foraging widely when conditions are adverse (dry season), but staying more sedentary when food is abundant (wet season) (see contributions in Pianka *et al.* 2004). The climate at Messel is thought to have shown seasonality with respect to temperature and, more clearly, precipitation (Grein *et al.* 2011). Thus it is conceivable that *P. feisti* n. comb. displayed similar behavioral plasticity. However, it is also possible that *P. feisti* n. comb. was more specialized in its food preferences, requiring it to forage more widely.

Sensory physiology

It was noted above that the labial and mental foramina are very numerous in *Paranecrosaurus feisti* n. comb. The inferior and superior alveolar nerves send numerous fine branches through these foramina, from which fibers fan out to innervate the skin of the lips (Watkinson 1906; Willard 1915; Oelrich 1956). It is thought that these are principally somatic sensory fibers, unlike those coming with the palatine branch of the facial nerve (Willard 1915; Adams 1942; Bellairs 1949). It seems likely, although it has not to our knowledge been demonstrated anatomically, that these fibers of the alveolar nerves innervate the scale organs, which in iguanian and varanid lizards and other squamates are particularly numerous on the head and especially the snout and lips (Miller & Kasahara 1967; Maclean 1980; Matveyeva & Ananjeva 1995). In examined *Varanus*, the scale organs ("sensory plaques" of Miller & Kasahara 1967) are particularly numerous on the head and invested with numerous expanded sensory terminals of nerve fibres (Miller & Kasahara 1967). Scale organs are considered to be tactile sensory organs (Miller & Kasahara 1967; Sherbrooke & Nagle 1996).

The size of a foramen may be correlated with the number of nerve fibers that pass through it, allowing inferences about the sensory biology of extinct species (e.g. Muchlinski 2008). For instance, Scanferla & Smith (2020) used foramen size to infer the presence of pit organs, sensitive to radiant heat, in the extinct booid snake *Eoconstrictor fischeri* from Messel. It is tempting, therefore, to hypothesize that the high number of labial foramina in *Paranecrosaurus feisti* n. comb. indicates an abundance of scale organs and a particularly sensitive snout. However, certain steps will be necessary to study the problem: 1) determining the course of the afferent neurons stimulated by the receptors in the scale organs (i.e., whether they are really associated with the alveolar nerves); and 2) establishing a correlation between the number of scale organs and the number or total size of the labial foramina.

Diet and feeding biology

In only one specimen, the Pohl-Perner specimen, could contents of the digestive tract be identified. It contains a small lizard with a skull length of 15.8 mm. The specimen is primarily preserved on the counterpart, where it lies between the ventral surface of the vertebrae of *Paranecrosaurus feisti* n. comb. and the ventral osteoderms (Fig. 26A, B). It is thus quite certain

that it was contained in the body of *P. feisti* n. comb. Based on size and a suite of morphological features, such as the fine dermal sculpture, the constriction of the supratemporal fenestra by the postorbitofrontal, the fine frontoparietal and coarser interfrontal interdigitations, the reduced lateral concha of the quadrate, and the short tooth row (11 positions) with enlarged posterior teeth (Fig. 26C), we identify the lizard as *Cryptolacerta hassiaca* Müller, Hipsley, Head, Kardjilov, Hilger, Wuttke & Reisz, 2011[112], only the second-known specimen of this species. Apart from the skull, associated metapodial elements and a couple of vertebrae of the small prey lizard could be identified, but strangely no more. It is possible, but difficult to establish with certainty, that the individual of *C. hassiaca* had been dismembered prior to ingestion.

The bones of the skull are well preserved with uncorroded exterior surfaces, so it is unlikely that the small lizard had been long in the body of the large one (see also Smith & Scanferla 2016). However, the teeth of the small lizard are poorly preserved. The digitally segmented dentary has teeth that taper strongly apically (are conical), and in some cases the pulp cavity may even be open (Fig. 25C). In any case, the distal dentary teeth do not display the bicuspid pattern seen in the holotype (pers. obs. of new CT scan). This cannot be ascribed to lower density of tooth tips, or to failure to fully segment those tips, because the tooth tips in lizards have much thicker enamel and should therefore show *greater* density contrast than the shafts.

Smith *et al.* (in press) distinguish between enteric and gastric digesters among gnathostome carnivores. In the former, a large proportion of the digestion takes place in the small intestine, and members with known physiology (mammalian carnivores) are characterized by a gastric fluids with higher acidity (lower pH) and lower digestive enzyme content. The latter, represented by part of Avialae, are characterized by gastric fluids with higher digestive enzyme content (and frequently lower acidity, or higher pH). These end-member physiologies have different effects on the pleurodont teeth of lizard prey (Smith *et al.* in press). In enteric digesters, the higher acidity in the stomach preferentially destroys the tooth crowns (which are not protected by the gingiva). Therefore, the preferential destruction of the tooth crowns in the *Cryptolacerta* prey are consistent with a high-acid, low-enzyme physiology. *Paranecrosaurus feisti* n. comb. would accordingly be an enteric digester, as expected given its phylogenetic position.

Gut contents could have been present in HLMD-Me 13709 but lost during preparation. SMNK-Me 1124, in turn, is disarticulated, and the posterior trunk vertebrae, pelvic girdles and appendages, and tail are missing; those facts, together with preparation, could explain the lack of gut contents here. Insect remains are known from many lower vertebrates at Messel, including lizards (Weber 2004; Smith & Wuttke 2012), but only in SMF-ME 10954 can we reasonably expect to find them if they were present. Consequently, sample size (2) is far too low to draw any reliable conclusions about the proportion of vertebrates versus invertebrates in the prey spectrum of *Paranecrosaurus feisti* n. comb.

Intramandibular joint

One of the classic features of the lower jaw of *Lanthanotus*, mosasaurs and snakes is a well-developed intramandibular hinge in which the overlap of dentary with post-dentary bones is reduced and the splenial and angular articulate via a ball-and-socket joint (Rieppel & Zaher 2000b). It is generally regarded as an important adaptation allowing the jaws to open more widely, thus facilitating the ingestion of larger – especially vertebrate – prey. Such a well-developed hinge (see Mandible), is not present in *Paranecrosaurus feisti* n. comb. Furthermore, there is little evidence of the lesser modifications seen in *Varanus* and *Heloderma*. *P. feisti* n. comb. merely shows the pinched angular at the ventral jaw margin but not its deep intrusion between splenial and dentary nor the reduced posterior portion of the splenial. Still, Frazzetta (1962: 293) and Gauthier (1982) have emphasized that movement can occur at the intramandibular joint by a bending of the elastic bones that span the joint, namely angular and splenial, so that even if a well-defined hinge is not present, some mobility is possible. Several lines of evidence – reduction of certain articulations in *P. feisti* n. comb. (such as between coronoid and dentary), the "pinched" angular, and the ventral displacement in death of the surangular-angular unit in two of four specimens – indeed suggest a limited degree of intramandibular movement in *P. feisti* n. comb..

Summary of hypotheses

Pough (1973) found that while smaller lizards (<300 g body mass) were generally insectivorous, larger lizards (>300 g body mass) tended to become herbivorous. When they stayed faunivorous, they either specialized on other lizards, showed morphological adaptations to reduce the energetic expense of food capture (chameleons), or showed adaptations to enable them to capture and subdue more energetic prey like mammals and birds (Varanidae). He explained his observation with energetics: as body size increases, the energetic returns on catching small insect prey are diminished, so that a shift to plants (which do not run away) or vertebrates (which offer greater energetic returns) is favored. On the other hand, Losos & Greene (1988) questioned the generality of this hypothesis, noting that some *Varanus* species exclusively take invertebrate, chiefly insect, prey, and occasional carnivory may be a primitive aspect of the feeding biology of Anguimorpha. For an example of competing hypotheses, see Čerňanský *et al.* (2015).

As a relatively large lizard (Table 2) with conical, recurved teeth, *Paranecrosaurus feisti* n. comb. would be expected to be at least partly carnivorous, and known gut contents (the lizard *Cryptolacerta hassiaca*) are consistent with this. That the only known prey item was probably semifossorial (Müller *et al.* 2011) suggests the possibility that *P. feisti* n. comb. might have been more specialized in its dietary preferences, which could have required a widely foraging strategy, as suggested by morphometric data. Furthermore, if the snout was as sensitive as tentatively inferred from the labial foramina, it may have served to assist foraging in leaf litter for both invertebrates and cryptozoic vertebrates. Nevertheless, available data on the autecology of *P. feisti* n. comb. remain meagre, and new

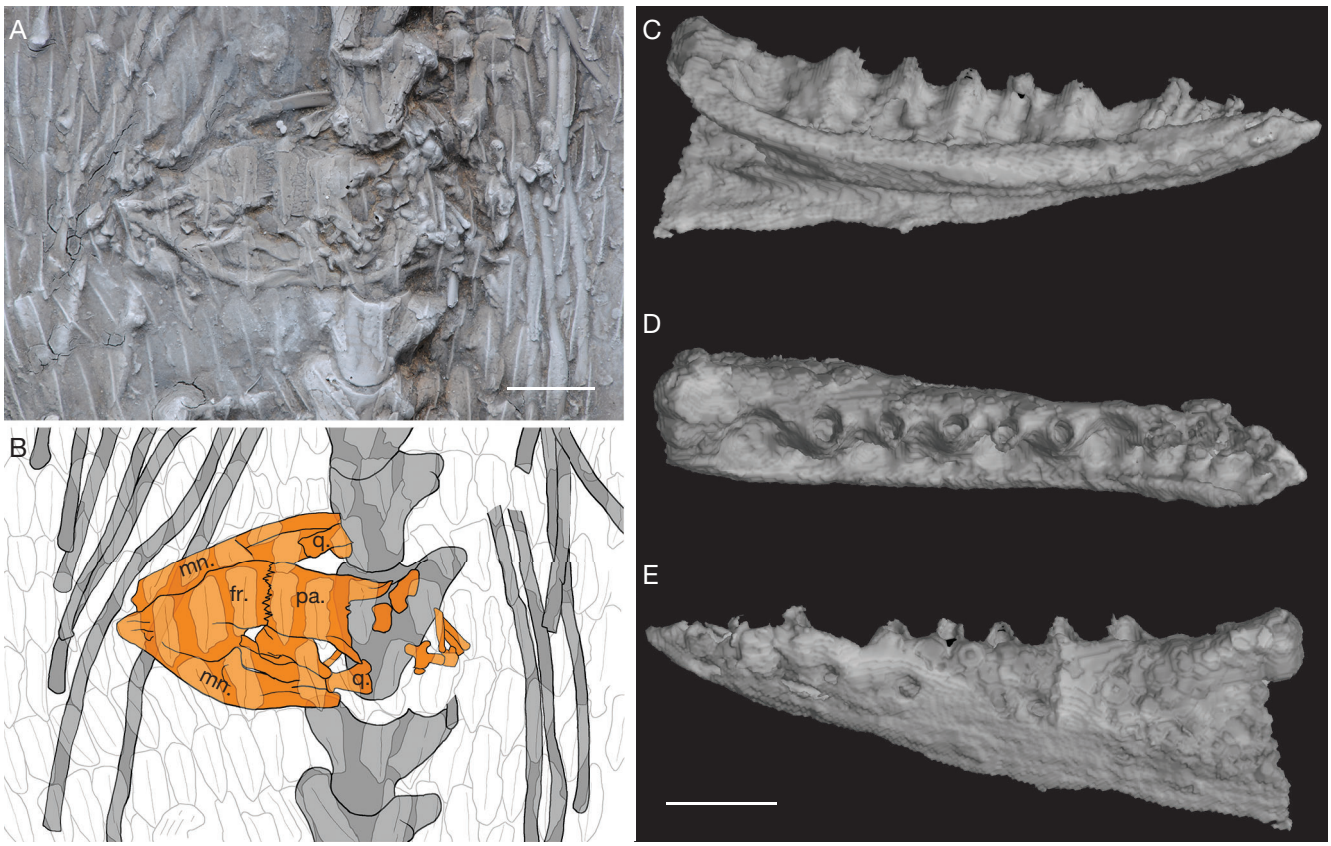

FIG. 26. — **A**, **B**, Photograph and interpretive drawing, respectively, of the skull of *Cryptolacerta hassiaca* Müller, Hipsley, Head, Kardjilov, Hilger, Wuttke & Reisz, 2011, seen in dorsal view (**orange**), in the gut of *Paranecrosaurus feisti* (Stritzke, 1983) n. comb. (Perner specimen, counterpart), seen in ventral view. Bones of *Paranecrosaurus feisti* n. comb. are shown in **gray**. Belly osteoderms of *Paranecrosaurus feisti* n. comb. are rendered semi-translucent and overlie the skull of *Cryptolacerta hassiaca*. **C**-**E**, Segmented left dentary of *C. hassiaca* in medial, dorsal and lateral views, respectively. Abbreviations: **fr.**, frontal; **mn.**, mandible; **pa.**, parietal; **q.**, quadrate. Scale bars: A, 5 mm; C-E, 1 mm.

specimens, especially those with preserved gut contents, would be important to further test these ideas. Additionally, the significance of the hyoid apparatus for swallowing and potential trade-offs in inertial feeding (Smith 1986) should be further explored. Finally, continuing work on microwear on lizard teeth (Winkler *et al.* 2019) might help elucidate the diet of *P. feisti* n. comb. over short time-scales.

CONCLUSIONS

Morphological evidence has universally supported a sister-group relationship between the extant carnivorous groups Varanidae and *Heloderma* since the advent of formal phylogenetic analyses (Pregill *et al.* 1986). In contrast, molecular evidence has supported their separation, with Varanidae part of an Asian clade (Paleoanguimorpha) and *Heloderma* part of a North American clade (Neoanguimorpha) (e.g. Vidal *et al.* 2012). The molecular tree implies that the derived features shared by Varanidae and *Heloderma* arose in parallel. In some, but not all (Gauthier *et al.* 2012), cases these features can be interpreted as adaptations to a carnivorous diet and potentially arose in parallel also in Mosasauria and/or Serpentes.

In the foregoing combined-evidence analyses, Palaeovaranidae, including *Paranecrosaurus feisti* n. comb., was inferred to be a stem representative of Varanidae, basal to the Cretaceous taxa from Mongolia like *Aiolosaurus*. Indeed, it is primitive with respect to Varanidae in most characters that have classically been viewed as synapomorphies of Varanoidea: nares not retracted, plicidentine poorly developed, and tooth row not reduced in extent. Palaeovaranidae share some distinctive apomorphic characters with Varanidae and/or *Shinisaurus*, such as the shape of the palpebral and the presence of cervical hypapophyses. Yet *P. feisti* n. comb., despite its extraordinary preservation, is insufficient to resolve the conflict between morphological and molecular evidence; that is, morphology-only analyses continue to result in a monophyletic Varanoidea, and combined analyses continue to result in a polyphyletic Varanoidea. If the molecular topology is correct, a reconciliation with morphology will require the discovery of equally primitive stem representatives of *Heloderma*, i.e., more primitive than *Eurheloderma*.

If the inferred phylogenetic position of Palaeovaranidae as a basal member of the total clade of Varanidae is correct, then *Paranecrosaurus feisti* n. comb. offers new insight into the evolution of that clade. Losos & Greene (1988) concluded that the common ancestor of ("a primitive") *Varanus* was

characterized as follows: "it hunted over wide areas, occasionally climbing trees and entering water; it used chemoreception to search for hidden prey in particular microhabitats; it fed frequently on large numbers of relatively small prey; the occasional ingestion of relatively larger vertebrates, perhaps as carrion, was energetically significant; and the latter perhaps involved dismemberment prior to ingestion" (p. 397). Insofar as the autecology of *P. feisti* n. comb. could be illuminated, it largely corresponds to this description. The extent of chemoreception could not be addressed, but we have suggested that tactile sense may have been enhanced with respect to many other anguimorphs.

The significance of *Paranecrosaurus feisti* n. comb. may then lie in suggesting that these aspects of feeding biology were primitive for the total clade of Varanidae, and that the divergent autecology of *Lanthanotus* (Losos & Greene 1988) is derived. While the latter point may at one time have seemed obvious, molecular data support Paleoanguimorpha, and *Shinisaurus* and *Lanthanotus* share an affinity for water and sit-and-wait predation. It further suggests that certain soft-tissue modifications – the "fibrous connection" of Pregill *et al.* (1986) – may have permitted a degree of movement between the dentary and postdentary bones, despite the lack of evidence of osteological modifications. This observation may be significant in understanding the evolution of an intramandibular hinge in Varanidae, *Heloderma*, snakes and mosasaurs. Losos & Greene (1988) noted that even in many *Varanus* known to take vertebrate prey, invertebrates still dominate numerically. Even so, they noted that the contribution of vertebrate prey to total energy intake can be very high, disproportionate to abundance, due to the generally larger body size of vertebrates. In this context, the framework of "fallback foods" (Marshall & Wrangham 2007) may be useful. Vertebrate prey may be considered "important" if they contributed to a significant proportion of energy intake (Losos & Greene 1988). For the same reason they are likely to have been "preferred" and so cannot be considered fallback foods. Marshall & Wrangham (2007) stated that, in primates, selection to exploit preferred foods will tend to enhance sensory and locomotory abilities (to find them), whereas selection to exploit fallback foods will tend to enhance food processing abilities (because of their low quality). If vertebrate prey such as lizards weighed high in importance and preference for basal stem varanids, selection may still have acted to enhance intramandibular mobility, even if feeding events were rare.

Acknowledgements
Financial support for this work came from the Senckenberg Research Institute and the Texas Memorial Museum to KTS, National Science Foundation grant DEB-0235628 to M. Kearney and O. Rieppel, and the Ermann Foundation to JH. KTS also received funding through SYNTHESYS (FR-TAF-218), which was made available by the European Community Research Infrastructure Action under the FP7 "Structuring the European Research Area" Programme. Eberhard "Dino" Frey (SMNK), Norbert Micklich (HLMD), H.-D. Sues (USNM), K. de Queiroz (USNM) and T. Daeschler (ANSP) generously provided access to specimens in their care. We are grateful to Achim Tandler and the late Manfred Keller for help in sorting out the full array of specimens from Messel, and to Dr. Burkhard Pohl and Thomas Perner for access to privately held specimens. T. Rowe and J. Maisano (University of Texas at Austin) kindly made available the CT scan of *Eosaniwa koehni*. We thank G. Georgalis, O. Rieppel, R. Sprackland and K. de Queiroz for discussion, and one anonymous reviewer and A. Čerňanský for their constructive criticism.

REFERENCES

Adams W. E. 1942. — Observations on the lacertilian sympathetic system. *Journal of Anatomy* 77 (1): 6-11.
Augé M. 2005. — Évolution des lézards du Paléogène en Europe. *Mémoires du Muséum National d'Histoire Naturelle* 192: 1-369.
Barrows S. & Smith H. M. 1947. — The skeleton of the lizard *Xenosaurus grandis* (Gray). *University of Kansas Science Bulletin* 31, part II (12): 227-281.
Behnke C., Eikamp H. & Zollweg M. 1986. — *Die Grube Messel: Paläontologische Schatzkammer und unersetzliches Archiv für die Geschichte des Lebens; Geologie, Bergbaugeschichte, Fossilien*. Goldschneck, Korb, 168 p.
Bellairs A. D. A. 1949. — Observations on the snout of *Varanus*, and a comparison with that of other lizards and snakes. *Journal of Anatomy* 83 (2): 116-147.
Bellairs A. D. A. & Boyd J. D. 1947. — The lachrymal apparatus in lizards and snakes. The brille, the orbital glands, lachrymal canaliculi and origin of the lachrymal duct. *Proceedings of the Zoological Society of London* 117: 81-108. https://doi.org/10.1111/j.1096-3642.1947.tb00500.x
Bernstein P. 1999. — Morphology of the nasal capsule of *Heloderma suspectum* with comments on the systematic position of helodermatids (Squamata: Helodermatidae). *Acta Zoologica* 80: 219-230. https://doi.org/10.1046/j.1463-6395.1999.00020.x
Bever G. S., Bell C. J. & Maisano J. A. 2005. — The ossified braincase and cephalic osteoderms of *Shinisaurus crocodilurus* (Squamata, Shinisauridae). *Palaeontologia Electronica* 8 (1): 1-36.
Bhullar B.-A. S. 2011. — The power and utility of morphological characters in systematics: a fully resolved phylogeny of *Xenosaurus* and its fossil relatives (Squamata: Anguimorpha). *Bulletin of the Museum of Comparative Zoology* 160 (3): 65-181. https://doi.org/10.3099/0027-4100-160.3.65
Bhullar B.-A. S. & Smith K. T. 2008. — Helodermatid lizard from the Miocene of Florida, the evolution of the dentary in Helodermatidae, and comments on dentary morphology in Varanoidea. *Journal of Herpetology* 42 (2): 286-302. https://doi.org/10.1670/07-185.1
Blob R. W. 1998. — Evaluation of vent position from lizard skeletons for estimation of snout–vent length and body mass. *Copeia* 1998 (3): 792-801. https://doi.org/10.2307/1447817
Borsuk-Białynicka M. 1984. — Anguimorphans and related lizards from the Late Cretaceous of the Gobi Desert, Mongolia. *Palaeontologia Polonica* 46: 5-105.
Caldwell M. W. 2012. — A challenge to categories: "What, if anything, is a mosasaur?". *Bulletin de la Société Géologique de France* 183 (1): 7-34. https://doi.org/10.2113/gssgfbull.183.1.7
Camp C. L. 1923. — Classification of the lizards. *Bulletin of the American Museum of Natural History* 48 (11): 289-481.
Camp C. L. 1942. — California mosasaurs. *Memoirs of the University of California* 13 (1): 1-68.
Čerňanský A., Smith K. T. & Klembara J. 2014. — Variation in the position of the jugal medial ridge among lizards (Reptilia: Squamata): its functional and taxonomic significance. *Anatomical Record* 297: 2262-2272. https://doi.org/10.1002/ar.22989

ČERŇANSKÝ A., KLEMBARA J. & SMITH K. T. 2015. — Fossil lizard from central Europe resolves the origin of large body size and herbivory in giant Canary Island. *Zoological Journal of the Linnean Society* 176 (4): 861-877. https://doi.org/10.1111/zoj.12340

CHRISTIAN A. & GARLAND JR. T. 1996. — Scaling of limb proportions in monitor lizards (Squamata: Varanidae). *Journal of Herpetology* 30 (2): 219-230. https://doi.org/10.2307/1565513

CONRAD J. L. 2004. — Skull, mandible, and hyoid of *Shinisaurus crocodilurus* Ahl (Squamata, Anguimorpha). *Zoological Journal of the Linnean Society* 141 (3): 399-434. https://doi.org/10.1111/j.1096-3642.2004.00128.x

CONRAD J. L. 2006a. — An Eocene shinisaurid (Reptilia, Squamata) from Wyoming, U.S.A. *Journal of Vertebrate Paleontology* 26 (1): 113-126. https://doi.org/cggh78

CONRAD J. L. 2006b. — Postcranial skeleton of *Shinisaurus crocodilurus* (Squamata: Anguimorpha). *Journal of Morphology* 267: 759-775. https://doi.org/10.1002/jmor.10291

CONRAD J. L. 2008. — Phylogeny and systematics of Squamata (Reptilia) based on morphology. *Bulletin of the American Museum of Natural History* 310: 1-182. https://doi.org/10.1206/310.1

CONRAD J. L. & NORELL M. A. 2007. — A complete Late Cretaceous iguanian (Squamata, Reptilia) from the Gobi and identification of a new iguanian clade. *American Museum Novitates* 3584: 1-47. https://doi.org/10.1206/0003-0082(2007)3584[1:ACLCIS]2.0.CO;2

CONRAD J. L., RIEPPEL O., GAUTHIER J. A. & NORELL M. A. 2011a. — Osteology of *Gobiderma pulchrum* (Monstersauria, Lepidosauria, Reptilia). *Bulletin of the American Museum of Natural History* 362: 1-88. https://doi.org/10.1206/740.1

CONRAD J. L., AST J. C., MONTANARI S. & NORELL M. A. 2011b. — A combined evidence phylogenetic analysis of Anguimorpha (Reptilia: Squamata). *Cladistics* 27: 230-277. https://doi.org/10.1111/j.1096-0031.2010.00330.x

COPE E. D. 1892. — The osteology of the Lacertilia. *Proceedings of the American Philosophical Society* 30: 185-221. http://www.jstor.org/stable/983170

COPE E. D. 1898. — The crocodilians, lizards, and snakes of North America. *Report of the U.S. National Museum* [1898]: 153-1270.

DE AVILA PIRES T. C. S. 1995. — Lizards of Brazilian Amazonia (Reptilia: Squamata). *Zoologische Verhandellingen* 299: 1-706.

DE FEJÉRVÁRY G. J. 1918. — Contributions to a monography on fossil Varanidae and on Megalanidae. *Annales Historico-Naturales Musei Nationalis Hungarici* 16: 341-467.

DE FEJÉRVÁRY G. J. 1935. — Further contributions to a monograph of the Megalanidae and the fossil Varanidae - with notes on recent varanians. *Annales Musei Nationalis Hungarici, Pars Zoologica* 29: 1-130.

DE QUEIROZ K. 1987. — Phylogenetic systematics of iguanine lizards: a comparative osteological study. *University of California Publications in Zoology* 118: 1-203. https://doi.org/10.5962/bhl.title.4857

DE STEFANO G. 1903. — I sauri del Quercy appartenenti alla collezione Rossignol. *Atti della Società italiana di Scienze naturali e del Museo civico di Storia naturale in Milano* 42: 382-418.

DEBRAGA M. & CARROLL R. L. 1993. — The origin of mosasaurs as a model of macroevolutionary patterns and processes, *in* HECHT M. K., MACINTYRE R. J. & CLEGG M. T. (eds), *Evolutionary Biology*, vol. 27. Springer, Boston: 245-322. https://doi.org/10.1007/978-1-4615-2878-4_7

EDMUND A. G. 1960. — Tooth replacement phenomena in the lower vertebrates. *Royal Ontario Museum, Life Sciences Division, Contributions* 52: 1-190. https://doi.org/10.5962/bhl.title.52196

ESTES R. 1983. — *Sauria Terrestria, Amphisbaenia (Handbuch der Paläoherpetologie, v. 10A)*. Gustav Fischer Verlag, Stuttgart, Handbuch der Paläoherpetologie, 249 p.

ESTES R., DE QUEIROZ K. & GAUTHIER J. A. 1988. — Phylogenetic relationships within Squamata, *in* ESTES R. & PREGILL G. K. (eds), *Phylogenetic Relationships of the Lizard Families*. Stanford University Press, Stanford: 119-281.

ETHERIDGE R. 1965. — The Abdominal Skeleton of Lizards in the Family Iguanidae. *Herpetologica* 21 (3): 161-168. https://www.jstor.org/stable/3891103

EVANS S. E. 2008. — The skull of lizards and tuatara, *in* GANS C., GAUNT A. S. & ADLER K. (eds), *Biology of the Reptilia, v. 20 (Morphology H). The Skull of Lepidosauria*. Society for the Study of Amphibians and Reptiles, Ithaca, New York: 1-347.

EVANS S. E. & BARBADILLO L. J. 1998. — An unusual lizard (Reptilia: Squamata) from the Early Cretaceous of Las Hoyas, Spain. *Zoological Journal of the Linnean Society* 124 (3): 235-265. https://doi.org/10.1111/j.1096-3642.1998.tb00576.x

EVERHART M. J. 2005. — *Oceans of Kansas: A Natural History of the Western Interior Sea*. Indiana University Press, Bloomington, Indiana, 322 p.

FILHOL H. 1873a. — Sur les vertèbrés fossiles trouvés dans les dépôts de phosphate de chaux du Quercy. *Bulletin de la Société philomathique de Paris* 10: 85-89.

FILHOL H. 1873b. — Sur des pièces fossiles provenant de Batraciens, de Lacertiens et d'Ophidiens, trouvées dans les dépôts de phosphate de chaux de l'Aveyron. *Comptes Rendus Hebdomadaires des Séances de l'Académie des Sciences* 77: 1556-1557.

FILHOL H. 1877. — *Recherches sur les Phosphorites du Quercy; Étude des fossiles qu'on y rencontre et spécialement des mammifères*. G. Masson, Paris, 561 p.

FRANZEN J. L. & FREY E. 1993. — *Europolemur* completed. *Kaupia* 3: 113-130.

FRAZZETTA T. H. 1962. — A functional consideration of cranial kinesis in lizards. *Journal of Morphology* 111: 287-319. https://doi.org/10.1002/jmor.1051110306

FROST D. R. & ETHERIDGE R. 1989. — A phylogenetic analysis and taxonomy of iguanian lizards (Reptilia: Squamata). *Miscellaneous Publications, University of Kansas Museum of Natural History* 81: 1-65. https://doi.org/10.5962/bhl.title.16288

FÜRBRINGER M. 1900a. — Beitrag zur Systematik und Genealogie der Reptilien. *Jenaische Zeitschrift für Naturwissenschaft (Neue Folge)* 27: 597-685.

FÜRBRINGER M. 1900b. — Zur vergleichenden Anatomie des Brustschulterapparates und der Schultermuskeln. *Jenaische Zeitschrift für Naturwissenschaft* 34: 215-718. https://doi.org/10.5962/bhl.title.15346

GAO K. & NORELL M. A. 1998. — Taxonomic revision of *Carusia* (Reptilia: Squamata) from the Late Cretaceous of the Gobi Desert and phylogenetic relationships of anguimorphan lizards. *American Museum Novitates* 3230: 1-51. http://hdl.handle.net/2246/3367

GAO K. & NORELL M. A. 2000. — Taxonomic composition and systematics of Late Cretaceous lizard assemblages from Ukhaa Tolgod and adjacent localities, Mongolian Gobi Desert. *Bulletin of the American Museum of Natural History* 249: 1-118. https://doi.org/bzjf3n

GAUTHIER J., KEARNEY M., MAISANO J. A., RIEPPEL O. & BEHLKE A. 2012. — Assembling the squamate tree of life: Perspectives from the phenotype and the fossil record. *Bulletin of the Peabody Museum of Natural History* 53: 3-308. https://doi.org/10.3374/014.053.0101

GAUTHIER J. A. 1982. — Fossil xenosaurid and anguid lizards from the early Eocene Wasatch Formation, southeast Wyoming, and a revision of the Anguioidea. *Contributions to Geology, University of Wyoming* 21 (1): 7-54.

GAUTHIER J. A., ESTES R. & DE QUEIROZ K. 1988. — A phylogenetic analysis of Lepidosauromorpha, *in* ESTES R. & PREGILL G. K. (eds), *Phylogenetic Relationships of the Lizard Families*. Stanford University Press, Stanford: 15-98.

GEORGALIS G. L. 2017. — *Necrosaurus* or *Palaeovaranus*? Appropriate nomenclature and taxonomic content of an enigmatic fossil lizard clade (Squamata). *Annales de Paléontologie* 103 (4): 293-303. https://doi.org/10.1016/j.annpal.2017.10.001

GEORGALIS G. L., ČERŇANSKÝ A. & KLEMBARA J. 2021. — Osteological atlas of new lizards from the Phosphorites du Quercy (France), based on historical, forgotten, fossil material. *Geodiversitas* 43 (9): 219-293. https://doi.org/10.5252/geodiversitas2021v43a9

GILMORE C. W. 1922. — A new description of *Saniwa ensidens* Leidy, an extinct varanid lizard from Wyoming. *Proceedings of the United States National Museum* 60 (23): 1-28. https://doi.org/10.5479/si.00963801.60-2418.1

GILMORE C. W. 1928. — Fossil lizards of North America. *Memoirs of the National Academy of Sciences* 22: 1-201.

GILMORE C. W. 1942. — Paleocene Faunas of the Polecat Bench Formation, Park County, Wyoming. Part II. Lizards. *Proceedings of the American Philosophical Society* 85 (2): 159-167. https://www.jstor.org/stable/985014

GOTH K. 1990. — Der Messeler Ölschiefer - ein Algenlaminit. *Courier Forschungsinstitut Senckenberg* 131: 1-141.

GREIN M., UTESCHER T., WILDE V. & ROTH-NEBELSICK A. 2011. — Reconstruction of the middle Eocene climate of Messel using palaeobotanical data. *Neues Jahrbuch für Geologie und Paläontologie, Abhandlungen* 260 (3): 305-318. https://doi.org/10.1127/0077-7749/2011/0139

HAINES R. W. 1942. — The tetrapod knee joint. *Journal of Anatomy* 76 (3): 270-301.

HALLERMANN J. 1994. — Zur Morphologie der Ethmoidalregion der Iguania (Squamata) - Eine vergleichend-anatomische Untersuchung. *Bonner Zoologische Monographien* 35: 1-133.

HARMS F.-J. 2000. — Arbeitsgruppe 1: Grabung und Präparation. *Natur und Museum* 130 (9): 307.

HARMS F.-J., ROSENBERG F., ADERHOLD G., NIX T. & HOFFMANN I. 1999. — Erläuterungen zur Grube Messel bei Darmstadt, Südhessen, *in* HOPPE A. & STEININGER F. F. (eds), Exkursionen zu Geotopen in Hessen und Rheinland-Pfalz sowei zu naturwissenschaftlichen Beobachtungspunkten Johann Wolfgang von Goethes in Böhmen. Kleine Senckenberg-Reihe no. 31, *Schriftenreihe der deutschen geologischen Gesellschaft* 8: 181-222.

HAUBOLD H. 1977. — Zur Kenntnis der Sauria (Lacertilia) aus dem Eozän des Geiseltals, *in* MATTHES H. W. & THALER B. (eds), *Eozäne Wirbeltiere des Geiseltales (Wissenschaftliche Beiträge 1977/2)*. Martin-Luther-Universität, Halle (Saale), Germany: 107-112.

HAUBOLD H. 1990. — Stratigraphische Revision der Wirbeltierfundstellen des Geiseltaleozäns. *Hallesches Jahrbuch für Geowissenschaften* 15: 3-20.

HILDEBRAND M. & GOSLOW G. 1998. — *Analysis of Vertebrate Structure*. Wiley, New York, 660 p.

HILLMER G., LEHMANN U., LIERL H.-J. & WEITSCHAT W. 1980. — *Fossile Schätze unter Müll? Messel - Leben vor 50 Millionen Jahren*. Geologisch-Paläontologisches Institut und Museum der Universität Hamburg, Hamburg, 46 p.

HOFFSTETTER R. 1943. — *Varanidae* et *Necrosauridae* fossiles. *Bulletin du Muséum nationale d'Histoire naturelle, Série 2* 15 (3): 134-141.

HOFFSTETTER R. 1954. — Sur la position systématique de *Necrosaurus*, Saurien de l'Éocène européen. *Comptes Rendus des Séances de la Société Géologique de France (Série 7)* 1 (9): 897-902.

HOFFSTETTER R. 1955. — Squamates de type moderne, *in* PIVETEAU J. (ed.), *Traité de Paléontologie, Vol. 5*. Masson, Paris: 605-662.

HOFFSTETTER R. 1962. — Revue des récentes acquisitions concernant l'histoire et la systématique des squamates, *Problèmes Actuels de Paléontologie – Évolution des Vertébrés.* Colloques internationaux du CNRS No. 104. CNRS, Paris: 243-279.

HOFFSTETTER R. & GASC J.-P. 1968. — Observations sur le squelette cervical et spécialement sur les hypapophyses des sauriens varanoides actuels et fossiles. *Bulletin du Muséum national d'Histoire naturelle, Série 2* 39 (6): 1028-1043.

HOFFSTETTER R. & GASC J.-P. 1969. — Vertebrae and ribs of modern reptiles, *in* GANS C. (ed.), *Biology of the Reptilia, v. 1: Morphology A*. Academic Press, New York: 201-310.

HSIANG A. Y., FIELD D. J., WEBSTER T. H., BEHLKE A. D. B., DAVIS M. B., RACICOT R. A. & GAUTHIER J. A. 2015. — The origin of snakes: revealing the ecology, behavior, and evolutionary history of early snakes using genomics, phenomics, and the fossil record. *BMC Evolutionary Biology* 15: 87. https://doi.org/10.1186/s12862-015-0358-5

HÜNERMANN K. A. 1978. — Ein varanoider Lacertilier (Reptilia, Squamata) aus einer alttertiären Spaltenfüllung von Dielsdorf (Kt. Zürich). *Eclogae Geologicae Helvetiae* 71 (3): 769-774.

JANDZÍK D. & BARTÍK I. 2004. — Differences in morphology of the atlas-axis complex in *Natrix natrix* and *N. tessellata* (Serpentes: Colubridae). *Biologia* 59 (Suppl. 15): 219-229.

KEARNEY M. & RIEPPEL O. 2006. — An investigation into the occurrence of plicidentine in the teeth of squamate reptiles. *Copeia* 2006 (3): 337-350. https://doi.org/c62jzj

KELLER T. 2009. — Beiträge zur Kenntnis von *Placosauriops abderhaldeni* KUHN, 1940 (Anguidae, Glyptosaurinae MARSH, 1872) aus dem Mitteleozän der Grube Messel - Skelettanatomie, Taphonomie und Biomechanik. *Kaupia* 16: 3-145.

KELLER T. & SCHAAL S. 1988. — Lizards: reptiles *en route* to success, *in* SCHAAL S. & ZIEGLER W. (eds), *Messel: An Insight into the History of Life and of the Earth*. Clarendon Press, Oxford: 119-134.

KERFOOT W. C. 1970. — The effect of functional changes upon the variability of lizard and snake body scale numbers. *Copeia* 1970 (2): 252-260. https://doi.org/10.2307/1441647

KLEMBARA J. 2008. — A new anguimorph lizard from the lower Miocene of north-west Bohemia, Czech Republic. *Palaeontology* 51 (1): 81-94. https://doi.org/10.1111/j.1475-4983.2007.00732.x

KLEMBARA J., BÖHME M. & RUMMEL M. 2010. — Revision of the anguine lizard *Pseudopus laurillardi* (Squamata, Anguidae) from the Miocene of Europe, with comments on paleoecology. *Journal of Paleontology* 84 (2): 159-196. https://doi.org/10.1666/09-033R1.1

KOCH A., ZIEGLER T., BÖHME W., ARIDA E. & AULIYA M. 2013. — Distribution, threats and conservation status of the monitor lizards (Varanidae: *Varanus* spp.) of southeast Asia and the Indo-Australian archipelago. *Herpetological Conservation and Biology* 8 (3): 1-62.

KONISHI T. & CALDWELL M. W. 2007. — New specimens of *Platecarpus planifrons* (Cope, 1874) (Squamata: Mosasauridae) and a revised taxonomy of the genus. *Journal of Vertebrate Paleontology* 27 (1): 59-72. https://doi.org/dn5rtr

KUHN O. 1940. — Die Placosauriden und Anguiden aus dem mittleren Eozän des Geiseltales. *Nova Acta Leopoldina* 8: 461-486.

KUHN O. 1966. — *Die Reptilien - System und Stammesgeschichte*. Verlag Oeben, Krailling bei München, 154 p.

LANDSMEER J. M. F. 1984. — Morphology of the anterior limb in relation to sprawling gait in *Varanus*, *in* FERGUSON M. W. J. (ed.), *The Structure, Development and Evolution of Reptiles (Symposium of the Zoological Society of London 52)*. Academic Press, London: 27-45.

LANG M. 1989. — Phylogenetic and biogeographic patterns of basiliscine iguanians (Reptilia: Squamata: "Iguanidae"). *Bonner Zoologische Monographien* 28: 1-172.

LANG M. 1991. — Generic relationships within Cordyliformes (Reptilia : Squamata). *Bulletin de l'Institut Royal des Sciences Naturelles de Belgique* 61: 121-188.

LÉCURU S. 1968a. — Remarques sur le scapulo-coracoïde des lacertiliens. *Annales des Sciences Naturelles, Zoologie* 10 (4): 475-510.

LÉCURU S. 1968b. — Étude des variations morphologiques du sternum, des clavicules, et de l'interclavicule des lacertiliens. *Annales des Sciences Naturelles, Zoologie* 10 (4): 511-544.

LEE M. S. Y. 1997. — The phylogeny of varanoid lizards and the affinities of snakes. *Philosophical Transactions of the Royal Society of London, Series B* 352 (1349): 53-91. https://doi.org/10.1098/rstb.1997.0005

LEMOS-ESPINAL J., SMITH G. R. & WOOLRICH-PIÑA G. 2012. — *La Familia Xenosauridae en México / The family Xenosauridae in Mexico*. ECO Herpetological Publishing and Distribution, Rodeo, New Mexico, 106 p.

LONGRICH N. R., BHULLAR B.-A. S. & GAUTHIER J. A. 2012. — Mass extinction of lizards and snakes at the Cretaceous-Paleogene boundary. *Proceedings of the National Academy of Sciences of the United States of America* 109 (52): 21396-21401. https://doi.org/10.1073/pnas.1211526110

LOSOS J. B. & GREENE H. W. 1988. — Ecological and evolutionary implications of diet in monitor lizards. *Biological Journal of the Linnean Society* 35: 379-407. https://doi.org/10.1111/j.1095-8312.1988.tb00477.x

LYDEKKER R. 1888a. — *Catalogue of the Fossil Reptilia and Amphibia in the British Museum (Natural History). Part I. Containing the Orders Ornithosauria, Crocodilia, Dinosauria, Squamata, Rhynchocephalia, and Proterosauria*. Taylor and Francis, London, 309 p. https://doi.org/10.5962/bhl.title.61848

LYDEKKER R. 1888b. — Notes on Tertiary Lacertilia and Ophidia. *Geological Magazine* 25: 110-113. https://doi.org/10.1017/S0016756800173480

MACLEAN S. 1980. — Ultrastructure of epidermal sensory receptors in *Amphibolurus barbatus* (Lacertilis [sic]: Agamidae). *Cell and Tissue Research* 210: 435-445. https://doi.org/10.1007/BF00220200

MAISANO J. A., BELL C. J., GAUTHIER J. A. & ROWE T. 2002. — The osteoderms and palpebral in *Lanthanotus borneensis* (Squamata: Anguimorpha). *Journal of Herpetology* 36 (4): 678-682. https://doi.org/10.2307/1565940

MALAN M. E. 1946. — Contributions to the comparative anatomy of the nasal capsule and the organ of Jacobson of the Lacertilia. *Annale van die Universiteit van Stellenbosch A* 24: 69-137. http://hdl.handle.net/10019.1/56295

MARSHALL A. J. & WRANGHAM R. W. 2007. — Evolutionary consequences of fallback foods. *International Journal of Primatology* 28: 1219-1235. https://doi.org/10.1007/s10764-007-9218-5

MATVEYEVA T. N. & ANANJEVA N. B. 1995. — The distribution and number of the skin sense organs of agamid, iguanid and gekkonid lizards. *Journal of Zoology, London* 235: 253-268. https://doi.org/10.1111/j.1469-7998.1995.tb05142.x

MAXWELL E. E., CALDWELL M. W. & LAMOUREUX D. O. 2011. — The structure and phylogenetic distribution of amniote plicidentine. *Journal of Vertebrate Paleontology* 31 (3): 553-561. https://doi.org/10.1080/02724634.2011.557117

MCDOWELL S. B. & BOGERT C. M. 1954. — The systematic position of*Lanthanotus*and the affinities of the anguinomorphan lizards. *Bulletin of the American Museum of Natural History* 105 (1): 1-142. http://hdl.handle.net/2246/1146

MEIRI S. 2010. — Length-weight allometries in lizards. *Journal of Zoology* 281 (3): 218-226. https://doi.org/10.1111/j.1469-7998.2010.00696.x

MERTENS R. 1942a. — Die Familie der Warane (Varanidae). Zweiter Teil: Der Schädel. *Abhandlungen der senckenbergischen naturforschenden Gesellschaft* 465: 117-234.

MERTENS R. 1942b. — Die Familie der Warane (Varanidae). Dritter Teil: Taxonomie. *Abhandlungen der senckenbergischen naturforschenden Gesellschaft* 466: 235-391.

MERTENS R. 1942c. — Die Familie der Warane (Varanidae). Erster Teil: Allgemeines. *Abhandlungen der senckenbergischen naturforschenden Gesellschaft* 462: 1-116.

MESZOELY C. A. M. 1970. — North American fossil anguid lizards. *Bulletin of the Museum of Comparative Zoology* 139 (2): 87-150.

MILLER M. R. & KASAHARA M. 1967. — Studies on the cutaneous innervation of lizards. *Proceedings of the California Academy of Sciences, Series 4* 34 (16): 549-568.

MUCHLINSKI M. N. 2008. — The relationship between the infraorbital foramen, infraorbital nerve, and maxillary mechanoreception: implications for interpreting the paleoecology of fossil mammals based on infraorbital foramen size. *Anatomical Record* 291: 1221-1226. https://doi.org/10.1002/ar.20742

MÜLLER J., HIPSLEY C. A., HEAD J. J., KARDJILOV N., HILGER A., WUTTKE M. & REISZ R. R. 2011. — Eocene lizard from Germany revelas amphisbaenian origins. *Nature* 473: 364-367. https://doi.org/10.1038/nature09919

NESSOV L. A. 1985. — Rare bony fishes, terrestrial lizards and mammals from the lagoonal zone of the littoral lowlands of the Cretaceous of the Kyzylkum. *Ezhegodnik Vsesouyuznogo Paleontologicheskogo Obshchestva, Leningrad* 28: 199-219 (in Russian).

NORELL M. A. & GAO K. 1997. — Braincase and phylogenetic relationships of *Estesia mongoliensis* from the Late Cretaceous of the Gobi Desert and the recognition of a new clade of lizards. *American Museum Novitates* 3211: 1-25. http://hdl.handle.net/2246/3612

NORELL M. A., GAO K.-Q. & CONRAD J. 2007. — A new platynotan lizard (Diapsida: Squamata) from the Late Cretaceous Gobi Desert (Ömnögov), Mongolia. *American Museum Novitates* 3605: 1-22. https://doi.org/10.1206/0003-0082(2008)3605[1:ANPLDS]2.0.CO;2

NYDAM R. L. 2000. — A new taxon of helodermatid-like lizard from the Albian–Cenomanian of Utah. *Journal of Vertebrate Paleontology* 20 (2): 285-294. https://doi.org/10.1671/0272-4634(2000)020[0285:ANTOHL]2.0.CO;2

OELRICH T. M. 1956. — The anatomy of the head of *Ctenosaura pectinata* (Iguanidae). *Miscellaneous Publications, Museum of Zoology, University of Michigan* 94: 1-122. http://hdl.handle.net/2027.42/56338

OPPEL M. 1811. — *Die Ordnungen, Familien, und Gattungen der Reptilien als Prodrom einer Naturgeschichte derselben*. Joseph Lindauer, Munich, 86 p. https://doi.org/10.5962/bhl.title.4911

PIANKA E. R., KING D. R. & KING R. A. 2004. — *Varanoid Lizards of the World*. Indiana University Press, Bloomington, Indiana, 588 p. https://doi.org/10.2307/j.ctt2005wjp

POLCYN M. J. & BELL G. L. 2005. — *Russelosaurus coheni*, n. gen., n. sp., a 92 million-year-old mosasaur from Texas (USA), and the definition of the parafamily Russellosaurina. *Netherlands Journal of Geosciences (Geologie en Mijnbouw)* 84 (3): 321-334. https://doi.org/10.1017/S0016774600021107

POLCYN M. J., TCHERNOV E. & JACOBS L. L. 1999. — The Cretaceous biogeography of the eastern Mediterranean with a description of a new basal mosasauroid from ‚Ein Yabrud, Israel, *in* TOMIDA Y., RICH T. H. & VICKERS-RICH P. (eds), *Proceedings of the Second Gondwanan Dinosaur Symposium (National Science Museum Monograph 15)*. National Science Museum, Tokyo: 259-290.

POUGH F. H. 1973. — Lizard energetics and diet. *Ecology* 54 (4): 837-844. https://doi.org/10.2307/1935678

PREGILL G. K., GAUTHIER J. A. & GREENE H. W. 1986. — The evolution of helodermatid squamates, with description of a new taxon and an overview of Varanoidea. *Transactions of the San Diego Society of Natural History* 21 (11): 167-202.

R CORE TEAM. 2016. — R: A Language and Environment for Statistical Computing. Vienna, R Foundation for Statistical Computing.

RAGE J.-C. 1978. — La poche à phosphate de Ste-Néboule (Lot) et sa faune de vertébrés du Ludien supérieur. 5 - Squamates. *Palaeovertebrata* 8 (2-4): 201-215.

RAGE J.-C. & AUGÉ M. 1993. — Squamates from the Cainozoic of the western part of Europe: a review. *Revue de Paléobiologie, Volume Spécial* 7: 199-216.

REEDER T. W., TOWNSEND T. M., MULCAHY D. G., NOONAN B. P., WOOD P. L., JR., SITES J. W. & WIENS J. J. 2015. — Integrated analyses resolve conflicts over squamate reptile phylogeny and reveal unexpected placements for fossil taxa. *PLoS ONE* 10 (3): e0118199. https://doi.org/10.1371/journal.pone.0118199

RENOUS-LÉCURU S. 1973. — Morphologie comparée du carpe chez les Lepidosauriens actuels (Rhynchocéphales, Lacertiliens, Amphisbéniens). *Gegenbaurs Morphologisches Jahrbuch* 119 (5): 727-766.

RIEPPEL O. 1978. — Tooth replacement in anguinomorph lizards. *Zoomorphologie* 91: 77-90. https://doi.org/10.1007/BF00994155

RIEPPEL O. 1980a. — The postcranial skeleton of *Lanthanotus borneensis* (Reptilia, Lacertilia). *Amphibia-Reptilia* 1: 95-112. https://doi.org/10.1163/156853880X00105

RIEPPEL O. 1980b. — The phylogeny of anguinomorph lizards. *Denkschriften der Schweizerischen Naturforschenden Gesellschaft* 94: 1-86.

RIEPPEL O. & ZAHER H. 2000a. — The braincases of mosasaurs and *Varanus*, and the relationships of snakes. *Zoological Journal of the Linnean Society* 129: 489-514. https://doi.org/10.1111/j.1096-3642.2000.tb00614.x

RIEPPEL O. & ZAHER H. 2000b. — The intramandibular joint in squamates, and the phylogenetic relationships of the fossil snake *Pachyrhachis problematicus* Haas. *Fieldiana Geology* 43: 1-69. https://doi.org/10.5962/bhl.title.3584

RIEPPEL O. & GRANDE L. 2007. — The anatomy of the fossil varanid lizard *Saniwa ensidens* Leidy, 1870, based on a newly discovered complete skeleton. *Journal of Paleontology* 81 (4): 643-665. https://doi.org/czrx82

RIEPPEL O., CONRAD J. L. & MAISANO J. A. 2007. — New morphological data for *Eosaniwa koehni* Haubold, 1977 and a revised phylogenetic analysis. *Journal of Paleontology* 81 (4): 760-769. https://doi.org/ch2j37

RIEPPEL O., GAUTHIER J. A. & MAISANO J. A. 2008. — Comparative morphology of the dermal palate in squamate reptiles, with comments on phylogenetic implications. *Zoological Journal of the Linnean Society* 152 (1): 131-152. https://doi.org/10.1111/j.1096-3642.2007.00337.x

ROBINSON P. L. 1967. — The evolution of the Lacertilia, *in* LEHMAN J.-P. (ed.), *Problèmes actuels de Paléontologie (Évolution des Vertébrés) (Colloques internationaux du Centre national de la Recherche scientifique, No. 163)*. Anatole-France, Paris: 395-407.

ROMER A. S. 1922. — The locomotor apparatus of certain primitive and mammal-like reptiles. *Bulletin of the American Museum of Natural History* 46: 517-606. http://hdl.handle.net/2246/929

ROMER A. S. 1956. — *Osteology of the Reptiles*. University of Chicago Press, Chicago, 772 p. https://doi.org/10.5962/bhl.title.6573

RONQUIST F., TESLENKO M., VAN DER MARK P., AYRES D. L., DARLING A., HÖHNA S., LARGET B., LIU L., SUCHARD M. A. & HUELSENBECK J. P. 2012. — MrBayes 3.2: efficient Bayesian phylogenetic inference and model choice across a large model space. *Systematic Biology* 61 (3): 539-542. https://doi.org/10.1093/sysbio/sys029

RUSSELL D. A. 1967. — Systematics and morphololgy of American mosasaurs (Reptilia, Sauria). *Peabody Museum of Natural History Bulletin* 23: 1-241.

SAVAGE J. M., LIPS K. R. & IBÁÑEZ D. 2008. — A new species of *Celestus* from west-central Panama, with consideration of the status of the genera of the Anguidae: Diploglossinae (Squamata). *Revista de Biología Tropical* 56 (2): 845-859. https://doi.org/10.15517/rbt.v56i2.5628

SCANFERLA A. & SMITH K. T. 2020. — Exquisitely preserved fossil snakes of Messel: insight into the evolution, biogeography, habitat preferences and sensory ecology of early boas. *Diversity* 12 (3): 100. https://doi.org/10.3390/d12030100

SCHACHNER E. R., CIERI R. L., BUTLER J. P. & FARMER C. G. 2014. — Unidirectional pulmonary airflow patterns in the savannah monitor lizard. *Nature* 506: 367-370. https://doi.org/10.1038/nature12871

SCHWANDT H.-J. 2019. — *The Gila Monster: Heloderma suspectum*. Chimaira, Frankfurt am Main, 272 p.

SCHWENK K. 1988. — Comparative morphology of the lepidosaur tongue and its relevance to squamate phylogeny, *in* ESTES R. & PREGILL G. K. (eds), *Phylogenetic Relationships of the Lizard Families*. Stanford University Press, Stanford, California: 569-598.

SHERBROOKE W. C. & NAGLE R. B. 1996. — *Phrynosoma* intraepidermal receptor: a dorsal intraepidermal mechanoreceptor in horned lizards (*Phrynosoma*; Phrynosomatidae; Reptilia). *Journal of Morphology* 228: 145-154.

SIMÕES T. R., CALDWELL M. W., PALCI A. & NYDAM R. L. 2017. — Giant taxon-character matrices: quality of character constructions remains critical regardless of size. *Cladistics* 33 (2): 198-219. https://doi.org/10.1111/cla.12163

SMITH K. K. 1986. — Morphology and function of the tongue and hyoid apparatus in *Varanus* (Varanidae, Lacertilia). *Journal of Morphology* 187: 261-287. https://doi.org/10.1002/jmor.1051870302

SMITH K. T. 2009a. — A new lizard assemblage from the earliest Eocene (zone Wa0) of the Bighorn Basin, Wyoming, USA: Biogeography during the warmest interval of the Cenozoic. *Journal of Systematic Palaeontology* 7 (3): 299-358. https://doi.org/10.1017/S1477201909002752

SMITH K. T. 2009b. — Eocene lizards of the clade *Geiseltaliellus* from Messel and Geiseltal, Germany, and the early radiation of Iguanidae (Squamata: Iguania). *Bulletin of the Peabody Museum of Natural History* 50 (2): 219-306. https://doi.org/10.3374/014.050.0201

SMITH K. T. 2011. — The evolution of mid-latitude faunas during the Eocene: late Eocene lizards of the Medicine Pole Hills reconsidered. *Bulletin of the Peabody Museum of Natural History* 52 (1): 3-105. https://doi.org/10.3374/014.052.0101

SMITH K. T. 2017a. — First crocodile-tailed lizard (Squamata:*Pan-Shinisaurus*) from the Paleogene of Europe. *Journal of Vertebrate Paleontology* 37: e1313743. https://doi.org/10.1080/02724634.2017.1313743

SMITH K. T. 2017b. — The squamation of the stem-basilisk *Geiseltaliellus maarius* (Squamata: Iguanidae) from the Eocene of Messel, Germany. *Salamandra* 53 (4): 519-530.

SMITH K. T. & BUCHY M.-C. 2008. — A new aigialosaur (Squamata: Anguimorpha) with soft tissue remains from the Upper Cretaceous of Nuevo León, Mexico. *Journal of Vertebrate Paleontology* 28 (1): 85-94. https://doi.org/10.1671/0272-4634(2008)28[85:ANASAW]2.0.CO;2

SMITH K. T. & GAUTHIER J. A. 2013. — Early Eocene lizards of the Wasatch Formation near Bitter Creek, Wyoming: diversity and paleoenvironment during an interval of global warming. *Bulletin of the Peabody Museum of Natural History* 54 (2): 135-230. https://doi.org/10.3374/014.054.0205

SMITH K. T. & SCANFERLA A. 2016. — Fossil snake preserving three trophic levels and evidence for an ontogenetic dietary shift. *Palaeobiodiversity and Palaeoenvironments* 96 (4): 589-599. https://doi.org/10.1007/s12549-016-0244-1

SMITH K. T. & WUTTKE M. 2012. — From tree to shining sea: Taphonomy of the arboreal lizard*Geiseltaliellus maarius*from Messel, Germany. *Palaeobiodiversity and Palaeoenvironments* 92 (1): 45-65. https://doi.org/10.1007/s12549-011-0064-2

SMITH K. T., SCHAAL S. F. K. & HABERSETZER J. 2018a. — *Messel: An Ancient Greenhouse Ecosystem*. Stuttgart, Schweizerbart: 355.

SMITH K. T., BHULLAR B.-A. S., KÖHLER G. & HABERSETZER J. 2018b. — The only known jawed vertebrate with four eyes and the *Bauplan* of the pineal complex. *Current Biology* 28: 1101-1107. https://doi.org/10.1016/j.cub.2018.02.021

SMITH K. T., ČERŇANSKÝ A., SCANFERLA A. & SCHAAL S. F. K. 2018c. — Lizards and snakes: warmth-loving sunbathers, *in* SMITH K. T., SCHAAL S. F. K. & HABERSETZER J. (eds), *Messel: An Ancient Greenhouse Ecosystem*. Schweizerbart, Stuttgart: 122-147.

SMITH K. T., COMAY O., MAUL L., WEGMÜLLER F., LE TENSORER J.-M. & DAYAN T. in press. — A model of digestive tooth corrosion in lizards: experimental tests and taphonomic implications. *Scientific Reports*.

SNYDER R. C. 1954. — The anatomy and function of the pelvic girdle and hindlimb in lizard locomotion. *American Journal of Anatomy* 95 (1): 1-36. https://doi.org/10.1002/aja.1000950102

STEINDACHNER F. 1878. — Über zwei neue Eidechse-Arten aus Süd-Amerika und Borneo. *Denkschriften der kaiserlichen Akademie der Wissenschaften, mathematisch-naturwissenschaftliche Classe* 38: 93-96, pl. 91-92.

STRITZKE R. 1983. — *Saniwa feisti* n. sp., ein Varanide (Lacertilia, Reptilia) aus dem Mittel-Eozän von Messel bei Darmstadt. *Senckenbergiana Lethaea* 64 (5/6): 497-508.

SULLIVAN R. M. 1979. — Revision of the Paleogene genus *Glyptosaurus* (Reptilia, Anguidae). *Bulletin of the American Museum of Natural History* 163 (1): 1-72. http://hdl.handle.net/2246/1289

SULLIVAN R. M. 1986. — The skull of *Glyptosaurus sylvestris* Marsh, 1871 (Lacertilia: Anguidae). *Journal of Vertebrate Paleontology* 6 (1): 28-37. https://doi.org/10.1080/02724634.1986.10011596

SWOFFORD D. L. 2003. — PAUP*: Phylogenetic Analysis Using Parsimony (* and Other Methods). Version 4. Sunderland, Massachusetts, Sinauer Associates. https://paup.phylosolutions.com/

THOMPSON G. G. & WITHERS P. C. 1997. — Comparative morphology of western Australian varanid lizards (Squamata: Varanidae). *Journal of Morphology* 233 (2): 127-152.

TSUIHIJI T. 2005. — Homologies of the *Transversospinalis* muscles in the anterior presacral region of Sauria (crown Diapsida). *Journal of Morphology* 263: 151-178. https://doi.org/10.1002/jmor.10294

VERSLUYS J. 1912. — Das Streptostylie-Problem und die Bewegung im Schädel bei Sauropsida. *Zoologische Jahrbücher* Suppl. 15 (2): 545-716, pl. 531.

VIDAL N. & HEDGES S. B. 2005. — The phylogeny of squamate reptiles (lizards, snakes, and amphisbaenians) inferred from nine nuclear protein-coding genes. *Comptes Rendus Biologies* 328 (10-11): 1000-1008. https://doi.org/10.1016/j.crvi.2005.10.001

VIDAL N., MARIN J., SASSI J., BATTISTUZZI F. U., DONNELLAN S., FITCH A. J., FRY B. G., VONK F. J., RODRIGUEZ DE LA VEGA R. C., COULOUX A. & HEDGES S. B. 2012. — Molecular evidence for an Asian origin of monitor lizards followed by Tertiary dispersals to Africa and Australasia. *Biology Letters* 8: 853-855. https://doi.org/10.1098/rsbl.2012.0460

VOIGT E. 1988. — Preservation of soft tissues in the Eocene lignite of the Geiseltal near Halle/S. *Courier Forschungsinstitut Senckenberg* 107: 325-343.

VON FEJÉRVÁRY-LÁNGH A. M. 1923. — Beiträge zu einer Monographie der fossilen Ophisaurier. *Palaeontologia Hungarica* 1: 123-220.

WATKINSON G. B. 1906. — The cranial nerves of *Varanus bivittatus*. *Gegenbaurs Morphologisches Jahrbuch* 35: 450-472.

WEBER S. 2004. — *Ornatocephalus metzleri* gen. et spec. nov. (Lacertilia, Scincoidea) – taxonomy and paleobiology of a basal scincoid lizard from the Messel Formation (middle Eocene: basal Lutetian, Geiseltalium), Germany. *Abhandlungen der senckenbergischen naturforschenden Gesellschaft* 561: 1-159.

WEDMANN S., HABERSETZER J., LEHMANN T., RUF I., SCHAAL S. F. K. & SMITH K. T. 2018. — Messel research – methods and concepts, *in* SMITH K. T., SCHAAL S. F. K. & HABERSETZER J. (eds), *Messel: An Ancient Greenhouse Ecosystem*. Schweizerbart, Frankfurt am Main: 34-41.

WELLSTEAD C. F. 1982. — Lizards from the lower Valentine Formation (Miocene) of northern Nebraska. *Journal of Herpetology* 16 (4): 364-375. https://doi.org/10.2307/1563566

WILLARD W. A. 1915. — The cranial nerves of Anolis carolinensis. *Bulletin of the Museum of Comparative Zoology* 59 (2): 16-116.

WILLISTON S. W. 1898. — Paleontology (Part I. Upper Cretaceous.) V. Mosasaurs. *The University Geological Survey of Kansas* 4: 81-221, pls. X-LXXII.

WINKLER D. E., SCHULZ-KORNAS E., KAISER T. M. & TÜTKEN T. 2019. — Dental microwear texture reflects dietary tendencies in extant Lepidosauria despite their limited use of oral food processing. *Proceedings of the Royal Society of London, Series B* 286: 20190544. https://doi.org/10.1098/rspb.2019.0544

YI H.-Y. & NORELL M. A. 2013. — New materials of *Estesia mongoliensis* (Squamata: Anguimorpha) and the evolution of venom grooves in lizards. *American Museum Novitates* 3767: 1-31. https://doi.org/10.1206/3767.2

ZITTEL K. A. 1887-1890. — *Handbuch der Palæontologie. Erste Abtheilung. Dritter Band. Vertebrata (Pisces, Amphibia, Reptilia, Aves)*. R. Oldenbourg, Munich, 900 p. https://doi.org/10.5962/bhl.title.34265

ZOLLWEG M. & KÜHNE H. 2013. — *Krokodilschwanzechsen,* Shinisaurus crocodilurus*: Lebensweise, Haltung, Nachzucht*. Natur- und Tierverlag, Münster, Germany, 95 p.

Submitted on 16 March 2020;
accepted on 28 April 2020;
published on 9 June 2021.

APPENDICES — SUPPLEMENTARY MATERIAL

APPENDIX 1. — *Paranecrosaurus feisti* (Stritzke, 1983) n. comb. SMF-ME 10954 (referred specimen), nearly complete skeleton. Scale bar: 5 cm.

Appendix 2. — X-radiograph of *Paranecrosaurus feisti* (Stritzke, 1983) n. comb. SMF-ME 10954 (referred specimen), nearly complete skeleton. Scale bar: 5 cm.

Appendix 3. — *Paranecrosaurus feisti* (Stritzke, 1983) n. comb. (referred specimen), nearly complete skeleton. Coated with ammonium chloride. **A**, part (Pohl collection, dorsal view); **B**, counterpart (Perner collection, ventral view). Scale bar: 5 cm.

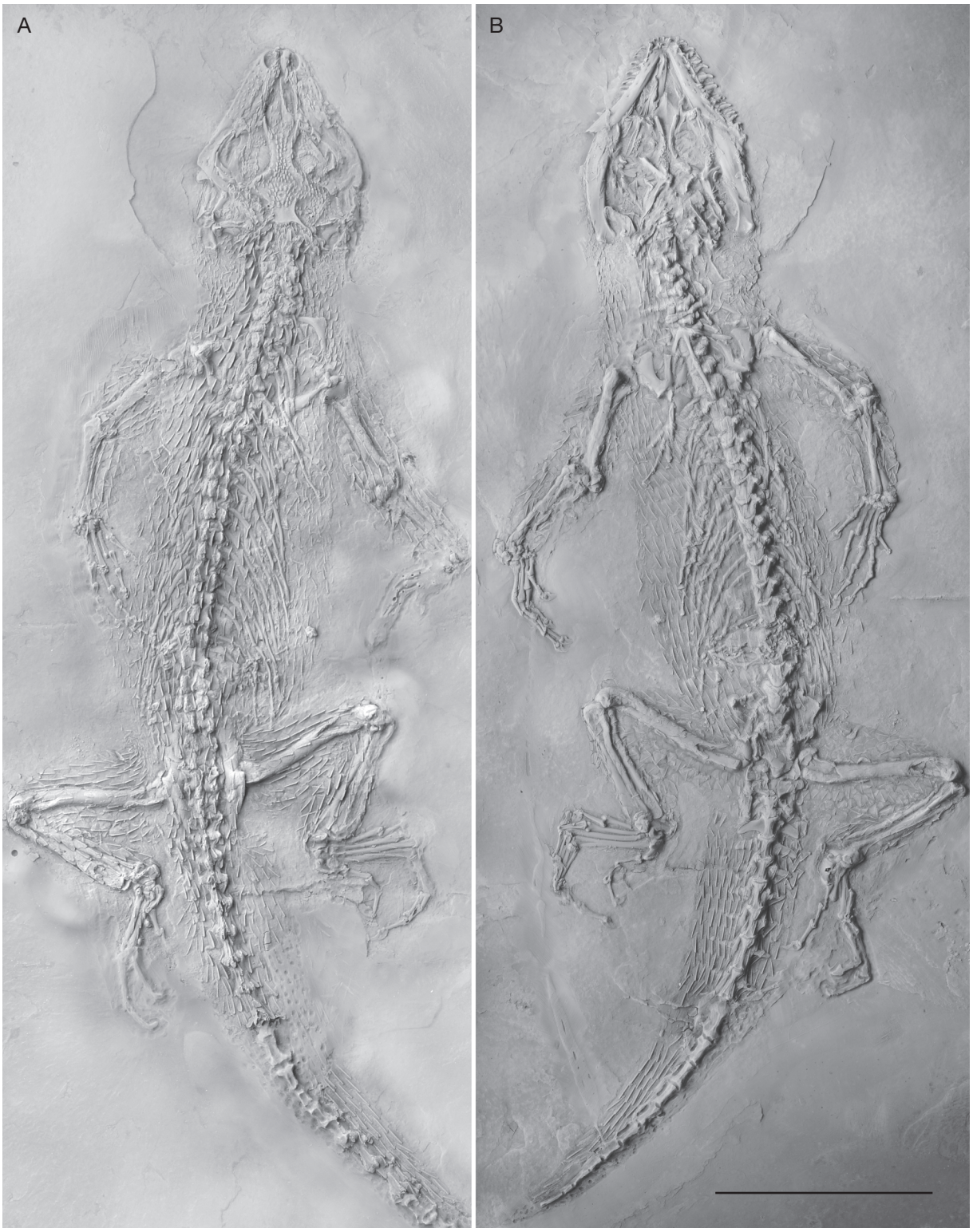

Appendix 4. — *Paranecrosaurus feisti* (Stritzke, 1983) n. comb. HLMD-Me 13709 (holotype), nearly complete skeleton. Coated with ammonium chloride. Scale bar: 5 cm.

Appendix 5. — **A**, *Paranecrosaurus feisti* (Stritzke, 1983) n. comb. SMNK-Me 1124 (paratype, part), partial disarticulated skeleton. The specimen has been painted over. **B**, **C**, *Paranecrosaurus feisti* SMNK-Me 1124 (paratype, part), CT scan of skull elements, topside and underside, respectively. **D**, *Paranecrosaurus feisti* n. comb. SMF-ME A258 (cast of paratype, counterpart), partial disarticulated skeleton. The cast has been painted, presumably, to look like the original counterpart. Scale bar: A, D, 5 cm; B, C, 10 mm.

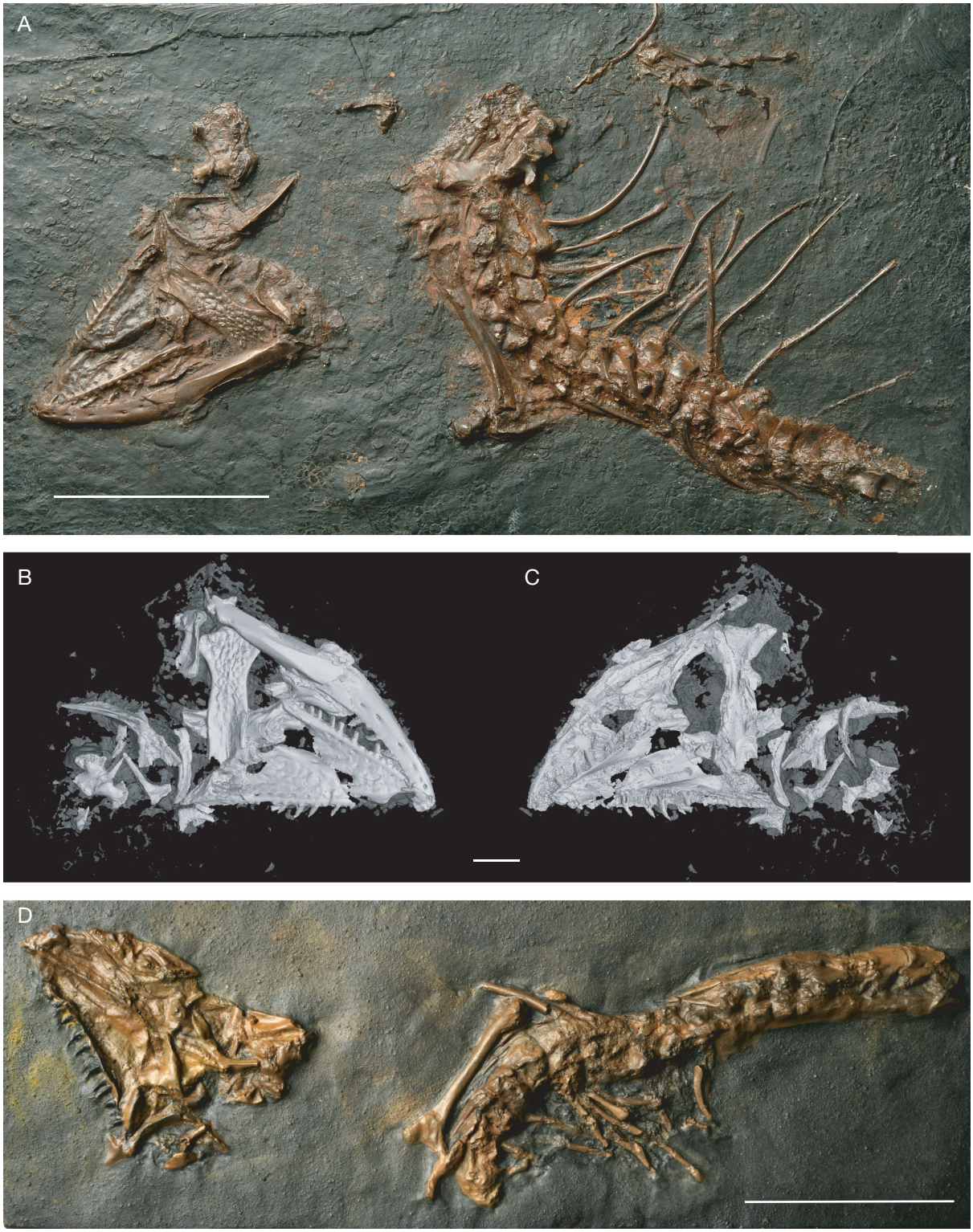

Appendix 6. — Stereo-X-radiograph of whole specimen, SMF-ME 10954. The stereo-X-radiographs of Appendices 6-11 are available in digital format as JPS files at the following address: https://doi.org/10.5852/cr-palevol2021v20a23_s1

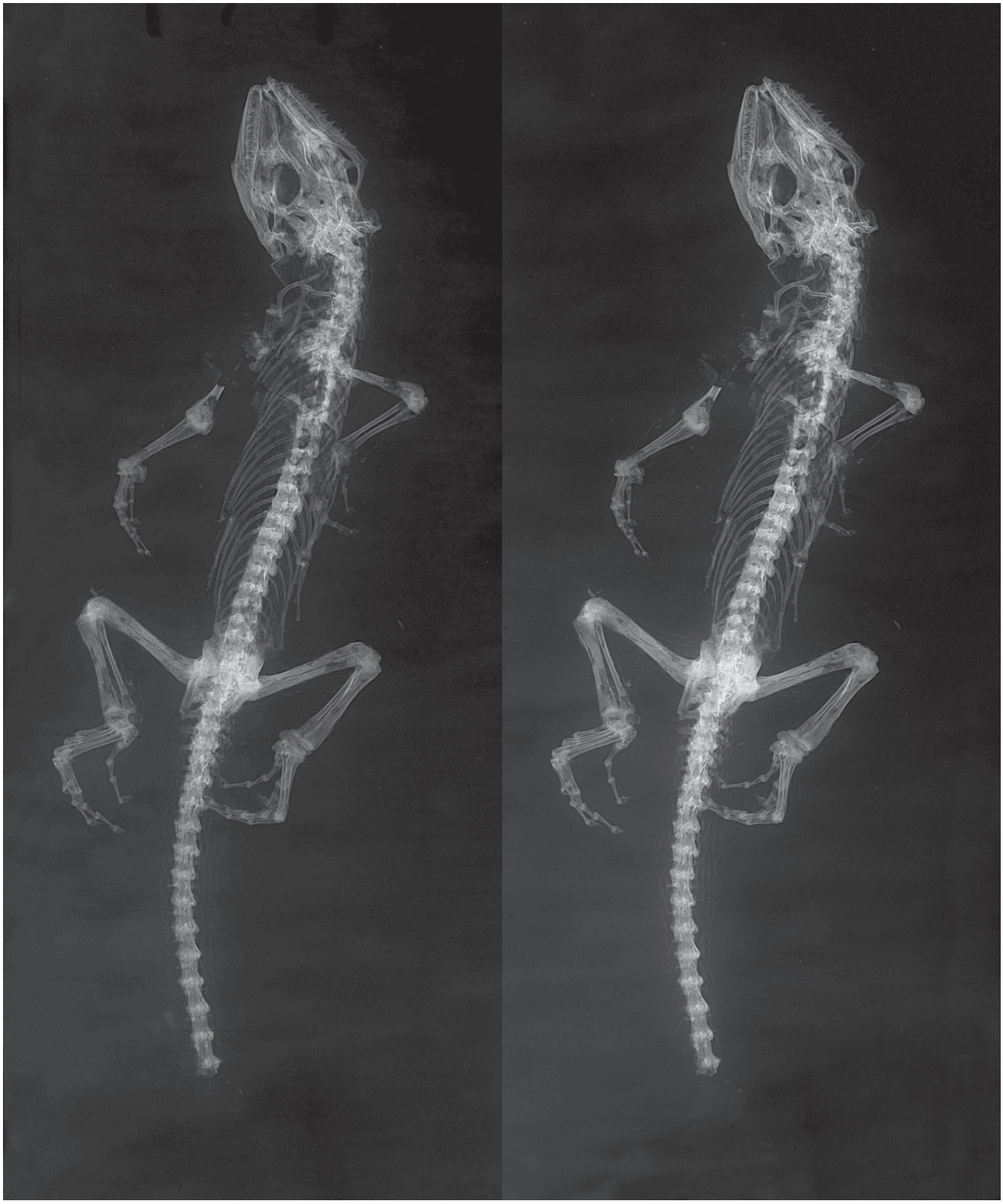

Appendix 7. — Stereo-X-radiograph of skull, SMF-ME 10954.

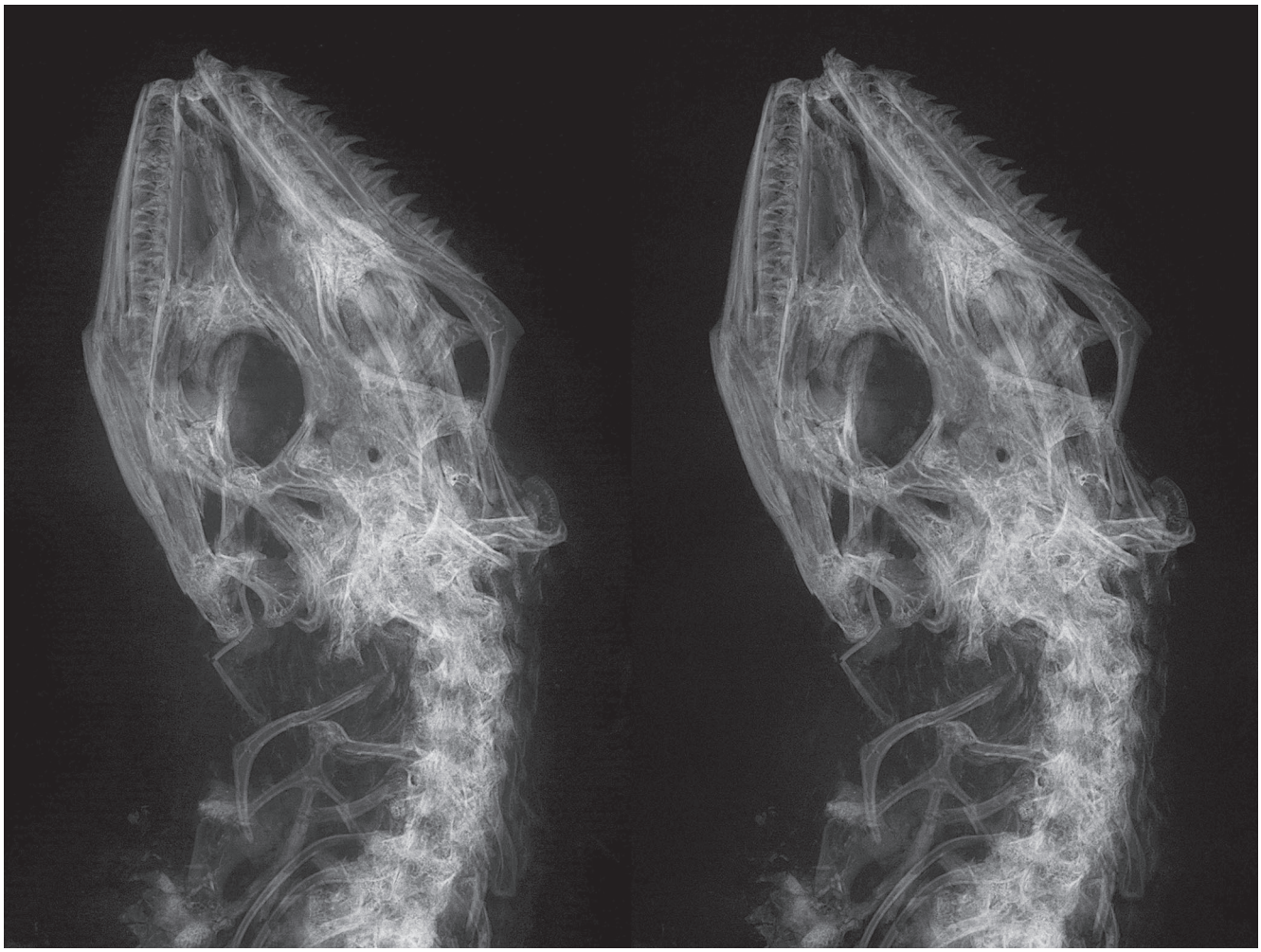

APPENDIX 8. — Stereo-X-radiograph of left forelimb, SMF-ME 10954.

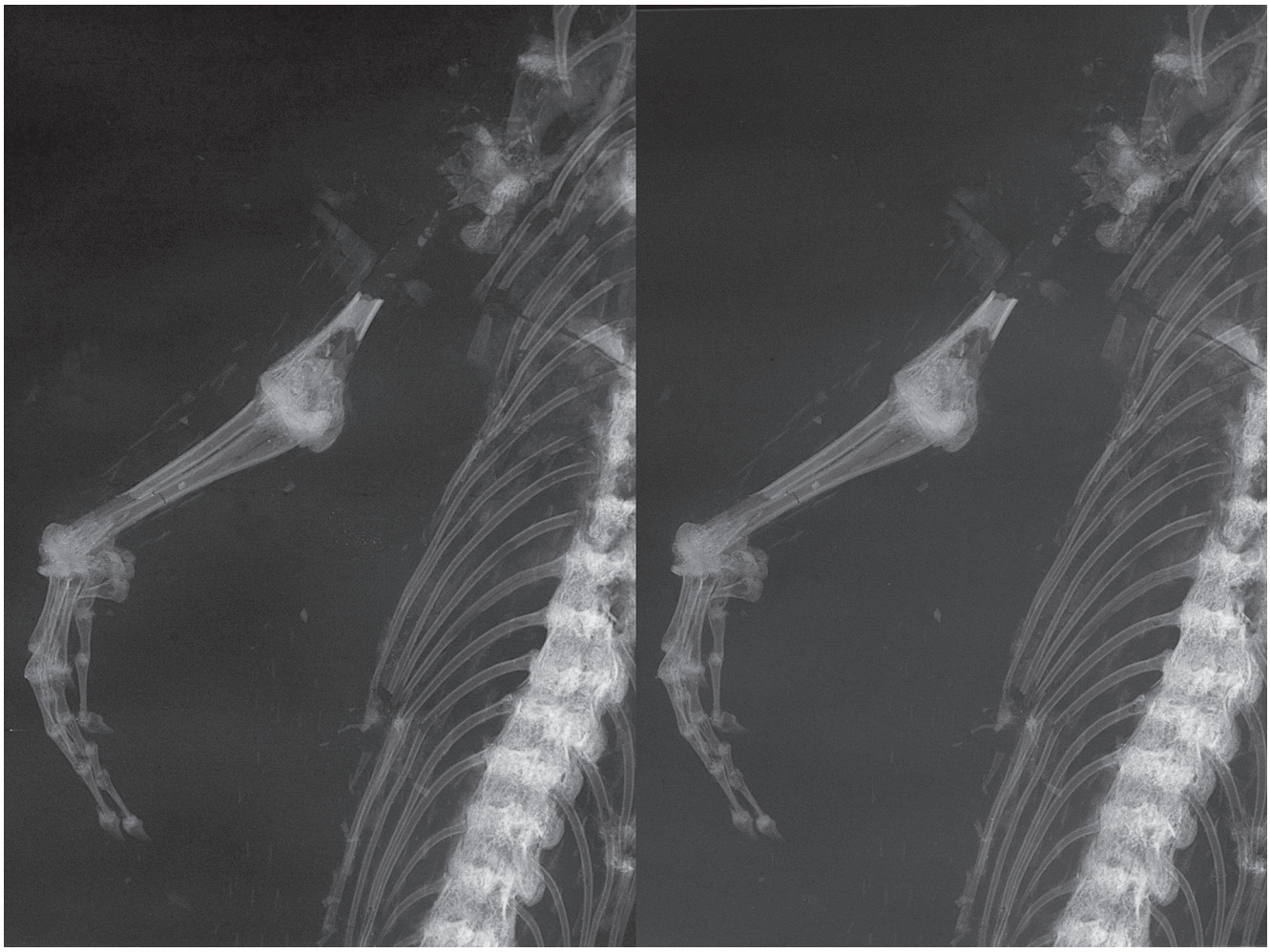

Appendix 9. — Stereo-X-radiograph of right forelimb, SMF-ME 10954.

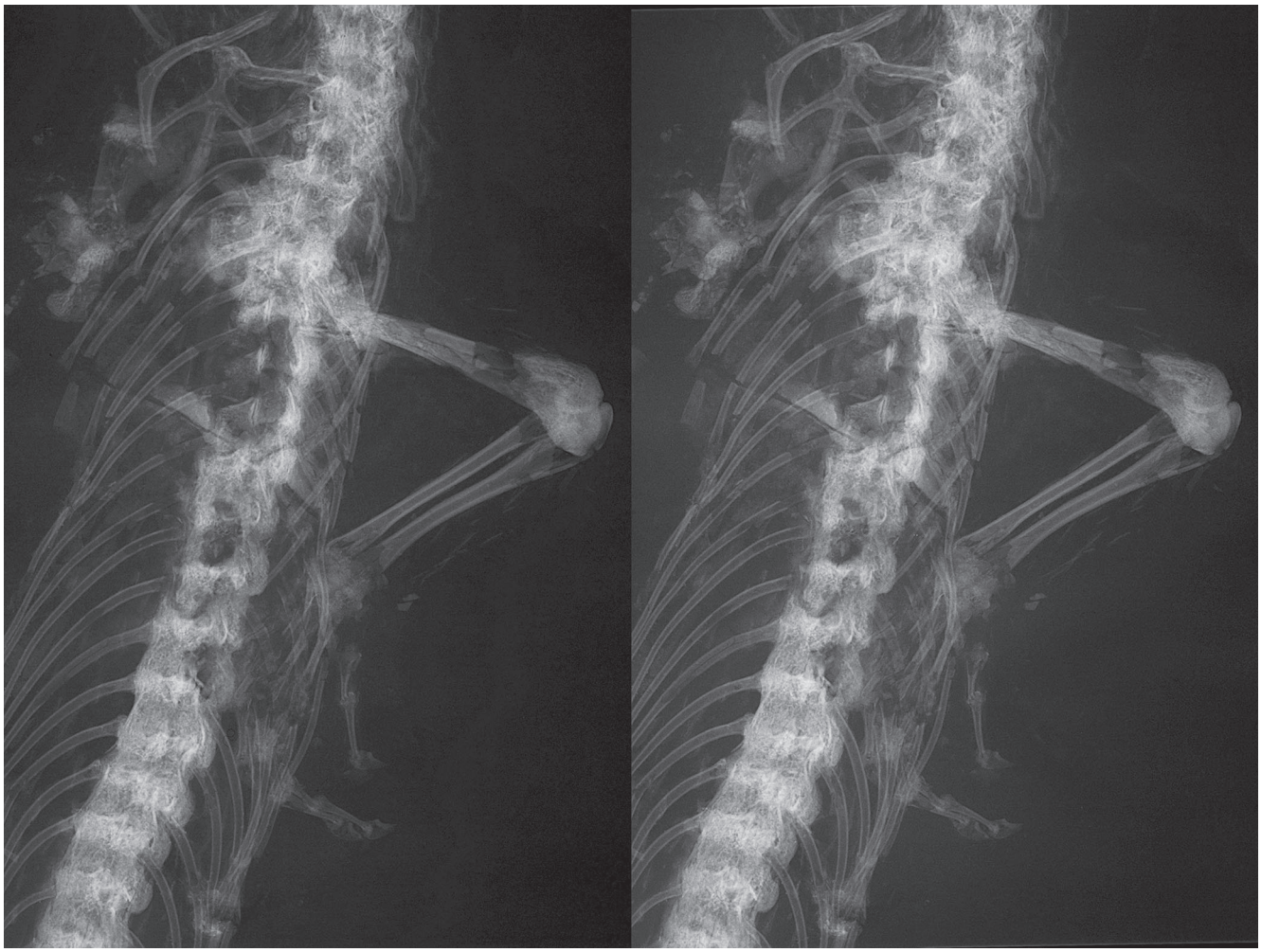

Appendix 10. — Stereo-X-radiograph of left hind limb, SMF-ME 10954.

Appendix 11. — Stereo-X-radiograph of right hind limb, SMF-ME 10954.

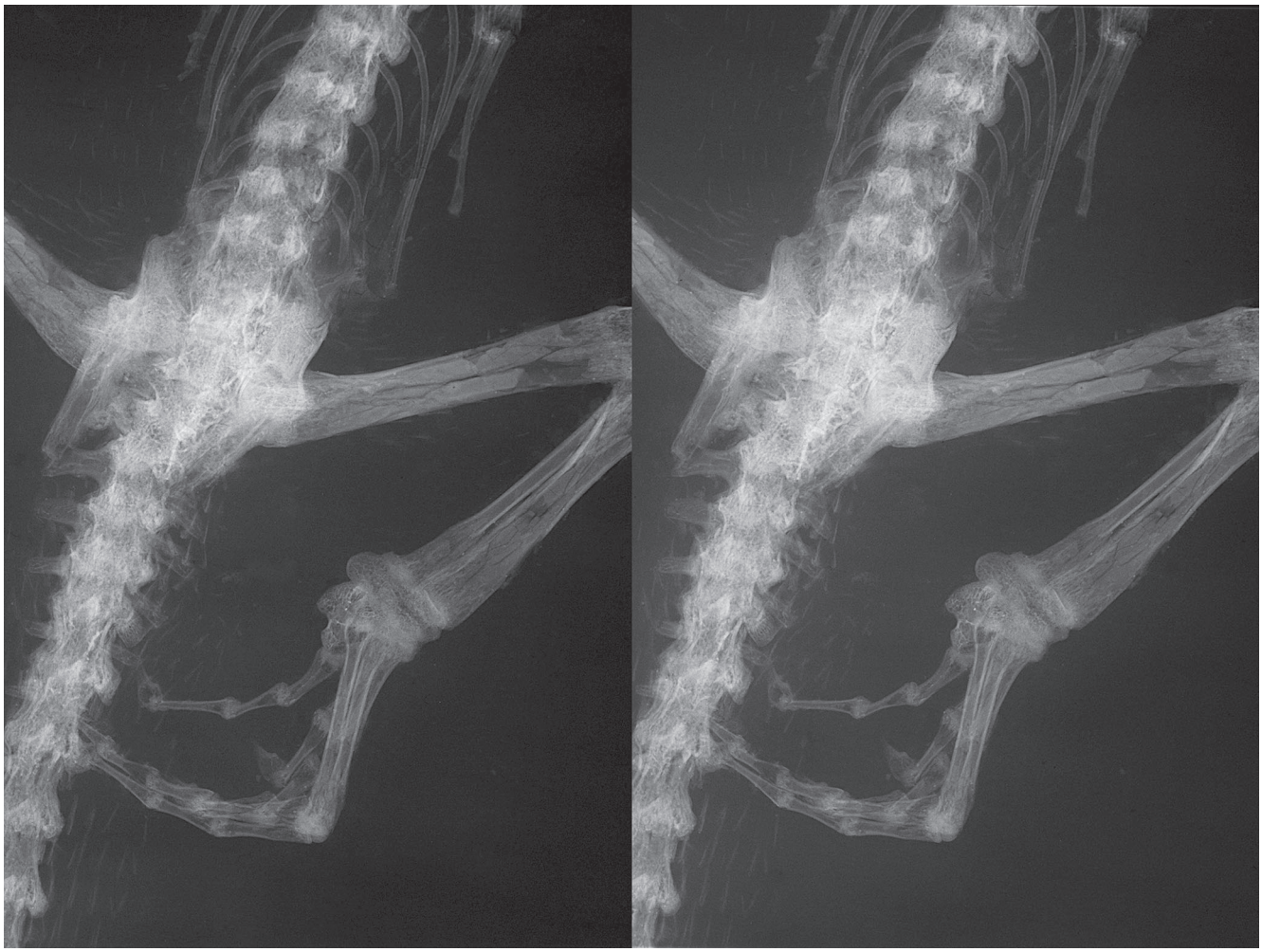

Appendix 12. — Morphological characters used in the phylogenetic analysis: https://doi.org/10.5852/cr-palevol2021v20a23_s2

Appendix 13. — Nexus file including both morphological and molecular data: https://doi.org/10.5852/cr-palevol2021v20a23_s3

Appendix 14. — R code for ecomorphological data analysis: https://doi.org/10.5852/cr-palevol2021v20a23_s4

Appendix 15. — Data on body proportions for *Varanus* Merrem, 1820, taken from Mertens (1942c): https://doi.org/10.5852/cr-palevol2021v20a23_s5

Appendix 16. — Data on body proportions for Australian *Varanus* Merrem, 1820, taken from Thompson & Withers (1997): https://doi.org/10.5852/cr-palevol2021v20a23_s6